Combined Path Tracking and Stability Control using Model Predictive Control

Daan Lenssen

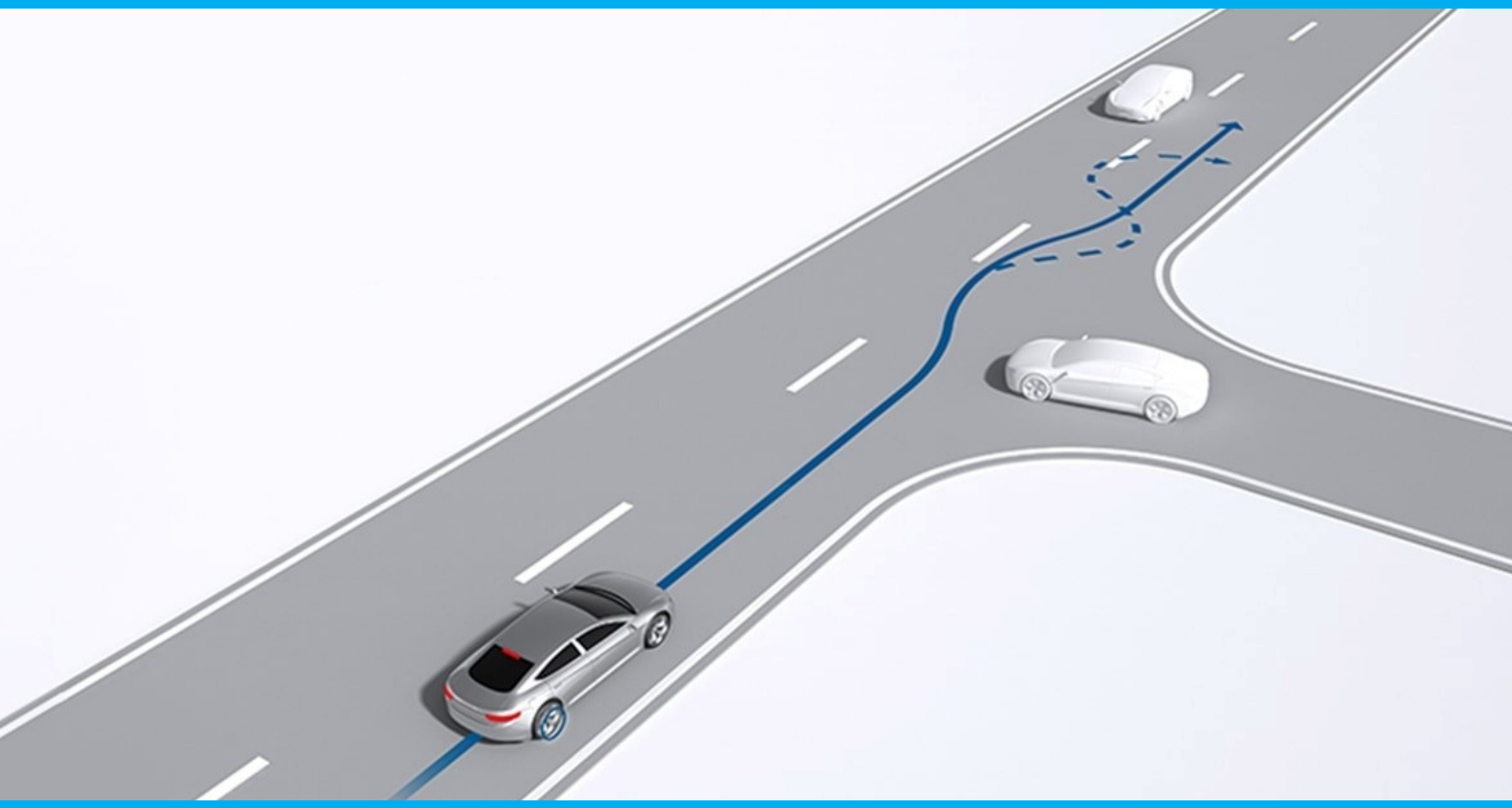

TU Delft

Combined Path Tracking and Stability Control using Model Predictive Control

by

Daan Lenssen

For the degree of Master of Science in Vehicle Engineering

at Delft University of Technology,

to be defended publicly on Friday 11 November 2022 at 09:00 AM.

Thesis committee:	Prof. Dr. ir. R. Happee,	TU Delft, chair
	Dr. ir. B. Shyrokau,	TU Delft, supervisor
	A. Bertipaglia,	TU Delft, daily supervisor

TU Delft


TU Delft
Delft
University of
Technology


Cognitive
Robotics

Abstract

This thesis presents a new MPC controller which integrates path tracking and stability control into one controller. Previously these tasks were done by separate controllers, where one controller handled the path tracking while another controller ensured the vehicle was kept in the stable operating region. A drawback of this method is that the controllers have opposing objectives. The path tracker could require a higher steering wheel angle to follow the path, while the Vehicle Stability Controller (VSC) might require a lower angle to keep the vehicle stable. By integrating these two controllers into one controller, the new controller is able to take both tasks into account and optimise the control output such that both objectives are satisfied.

This is achieved by implementing two extra yaw rates into the MPC model. These are the expected yaw rates based on the steering wheel angle and lateral acceleration of the vehicle. By comparing these two yaw rates to the actual yaw rate, the stability of the vehicle can be determined. The MPC controller is then able to prioritise path tracking or vehicle stability. This is achieved by actively varying the weights in the cost function depending on the vehicle state.

To compare the new MPC controller, 8 benchmark controllers have been created. These controllers can be divided into two groups of four controllers. The first group is able to use differential braking in the control output, while the second group can only output an equal brake torque for all wheels. The benchmark controllers use different methods for path tracking and stability control, to get an understanding of the performance benefits of each method. These different methods include: adding an extra target yaw rate based on path curvature and speed for tracking, adding constraints to ensure vehicle stability and using a separate stability controller to stabilise the vehicle.

All controllers are evaluated using the industry standard Moose test as well as a double lane change in simulations. These manoeuvres are used in industry to evaluate stability and can also be used to evaluate path tracking. Furthermore the robustness of the controllers was evaluated by changing various parameters. These variations include: changing vehicle speed, adding extra weight to the vehicle, lowering the road μ level and performing a lane change where each lane has a different μ level.

The results were evaluated using objective Key Performance Indicators regarding tracking performance and vehicle stability. The results show that the new MPC controller with the combined path tracking and stability control improves performance in both objectives. The new controller improves path tracking by 8% compared to the pure path tracking controller. While the stability is improved by 11% compared to the controller with a separate VSC. Furthermore the new controller was able to keep the vehicle stable at higher speeds and was more robust to varying conditions.

Contents

List of Figures

List of Tables

Acronyms

AD Automated Drive. 1, 3, 9, 15

ESC Electronic Stability Control. vii, 1, 2, 9

ESP Electronic Stability Protocol. 1

Euro NCAP European Euro New Car Assessment Programme. 9

KPI Key Performance Indicator. 4, 5, 8, 10, 11, 18, 39–42, 44–49, 51, 53, 55, 56

MPC Model Predictive Control. vii, 3, 5, 6, 10, 11, 13, 15, 18, 20–27, 29, 34–37, 50, 52, 59–61, 63, 64

NHTSA National Highway Traffic Safety Administration. 9

NRMSE Normalised Root Mean Square Error. 33, 35, 39, 42, 46, 48

RMSE Root Mean Square Error. 10, 11, 33–35, 39, 42, 46, 48, 50, 51, 53, 60, 61

RPM Revolutions per Minute. 15

TME Toyota Motor Europe. 19, 27

VSC Vehicle Stability Control. vii, 1, 13, 19–23, 26, 27, 41, 48, 52, 63, 64

1 Introduction

Path tracking and Stability Control are the two main components in controlling a vehicle. Before active safety systems were developed, the human driver was tasked with doing both of these actions. The driver has to control the vehicle to follow the route to his destination, while at the same time keep the vehicle in the stable region. However, when an unexpected evasive manoeuvre or braking had to be done, the driver would often not be able to control the vehicle resulting in an accident. The development of stability controllers made vehicles safer by aiding the driver in the control of the vehicle at the limit of handling. A further advancement to increase vehicle safety is the recent development of Automated Drive (AD) vehicles. These controllers take over the general path tracking task from the driver, removing the possibility of human driver error. In this chapter an introduction to stability controllers and path tracking for automated drive vehicles will be given, followed by defining the scope of this thesis and an outline of the structure of this report.

1.1. Stability Control Systems

Stability control systems (also called Vehicle Stability Control (VSC), Electronic Stability Control (ESC) or Electronic Stability Protocol (ESP) systems) are controllers which are used to stabilise the vehicle when the driver is at risk of losing control of the vehicle. This can happen in many cases, such as in evasive manoeuvres or when driving in bad weather conditions. An example of what can happen without a stability controller is shown in figure 1.1. The green path shows the intended path. However, if the driver's inputs are too aggressive or the road conditions are bad the vehicle becomes unstable resulting in a spin. Without a stability controller the vehicle would spin and follow the red path. When the stability controller is activated, the driver is able to maintain control and keep the vehicle on the desired path.

The first generation of stability controllers were implemented in vehicles in 1995 [1]. Since then stability controllers have become more advanced and more widely used. The implementation of stability control systems in vehicles has had a major impact in increasing the safety of road vehicles. A study on the effectiveness of stability control showed that ESC systems reduce fatal single-vehicle accidents by about 30-50% for passenger cars and even up to 50-70% for SUVs [2]. In absolute terms, the National Highway Traffic Safety Administration (NHTSA) in the US estimated in 2007 that if all vehicle were equipped with an ESC, 1547-2534 lives would be saved and 46,896-65,801 injuries would be prevented annually in the US alone. As it is so effective in reducing accidents, stability control systems have been mandatory in all new cars sold in the US since 2012 [3] and since 2014 for all new cars sold in the EU [4].

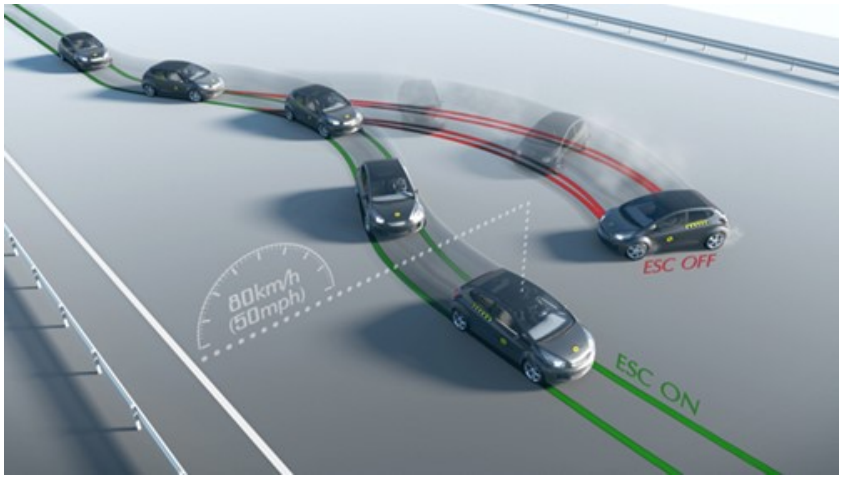

Figure 1.1: Vehicle path with and without ESC enabled. [4]

The stability control system calculates the desired vehicle yaw rate and compares this to the actual yaw rate measured from sensors. If the actual yaw rate deviates too much from the desired yaw rate, the system intervenes. The most common method of intervention is by the use of differential braking. This control strategy applies a braking force on one side of the vehicle, in order to create a yawing moment in the desired direction. If the vehicle is about to oversteer, the controller would apply the outside brakes. While if the vehicle is understeering the inside brakes would be used to increase the yawing moment of the vehicle.

1.2. Automated Driving Path Tracking

Path tracking is the core task of the automated driving controllers. These path followers should be able to follow a target path set by the path planner. This path is usually a relatively simple path which makes the vehicle follow the road, make a lane change or avoid an obstacle. Such a path is shown in figure 1.2. In order to follow this path, the controller most often uses the steering wheel for lateral path tracking and braking and throttle for longitudinal speed control. The vehicle not only needs a controller to follow a path, but also a path planner to generate this path. Furthermore sensors are required to detect obstacles, determine the vehicle's position and know the destination to even be able to generate the path. However, in this thesis only the path tracking and stability controller will be analysed and a very simple path planner is used in order to keep the main focus on combined path tracking and stability control.

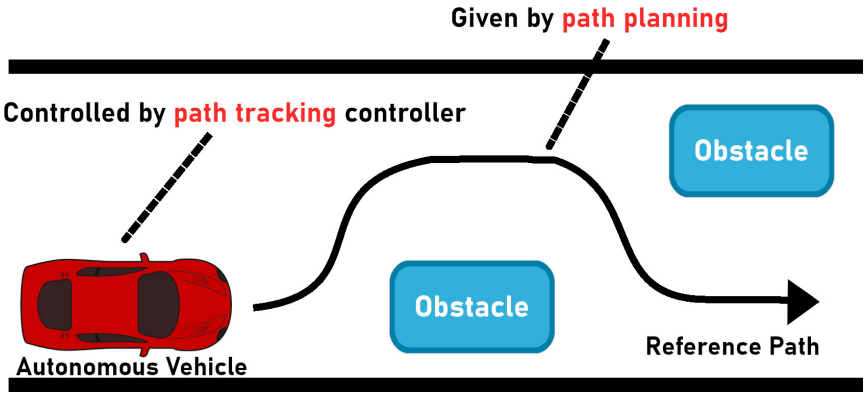

Figure 1.2: Path tracking controller schematic

The path tracking controller should be able to control the vehicle during extreme manoeuvres and with uncertainty in the vehicle parameters. Examples of these extreme manoeuvres include evading sudden obstacles and driving in low grip conditions. In this scenarios there is an added difficulty as the tires are operating in the non-linear region. If the controller is not able to take this into account, the result could be a control output that does not follow the reference path and could even lead to the vehicle losing control. The second difficulty comes from the uncertainty in the vehicle parameters. There are many factors which influence the vehicle behaviour like total mass, location of the center of gravity, which tires are used and road conditions. All these parameters affect the vehicle dynamics and can change over the lifetime of the vehicle or even while driving. This adds complexity as the controller needs to be able to control the vehicle in all conditions.

1.3. Scope of Thesis

During the initial literature review it was noticed that a lot of research has been done on vehicle stability control as well as on automated vehicle path tracking. However, there has been minimal investigation into controllers which combine these two functions. With the increased computational power that is now available, it is now possible to use Model Predictive Control (MPC) in real-time for vehicle control. This control method has already been researched for path tracking, but these controllers have limited to no stability control.

Most of the current AD vehicle controllers consist of a separate path tracking controller coupled with a separate stability controller. With this method the path tracking controller will control the vehicle to best follow the path, while the vehicle stability controller intervenes if the vehicle exceeds the predefined stability bounds. The advantage of this separate control is the easier formulation of each controller and a lower computational time. However, a disadvantage is that there is no collaboration between the path tracking and stability control. The path tracking controller will control the vehicle to follow the path, but if the vehicle exceeds the stability bounds, the path tracking control will suddenly face a completely new situation and the vehicle will not follow the intended path. With the rise of MPC becoming more common, this is also an area of control where MPC could provide improvements. By combining the path tracking and stability control into one MPC controller, it would be possible to have a single controller which optimises the path tracking while also staying within the stability bounds of the vehicle. The added benefit is that there is only one controller necessary to perform the two tasks. This also means there is a trade-off where the MPC is more complex and thus more computationally expensive.

Therefore the scope of this thesis is to design a new MPC controller which integrates the stability control into the path tracking controller. To fully compare the newly designed controller to existing solutions, 8 benchmark controllers have also been made. These baseline controllers use similar MPC path tracking or stability control methods as found in literature. Furthermore all controllers have been evaluated in varying conditions like different road μ, added vehicle weight and different speeds.

1.3.1. Goals of Thesis

The main goal of this thesis is as follows:

Design and evaluate an MPC controller which combines path tracking and stability control into one controller, using the steering wheel, throttle and brakes as actuation.

To achieve this goal, the following objectives were set:

- Extend the MPC prediction model to include throttle control to get a true AD vehicle

simulation.

- Develop and tune the 8 benchmark controllers.
- Create the reference generation to make a path for the vehicle to follow. This should be easily changeable between different manoeuvres.
- Develop the proposed controller which combines path tracking and stability control.
- Simulate all controllers in the Simulink / IPG Carmaker software for both default conditions as well as the manoevre variations.
- Compare the different controllers using the defined KPIs and analyse the strengths and weakness of the controllers.

1.3.2. Contribution of Thesis

The main contribution of this thesis is the novel controller which combines both path tracking and stability control into one single controller. This means the controller is able to take the stability of the vehicle into account when deciding on the control inputs to follow the path. This leads to an increased performance for both path tracking as well as stability when compared to a control structure where these tasks are achieved by separate controllers. Integrating the stability control into the path tracking controller means the controller can calculate the optimal path while taking both objectives into account.

Secondly, all controllers are designed to have good performance in a variety of conditions, not only in optimal scenarios. This is shown by the performance in low μ conditions, different speeds, as well as when weight is added.

Lastly, the used reference generator calculates the reference path using a very simple equation. This equation does not take the vehicle's performance limits into account and is only based on the geometric path that should be followed. This is done to have the vehicle controller be the only complex controller in the simulation and not have separate controllers for each task.

1.4. Thesis Structure

The thesis is divided into 7 chapters, summarised below:

- Chapter 2 introduces the key elements from the literature review. This review looks into the different path tracking an stability control methods that are used in literature, as well as the different test manoeuvres and KPIs used to evaluate the controllers.
- Chapter 3 shows the controller design. The vehicle and tire model that are used will also be shown, as well as the constraints and layout of each controller. This includes the 8 benchmark controllers as well as the proposed controller.
- Chapter 4 gives an overview of the simulation environment. The used simulation software is introduced as well as the different manoeuvres and KPIs used for evaluation.
- Chapter 5 shows the results from the different simulations with all controllers and manoeuvre variations.
- Chapter 6 discusses the results that are shown in Chapter 5. The key differences between controller performances will be highlighted, as well as some observations made during the simulation.
- Chapter 7 gives the conclusions as well as some recommendations for future work.

2

Literature Review

As part of this thesis, a literature study was done. In this chapter the main findings of this work will be shown. First an analysis of the different vehicle models that have been used in literature will be given. Next the same will be done for the different tire models. Then the methods for evaluation of the controllers will be shown. This includes the different manoeuvres that were used, as well as the Key Performance Indicator (KPI) used to give an objective assessment of the different controllers.

2.1. Vehicle Models

In literature there are mainly two vehicle models that are used. The simplest model is the bicycle model, this model consists of a simplified vehicle where the wheels on each axle are combined into one. These wheels are then linked together by a bar. The second model is the planar model. This model (also known as the four corner model or double track model) includes all four tires which are connected to the vehicle. In this section both vehicle models will be shown in more detail.

The bicycle model is shown in figure 2.1. It is often used in control structures when a simple vehicle model is sufficient in capturing the vehicle dynamics. This model uses some assumptions to simplify the vehicle model. It is assumed that there is no lateral load transfer and no body roll as both axles are collapsed into one tire. This single tire at the front and rear of the vehicle produces the same force as two tires would. Furthermore Ackermann geometry is not considered as only one wheel is modeled on each axle.

As the bicycle model only models two tires, the controller can only output a steering wheel angle, a correcting moment and tractive forces per axle. It is not possible to calculate independent forces on each of the four wheels directly from this model.

In order to apply a tractive force to individual tires, a secondary controller is required. This is done in [6] where the researchers use MPC to calculate a corrective moment which is then converted to braking forces by a secondary controller. A similar approach is taken in [7], where they use the bicycle model to calculate a corrective moment, which is fed into a brake force allocator which in turn feeds the output to the brake control logic which outputs the braking torques. In other research where the the bicycle model is used in MPC, the controller only controls the steering angle. In this case there is no need for a secondary controller to allocate individual wheel forces. This is done in [8], [5] and [9].

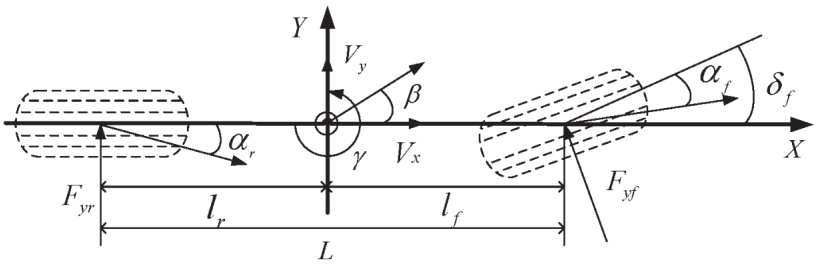

Figure 2.1: Bicycle model [5]

For controllers which only do path tracking, the bicycle model is by far the most commonly used model. As most of the path following controllers are designed for constant and relatively low speed, as well as low lateral acceleration conditions, there is less need for a complex model which also captures the lateral weight transfer and individual longitudinal wheel forces. Instead, the simpler bicycle model gives a good approximation of the vehicle which still leads to good performance as demonstrated in [10], [11] and [12].

The other vehicle model which is often used in literature, is the planar model (sometimes also called double track model). The double track or planar model consists of the four corners of a car connected to a center of mass, it is shown in figure 2.2. Using this model allows for easier application of individual tractive forces as all wheels are modeled and a secondary brake force allocator is therefore not required. Another advantage of this is that it is possible to set a constraint on the braking torques and variations of braking torques as done in [13], as the individual wheel forces can be calculated.

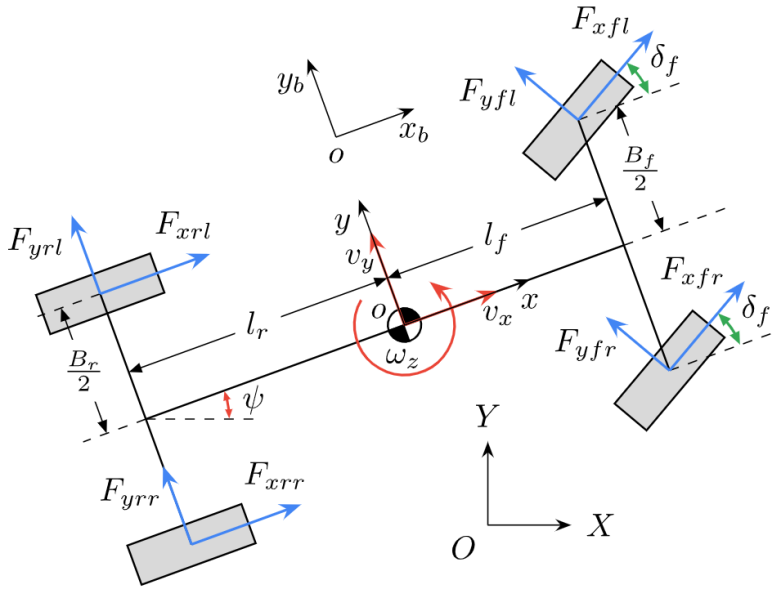

Figure 2.2: Planar model [14]

In [13], a direct comparison between the bicycle model and double track model in an MPC based yaw and lateral stability controller using active front steering and differential braking was done. In their findings they noted that the controller which uses the planar model was able to stabilise the vehicle at higher speeds than the controller which used the bicycle model. However, the planar model controller resulted in a much higher computational load. The au-

thors noted that the weight tuning of the controller with the planar model was significantly more time consuming, as the simulations took almost 15 minutes to complete. One thing to note is that this research was performed in 2008, with the increase in computational power the difference in computational time should be less of an issue now than it was then.

2.2. Tire Models

The tire model is used to link the slip angles of the tire with the forces the tire generates on the road. These forces can then be used in the vehicle model to calculate the control action. Tire models can generally be divided into two model classifications, physical models and empirical models [15]. The most commonly used tire model is the semi-empirical Pacejka ”Magic Formula” model. This model consists of a non linear equation with several parameters that need to be experimentally obtained [16]. The Pacejka model is shown in equation 2.1. The parameters D C B and E need to be obtained from testing in order to properly fit the model to the tire. These parameters are:

D - peak tire force value

C - shape factor which controls the stretching along the x-axis

B - cornering stiffness

E - curvature factor which determines the x-position of the peak force value

$$F = D\sin(C\arctan(Bx - E\arctan(Bx))) \tag{2.1}$$

In [17] a controller using the Pacejka model is compared to a controller using a simple linear tire model. The controller which utilises the Pacejka model indeed provided improved performance and was able to control the vehicle closer to the stability limits.

Another model that is often used in literature is the Dugoff model. This model is given by the following set of equations [18]:

$$F_x = C_\kappa \frac{\kappa}{1+\kappa} f(\lambda) \tag{2.2}$$

$$F_y = C_\alpha \frac{\tan\alpha}{1+\kappa} f(\lambda) \tag{2.3}$$

$$\lambda = \frac{\mu F_z (1+\kappa)}{2((C_\kappa \kappa)^2 + (C_\alpha \tan\alpha)^2)^{1/2}} \tag{2.4}$$

$$f(\lambda) = \begin{cases} (2-\lambda)\lambda & \lambda < 1 \\ 1 & \lambda \geq 1 \end{cases} \tag{2.5}$$

Where κ and α are the tires slip ratio and slip angle, C_κ and C_α the longitudinal and lateral tire stiffness. The main advantage of the Dugoff model is the fact that only the tire lateral and longitudinal stiffness need to be known. This is less time-consuming when the tire parameters that are required for the Magic Formula are not known. However, the Magic Formula does give a more accurate representation of the tire forces. In [18] the Dugoff model was modified by introducing a corrective factor to the calculation of the tire forces in equations 2.2 and 2.3. The corrective factors is shown in equations 2.6 and 2.7, with the new tire force equations shown in equations 2.8 and 2.9. This new modified Dugoff model is a closer approximation to the result of the Magic Formula as shown in figure 2.3. If the tire parameters for the Magic Formula are not known, this could give an improved accuracy over the original Dugoff model.

However, the numeric values in the corrective factors had to be changed by trial and error and could therefore be different if other tires are used.

$$g_x = (1.15 - 0.75\mu)\,\kappa^2 - (1.63 - 0.75\mu)\,\kappa + 1.5 \tag{2.6}$$

$$g_y = (\mu - 1.6)\tan\alpha + 1.5 \tag{2.7}$$

$$F_x = C_\kappa \frac{\kappa}{1+\kappa} f(\lambda) g_x \tag{2.8}$$

$$F_y = C_\alpha \frac{\tan\alpha}{1+\kappa} f(\lambda) g_y \tag{2.9}$$

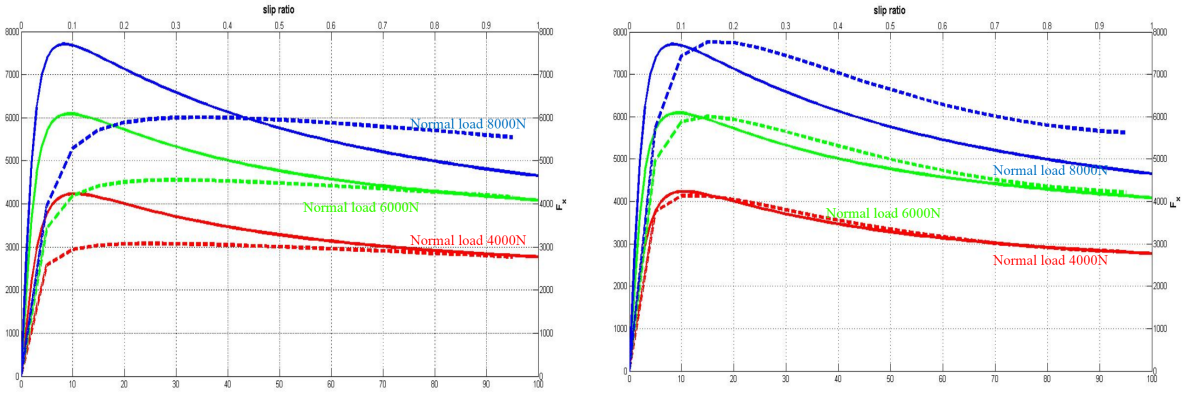

Figure 2.3: (a) original Dugoff model (dashed) vs Magic Formula (solid), (b) Modified Dugoff model vs Magic Formula [18]

2.3. Evaluation methods

After designing a controller, it needs to be tested and validated. Using the right test manoeuvre and performance evaluation is as important as the design of the controller. Without proper testing and evaluation, the performance of the new controllers can not be compared. The test manoeuvre should correspond a real world scenario where the limits of operation are tested. In this section, first the test manoeuvres that have been used in literature will be shown, followed by the most common KPIs that are used to objectively evaluate the performance of the controllers.

2.3.1. Manoeuvres

The most common testing manoeuvre that is used in literature is the double lane change. This manoeuvre is used for evaluating both path following as well as stability control. The double lane change is used to simulate an evasive manoeuvre. It has several variants which are used in literature. The two most commonly used ones are the two ISO standardised tests, ISO:3888-1 and ISO:3888-2. The first of these two is used to ”subjectively determine a double-lane change which is one part of vehicle dynamics and road-holding ability of passenger cars” [19]. The second manoeuvre is more commonly known as the Elk or Moose test and is used to simulate an evasive manoeuvre when the vehicle has to evade an object crossing the path of the vehicle [20]. This manoeuvre is shown in figure 2.4, the vehicle has to complete the manoeuvre at 72km/h without knocking over any of the cones to pass the test. The main difference between these two tests is the length of the manoeuvre and the width of the lanes. While the vehicle has 125 meters to complete the manoeuvre in ISO:3888-1, The track length of ISO 3888-2 is only 61 meters. To compensate for this the side and exit lane of the 3888-2 manoeuvre are slightly wider. However it is still a more difficult manoeuvre [21].

In literature these double lane changes are used for both stability controller evaluation as well as path following evaluation. However, often it is not clear which of the two manoeuvres is used or a slightly different manoeuvre length is used. In [14] the defined double lance change was followed the closest, while in [7] and [22] a distance plot is shown which corresponds the closest to the ISO:3888-1 manoeuvre.

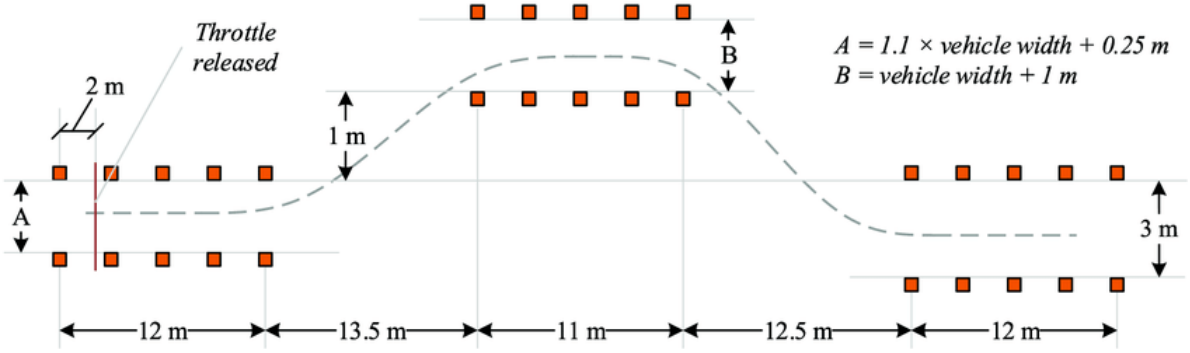

Figure 2.4: Path of the Elk test manoeuvre [23]

Another manoeuvre that is often used for the evaluation of stability controllers is the Sine-with-Dwell test. This test was used by the European Euro New Car Assessment Programme (Euro NCAP) for evaluating ESC behaviour on new cars before these systems became mandatory in 2014 [24] as well as the NHTSA [3]. The manoeuvre is done at 80km/h and consists of a predefined steering input, where the wheel is first turned to one side, then immediately back to the other side where it is held for 500ms and finally returned to center. This is shown in figure 2.5.

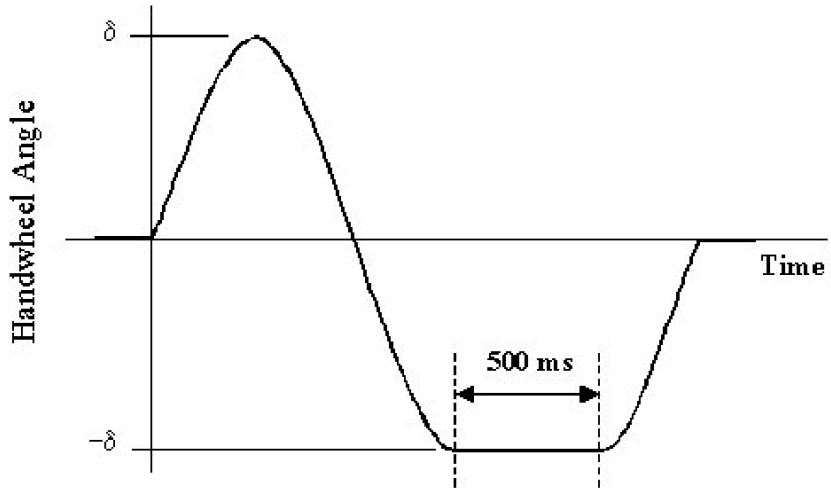

Figure 2.5: Steering input for the Sine-with-Dwell manoeuvre [25]

The big downside of using the Sine-with-Dwell test is that it is defined by a steering wheel input. In the case of evaluating an AD vehicle controller that does both stability control as well as path following, this predefined steering input doesn't allow the controller to function as it would normally as the control of the steering wheel is taken away. In the literature where the Sine-with-Dwell manoeuvre is used for evaluation, the proposed controller is always a pure stability controller without path following, as for path following the steering wheel is used as a control input.

2.3.2. KPIs

After the testing and simulation is completed, an objective and analytical way of judging the performance is required. This is not only important to be able to compare the different controllers within the test, but also to have a way of comparing different tests with each other. The most common method of objectively analysing performance is by the use of certain KPIs. Most KPIs found in literature are Root Mean Square Error (RMSE) of various parameters, integrals of some parameters or maximum values of some parameters. Some of the most used KPIs are the RMSE of the yaw angle ψ, yaw rate $\dot{\psi}$ and lateral position Y which is used in [13], [22] and [14]. These RMSEs give an indication of the accuracy in the tracking between the target value and actual value. The maximum values of these parameters is also used as a performance indicator in [13] and [14]. Furthermore, in [26] some other performance criteria are used like the integral of the control action for the complete manoeuvre, which shows how much the controller had to intervene in order to keep the vehicle from spinning out. As well as the average time consumed by the calculations of the algorithm that was used in that paper. This performance criteria is especially important for an MPC controller where a lot of calculations are performed on-line which need to be solved as fast as possible. This criteria was defined as follows:

$$Er_{time} = \frac{\sum_k^N T_{c_k}}{N}$$

Where T_{c_k} is the computational time of each iteration and N the amount of iterations. Another performance indicator which is used in [27] is the percentage of speed reduction during the test. Which is defined as:

$$\Delta V\% = 100 * \frac{V_m - V(t_f)}{V_m}$$

Where V_m is the initial velocity and $V(t_f)$ is the final velocity. Some other KPIs that can be used in order to account for the passenger comfort in case of a path follower is the average lateral acceleration as well as the average lateral jerk.

2.4. Summary

The two vehicle models that are used the most often in literature are the bicycle model and the planar model. From previous research that directly compared the two different models, it was found that using the planar model resulted in a controller with better stabilising properties. However, this increased performance comes at the cost of a higher computational time for the controller when using the planar model. Another consideration for the choice of model could also be depending on the used type of control actuation that is used. As the planar model uses all four tires directly in the calculation, the wheel torque control can be done directly. In contrast, the bicycle model lumps the wheels on each axle in one, so for individual wheel torque control a lower level controller is needed to assign the individual wheel torques.

The most well known tire model is the Pacejka ”Magic Formula” model. This is a semi empirical model where the parameters of the equations need to be experimentally obtained. There are also some other tire models which are based on more physical approaches. The most common of these physical models is the Dugoff model, which uses the tire cornering stiffness and peak tire force as tire parameters, and then uses the tire slip angle and slip ratio to calculate the tire forces. The advantage of this method is that those parameters can be more easily obtained than the Pacejka parameters but still give a good approximation of the tire force.

For evaluating the performance of the controller, there are mainly two manoeuvres that are used. The first one is the Double lane change, sometimes also called the Elk test. The second

manoeuvre which is used for testing the vehicle stability is the Sine-with-Dwell test. However, for testing autonomous vehicles or controllers which also do path following, the Sine-with-Dwell test can not be used, as it is defined by a predetermined steering wheel input.

After performing the manoeuvres, the obtained data needs to be evaluated to determine the performance of the controller. This objective evaluation can be done using KPIs. The most common KPIs that are used are summarised below:

- RMSE of: lateral position Y, yaw angle ψ, yaw rate $\dot{\psi}$
- Average of: lateral acceleration and lateral jerk
- MPC Computational Time
- Percentage of speed reduction during the manoeuvre

3

Controller Design

This chapter will show the different controller designs that have been used in this research. First the underlying vehicle and tire model which are used in all controllers will be explained. Then the imposed constraints on the MPC controllers will be shown, followed by the method of determining the cost function weights. Then the separate VSC will be shown and finally the different controller variations will be explained.

3.1. MPC introduction

Within the MPC, a prediction model and an optimization algorithm are used in order to calculate the optimum output and state evolution over the prediction horizon N_p. At each time step (which in this research is taken to be 0.035s [28]), the optimization algorithm takes the current available state information and calculates the optimum control inputs over the control horizon N_c. This is shown in figure 3.1 where N_p and N_c have the same length. In this research the prediction and control horizon both have a length of 30 steps, giving a time horizon of 1.05s. This was found to be the optimal value which gives the best performance while still being able to run in real-time [28]. The optimal control input sequence is calculated using an optimization algorithm which tries to minimize a predefined cost function, while taking imposed constraints into account. When the optimal control sequence is obtained, only the first control input is actually applied to the system. In the next time step, the new states are obtained and the MPC calculates the new output. In the next sections the models, constraints and cost function that are used in this thesis are explained.

3.2. Vehicle Model

The vehicle model that is used is a modified version of the model used in Chowdhri's paper [28], as this is a continuation of that project. Changes have been made to allow for control of the vehicle speed by the MPC. This is done by adding throttle control to the calculation of the longitudinal tire force. This allows the throttle position to be controlled by the MPC, instead of only the steering and brakes. The model consists of a planar car model as shown in figure 2.2. This model was chosen as this gives direct control over the braking output without the need of a secondary controller. The model also performs better when the vehicle is close to the stability limits, which will be the case for these stability controllers. The controller outputs the steering rate, brake rate and throttle position rate. The decision was made to control the rates in order to have a smoother operation of these control inputs to the vehicle. The equations

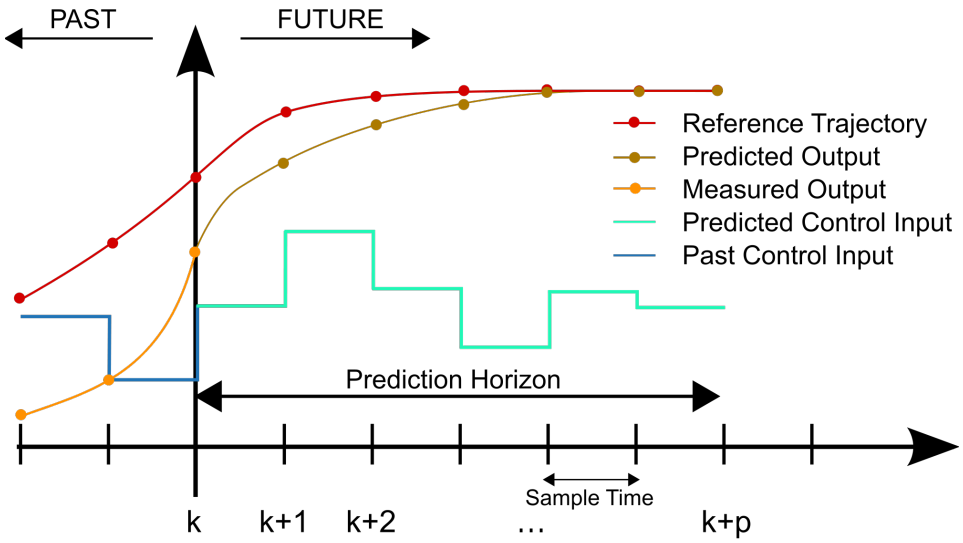

Figure 3.1: Model Predictive Control prediction horizon [29]

used in this model are as follows:

$$\dot{v}_x = \frac{(F_{x,fl} + F_{x,fr})\cos\delta - F_{aero} - (F_{y,fl} + F_{y,fr})\sin\delta + (F_{x,rl} + F_{x,rr})}{m} + v_y r \tag{3.1}$$

$$\dot{v}_y = \frac{(F_{x,fl} + F_{x,fr})\sin\delta + (F_{y,fl} + F_{y,fr})\cos\delta + (F_{y,rl} + F_{y,rr})}{m} - v_x r \tag{3.2}$$

$$\dot{r} = \frac{(F_{x,fl} + F_{x,fr})\sin\delta * l_f + (F_{y,fl} + F_{y,fr})\cos\delta * l_f - (F_{y,rl} + F_{y,rr}) * l_r}{I_z} + \frac{\frac{t_f}{2}(F_{x,fr} - F_{x,fl})\cos\delta + \frac{t_f}{2}(F_{y,fl} - F_{y,fr})\sin\delta + \frac{t_r}{2}(F_{x,rr} - F_{x,rl})}{I_z} \tag{3.3}$$

$$\psi = r \tag{3.4}$$

$$\dot{x}_p = v_x\cos\psi - v_y\sin\psi \tag{3.5}$$

$$\dot{y}_p = v_x\sin\psi + v_y\cos\psi \tag{3.6}$$

$$\dot{\delta} = u_\delta \tag{3.7}$$

$$\dot{T}_{b,fl} = u_{Tb,fl} \tag{3.8}$$

$$\dot{T}_{b,fr} = u_{Tb,fr} \tag{3.9}$$

$$\dot{T}_{b,rl} = u_{Tb,rl} \tag{3.10}$$

$$\dot{T}_{b,rr} = u_{Tb,rr} \tag{3.11}$$

$$\dot{Thr} = u_{Throttle} \tag{3.12}$$

In these equations $F_{x,ij}$ is the longitudinal force on each tire, $F_{y,ij}$ the lateral force on each tire, δ the steering wheel angle, F_{aero} the aerodynamic drag force acting on the vehicle, l_i the distance between the center of gravity and the front or rear axle, t_i the track width of the front or rear axle. For a full list of the car parameters and their values, see Appendix A.

The longitudinal tire forces are calculated as follows:

$$F_{x,f} = \frac{GearRatio((Trq_{full} - Trq_{drag})Thr + Trq_{drag}) - (T_{b,fl} + T_{b,fr})}{R_{eff,f}} \tag{3.13}$$

$$F_{x,r} = \frac{-(T_{b,fl} + T_{b,fr})}{R_{eff,r}} \tag{3.14}$$

Here the $GearRatio$ is the total gear ratio between the engine and the wheels, Trq_{full} and Trq_{drag} the maximum and minimum engine torque at the current Revolutions per Minute (RPM) of the engine, Thr the throttle position, $T_{b,ij}$ the braking torque on each wheel and $R_{eff,i}$ the effective tire radius on the front and rear of the vehicle.

As this vehicle is using a full AD controller, the longitudinal tire force needs to includes a calculation of the drive torque at the wheels as seen in equation 3.13. This is done by having some additional 'OnlineData' parameters, namely the current gear ratio, maximum torque at current engine operating RPM and minimum torque at current engine operating RPM. These maximum and minimum engine torques are taken from the engine torque curve shown in figure 3.2. The blue line shows the maximum engine torque achieved at 100% throttle, while the red line shows the minimum engine torque at 0% throttle.

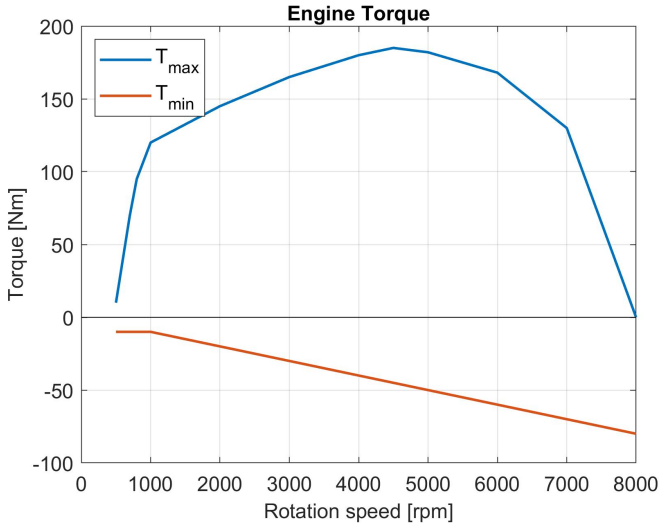

Figure 3.2: Minimum (red) and Maximum (blue) engine torque curves

The engine torque is then calculated as a linear interpolation between Trq_{full} and Trq_{drag} at the current RPM. Finally, this engine torque is then multiplied by the current gear ratio which is based on the final drive and currently selected gear in order to obtain the drive torque at the wheels. The MPC controller is then able to predict and change the engine power by varying the throttle position.

The lateral tire forces in equations 3.1 to 3.3 are calculated using the following equations:

$$F_{y,fl} = Ca_{fl}(\delta - \frac{v_y + l_f r}{v_x - \frac{t_f}{2} r}) \tag{3.15}$$

$$F_{y,fr} = Ca_{fr}(\delta - \frac{v_y + l_f r}{v_x + \frac{t_f}{2} r}) \tag{3.16}$$

$$F_{y,rl} = Ca_{rl}(-\frac{v_y - l_f r}{v_x - \frac{t_r}{2} r}) \tag{3.17}$$

$$F_{y,rr} = Ca_{rr}(-\frac{v_y - l_f r}{v_x + \frac{t_r}{2} r}) \tag{3.18}$$

Here Ca_{ij} are the cornering stiffnesses of the tires. These stiffnesses are assumed to be constant over the prediction horizon. However, at each time step they are updated using the Dugoff tire model. This tire model will be shown in more detail in the next section.

3.3. Tire Model

Instead of a constant cornering stiffness, the cornering stiffness of each tire is calculated at each time step using the Dugoff tire model. This adaptive tire model is used to increase the accuracy of the prediction, as the Dugoff model can be used to capture the non-linearities of the tire behaviour. This in turn results in a more accurate calculation of the tire forces and will make the controller able to make more accurate predictions. The Dugoff model for the lateral tire forces is described by the following set of equations:

$$\mu = \mu_0 \left(1 - e_r V_{xij} \sqrt{\kappa_{ij}^2 + \tan^2 \alpha_{ij}}\right) \tag{3.19}$$

$$\lambda = \frac{\mu F_{zij}(1-\kappa_{ij})}{2\sqrt{(C_{\kappa ij}\kappa_{ij})^2 + \left(C_{\alpha ij}\tan(\alpha_{ij})\right)^2}} \tag{3.20}$$

$$f(\lambda) = \begin{cases} \lambda(2-\lambda), & \lambda < 1 \\ 1, & \lambda \geq 1 \end{cases} \tag{3.21}$$

$$F_{yij} = \frac{C_{\alpha ij}\alpha_{ij}}{1-\kappa_{ij}} f(\lambda) \tag{3.22}$$

In these equations μ_0 and e_r are variables which can be tuned to fit the tire curve to the real tire force values. The values for C_κ and C_α are also obtained by fitting the resulting tire curve to the actual model. The velocities V_{xij} are the longitudinal velocities of each individual tire, which are different from the longitudinal velocity of the vehicle and are calculated using the following equations:

$$V_{xfl} = (v_x - t_f \frac{r}{2}) \cos\delta + (v_y + l_f r) \sin\delta \tag{3.23}$$

$$V_{xfr} = (v_x + t_f \frac{r}{2}) \cos\delta + (v_y + l_f r) \sin\delta \tag{3.24}$$

$$V_{xrl} = v_x - t_r \frac{r}{2} \tag{3.25}$$

$$V_{xrr} = v_x + t_r \frac{r}{2} \tag{3.26}$$

Where v_x and v_y are the vehicle longitudinal and lateral speed respectively, twf and twr the front and rear track width, δ the wheel angle and r the yaw rate. Lastly the vertical tire forces F_{zij} are calculated using the weight transfer that occurs due to the longitudinal and lateral accelerations as follows:

$$F_{zfs} = \frac{m g l_f}{2L} \tag{3.27}$$

$$F_{zrs} = \frac{m g l_r}{2L} \tag{3.28}$$

$$F_{z,long} = \frac{m a_x h_{cg}}{2L} \tag{3.29}$$

$$h = h_{cg} - \frac{l_r h_f + l_f h_r}{L} \tag{3.30}$$

$$F_{z,lat}^{f} = \frac{ma_y}{t_f}\left(\frac{l_r h_f}{L} + \frac{C_{r,f}h}{C_{r,f} + C_{r,r} - mgh}\right) \tag{3.31}$$

$$F_{z,lat}^{r} = \frac{ma_y}{t_r}\left(\frac{l_f h_r}{L} + \frac{C_{r,r}h}{C_{r,f} + C_{r,r} - mgh}\right) \tag{3.32}$$

$$F_{z,fl} = F_{z,fs} - F_{z,long} - F_{z,lat}^{f} \tag{3.33}$$

$$F_{z,fr} = F_{z,fs} - F_{z,long} + F_{z,lat}^{f} \tag{3.34}$$

$$F_{z,rl} = F_{z,rs} + F_{z,long} - F_{z,lat}^{r} \tag{3.35}$$

$$F_{z,rr} = F_{z,rs} + F_{z,long} + F_{z,lat}^{r} \tag{3.36}$$

Here it is assumed that the weight transfer due to the roll and pitch of the vehicle is small.

3.4. Constraints

In this section the baseline constraints that are used in all of the controllers will be shown. Some controllers have additional constraints which will be shown in section 3.7. The main point of the baseline constraints is to limit the control outputs by limiting the maximum values as well as the maximum rates for the control outputs. These main constraints are shown below:

$$0 \leq v_x \leq \frac{170}{3.6} \tag{3.37}$$

$$0 \leq Thr \leq 1 \tag{3.38}$$

$$-1 \leq \dot{Thr} \leq 1 \tag{3.39}$$

$$\frac{-2.76 * 360\pi}{180 S_{rat}} \leq \delta \leq \frac{2.76 * 360\pi}{180 S_{rat}} \tag{3.40}$$

$$\frac{-800\pi}{180 S_{rat}} \leq \dot{\delta} \leq \frac{800\pi}{180 S_{rat}} \tag{3.41}$$

$$0 \leq T_b \leq 4885.8 \tag{3.42}$$

$$-7023.3 \leq \dot{T_b} \leq 7023.3 \tag{3.43}$$

The first constraint in this list limits the vehicle speed to the top speed of the vehicle. The second and third constraint limit the throttle input and input rate respectively. The throttle input is limited between a value of 0 and 1 where 0 means the throttle is closed, while a value of 1 corresponds to a fully open throttle. The throttle rate is limited to ensure a smooth operation of the throttle. Constraint 3.40 and 3.41 limit the steering wheel angle and steering wheel angle rate, with S_{rat} the steering ratio. The values for the bounds were determined in [28]. The final two constraints limit the brake torque as well as the brake torque rate. The values for these bounds were also determined in [28]. As previously mentioned, these constraints are the baseline constraints that all of the designed controllers have.

3.5. Cost Function Weights

During the optimisation of the MPC, the cost function is minimised. This minimisation gives the optimal control output over the prediction horizon. The weights in the cost function can be used to assign different priorities to states or outputs. If the weight that is used for a certain state is increased, that state will be tracked more closely. This is because the value of the cost function will increase more when this state deviates from its reference, than when a different state with a lower cost deviates from its reference. This also applies to the weights of different control outputs, which is especially helpful for MIMO controllers. By carefully tuning the weights, the controller can be tuned to prioritise tracking of certain states or control outputs. With a prediction horizon N_p the cost function can be defined as:

$$J = \sum_{i=1}^{N_p-1} \left(Q_i \left(x_i - r_i\right)^2 + R_i u_i^2 + P_i \Delta u_i^2 \right) + Q_N \left(x_{N_p} - r_{N_p} \right)^2 + R_N u_{N_p}^2 \tag{3.44}$$

Where Q_i, R_i and P_i are the weights on the state tracking, control use and change in control use respectively. In this thesis the output from the MPC is the change in the controls Δu. The selection of these weights is a non-trivial process. A set of weights that gives optimal results in one scenario, does not guarantee optimal results in a different scenario. For example the weights that lead to an optimal following of the speed profile along a straight path, will not give optimal results in an evasive manoeuvre. Even the weights for the same manoeuvre, but with different μ levels, could require different weights for optimal performance.

In this research the weights of the cost function change depending on the road μ and if the vehicle is turning or not. The dependence on the road μ level is done by multiplying or dividing the weights with the current road μ level, thereby increasing or decreasing the value of the weights. The amount of increase or decrease required for optimal performance was determined by a trial and error method. The weights were found by iteratively running the simulation while changing the weights, and using the KPIs to check if an improvement was achieved.

In order to have the weights change when the vehicle is turning, two sets of weights were defined. One set for straight line driving and another set for turning. The selection of which set to use was done by checking to see if the vehicle is turning or not. This was done using a modified version of the Cost Function Update method used by Chowdhri [28]. In his paper, Chowdhri introduced an algorithm which counts the amount of times the reference ψ and $\dot{\psi}$ exceed a certain threshold. If the values of ψ and $\dot{\psi}$ are above the threshold, these reference values are significant and the turning of the vehicle is critical in order to follow the path. The weights in the cost function then change to prioritise the cornering manoeuvre, instead of straight line driving. A similar method was used in this thesis, however instead of only looking at the upcoming 30 reference values, also the past 30 reference values were taken into account. This was done to remove the abrupt change in weights at the final phase of the corner, when the reference path is straight but the vehicle is still turning. In this updated method, the reference values both in front of the vehicle as well as behind the vehicle are used to determine if the vehicle is still cornering.

With this method of utilising the road μ and reference path to determine the cost function weights, the controller has better performance in varying conditions as the weights can be tuned depending on the scenario. One drawback of this method is that it is more time consuming, as for each scenario the weights have to be tuned for optimal performance. A full overview of the cost function weights for all controllers can be found in Appendix B. The method used for obtaining these weights is explained in more detail in section 4.5.

3.6. Separate VSC

The Vehicle Stability Control that is used in this research is a VSC that is a simplified version of a VSC that was developed in-house at TME. This simplified VSC checks the current state of the vehicle against some threshold values. If the vehicle exceeds one of these thresholds, the VSC will intervene and output a corrective brake torque for each individual wheel. The VSC can intervene in three different scenarios: When the vehicle is in oversteer, understeer or during a transient manoeuvre when the steering wheel changes direction. A generalised workflow of the VSC is shown in figure 3.3.

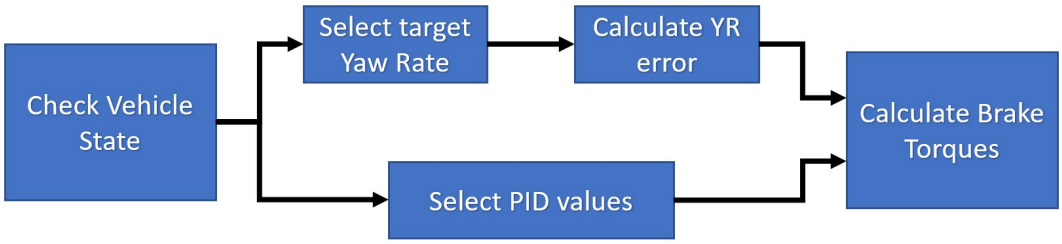

Figure 3.3: VSC generalised workflow

In the check vehicle state section, the VSC checks if the vehicle currently exceeds any of the thresholds for oversteer, understeer or transient manoeuvres. If this is not the case, the flags for these states will remain zero and the VSC does not intervene. If one or multiple thresholds are exceeded, a flag will be raised and the VSC will intervene. It is possible that both the transient manoeuvre as well as the under- or oversteer flag is active. In that case, the transient manoeuvre flag will take priority in the target yaw rate selection and PID value selection.

The target yaw rate selection block selects one of three target yaw rates. These yaw rates are: the current yaw rate of the vehicle, the expected yaw rate based on the lateral acceleration and longitudinal speed ($\dot{\psi}_{GY}$), and the expected yaw rate based on the steering wheel angle and car parameters ($\dot{\psi}_{Ack}$). The formulas to calculate $\dot{\psi}_{GY}$ and $\dot{\psi}_{Ack}$ are shown below.

$$\dot{\psi}_{GY} = \frac{a_y}{v_x} \tag{3.45}$$

$$\dot{\psi}_{Ack} = \frac{\delta v_x}{L(1 + K_h v_x^2)} \tag{3.46}$$

Where L is the wheelbase of the vehicle and K_h the stability factor.

In order to not have an extreme target yaw rate when the vehicle has a high wheel angle, which may be unachievable in low mu conditions, a weighted target yaw rate is used. This is a modified yaw rate which uses the theoretical maximum achievable yaw rate, using certain logic, and combines it with the target yaw rate found by equation 3.46. The theoretical maximum is calculated by:

$$\dot{\psi}_{max} = \frac{9.81\mu}{v_x} \tag{3.47}$$

When the target yaw rate is selected, the error between this target and the actual yaw rate can be calculated. This error is then used in the PID control selection block to obtain the PID control values. Each of the vehicle state flags also has a corresponding PID control weight block. This way, the weights can be tuned to fit the state that the vehicle is in.

Finally, the actual brake torques are calculated. This is done by having the output of the PID control block act as a desired Yaw acceleration. This desired yaw acceleration can then be converted into a yaw moment which can be achieved by applying more brake torque on one side of the car versus the other side. In order to prevent a large desired yaw acceleration to cause a large brake torque allocation and thereby locking of the wheels, an ABS controller is integrated in the VSC to prevent this situation.

3.7. Controller Variations

In this study a total of 9 different controller variations have been designed. The first 8 controllers can be split into two sets of four as shown in table 3.1. The first set is a simpler control structure where the braking output by the MPC is only a single brake pressure for all wheels (indicated by SB). In the second set the MPC can apply differential braking and thus can independently send a brake pressure to each individual wheel (indicated by DB). This makes the controller more complex but also gives more freedom in the control output.

Table 3.1: Overview of the 8 controllers

	1) Path Tracking	2) Stability by Y.R. in Cost Function	3) Stability by Constraints	4) Path Following + Separate VSC
Single Brake Output 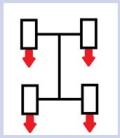	SB-PT	SB-PTY	SB-PTC	SB-PTS
Differential Braking 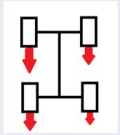	DB-PT	DB-PTY	DB-PTC	DB-PTS

The other differences in design relate to the method of path tracking and stability control integration. In this report four different methods are applied and compared. The first method is a simple path tracker with no stability control (PT). The second method tries to improve tracking and implement some stability control by including a target yaw rate in the cost function (PTY). The third controller implements stability control by including two additional constraints to the MPC formulation (PTC). These constraints limit the vehicle to the specified stability bounds. Finally, the fourth configuration uses the pure path following MPC from the first configuration and adds a separate VSC as described in section 3.6 to provide stability control (PTS).

The 9th controller is a novel controller that uses some of the equations that were used in the separate VSC and integrates those into the MPC controller. This method makes the MPC controller predict the stability of the vehicle more accurately. This is achieved not only because the equations are now actively used in the calculations, but also because there is no separate controller that interferes in the path following task when the vehicle becomes unstable.

In the next subsections each controller will be discussed in more detail. Each controller will have a short summary of the design, including a general layout of the controller.

SB-PT: Simple Path Tracking

The SB-PT controller is a simple path tracking controller. It outputs a steering wheel angle, throttle position and a single brake pressure that is the same for all wheels. This way it can accelerate and decelerate, as well as turn the vehicle. The reference values from the trajectory

consist of a reference lateral position and yaw angle. This is shown in a schematic layout in figure 3.4. The constraints in this controller are only the baseline constraints shown in section 3.4.

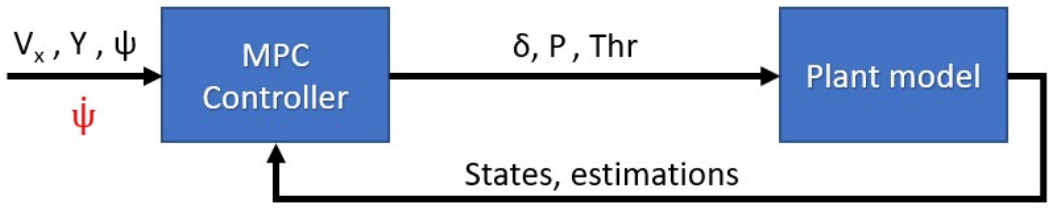

Figure 3.4: Layout of the SB-PT controller and SB-PTY Controller yaw rate addition

SB-PTY: Adding Yaw Rate to the Cost Function

The SB-PTY controller is similar to the SB-PT controller. However instead of only having a reference lateral position and yaw angle, now also a reference yaw rate is included. This reference yaw rate is based on the path curvature and the velocity that the vehicle is currently driving on. The layout is the same as the SB-PT controller and can be seen in figure 3.4, with the addition of a reference yaw rate. The constraints are also the same as the SB-PT controller.

SB-PTC: Stability by Constraints

In the SB-PTC controller, the stability of the baseline SB-PT controller is improved by adding constraints. These two extra constraints are used to keep the vehicle in the stable operating region. The first constraint is the error between the expected yaw rate as calculated by the Ackermann angle in equation 3.46 and the actual yaw rate of the vehicle. The second constraint is the error between the expected yaw rate based on the lateral acceleration and longitudinal speed from equation 3.45, and the actual yaw rate of the vehicle. These equations are shown below below:

$$\dot{\psi}_{GY,err} = \frac{a_y}{v_x} - r \tag{3.48}$$

$$\dot{\psi}_{Ack,err} = \frac{\delta v_x}{L(1 + K_h v_x^2)} - r \tag{3.49}$$

These two equations are then used in the constraints, where they are bounded to a minimum and maximum value to ensure vehicle stability. The layout of the SB-PTC controller is the same as the SB-PT controller in figure 3.4

SB-PTS: Stability by separate VSC

The SB-PTS controller structure combines the MPC path follower from SB-PT with a separate VSC controller. The MPC formulation is the same as in SB-PT and the VSC is as described in section 3.6. It should be noted that while the MPC does not have the ability of differential braking, the VSC can give individual wheel pressures. The final brake pressure is the combination of both these pressures, in formula form:

$$P_i = P_{MPC} + P_{VSC,i} \tag{3.50}$$

The layout of this controller is shown below in figure 3.5.

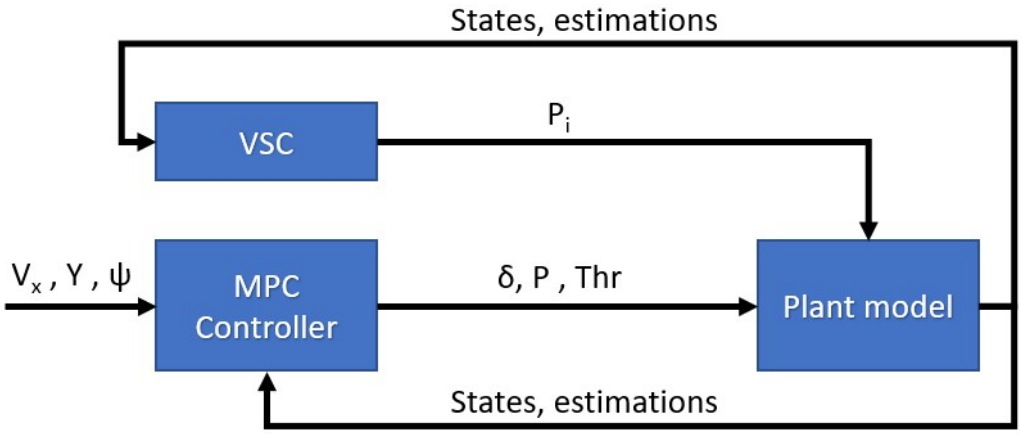

Figure 3.5: Layout of the SB-PTS Controller

DB-PT: Path Following with differential braking

The DB-PT controller adds the ability to use differential braking to the MPC formulation of the SB-PT controller. Instead of having a single brake output that is the same for each wheel, the controller is now able to individually assign a brake pressure to each wheel in order to have more control of the vehicle behaviour. This layout is shown in figure 3.6.

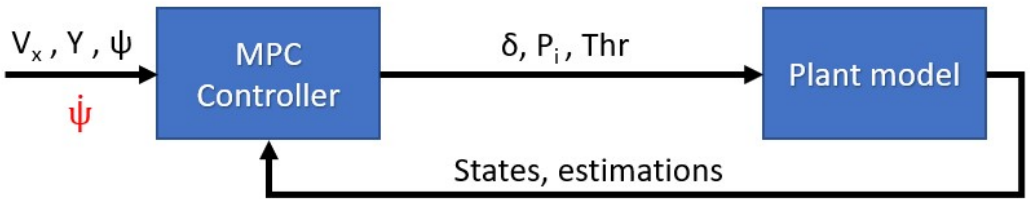

Figure 3.6: Layout of the DB-PT Controller and DB-PTY Controller yaw rate addition

DB-PTY: Differential braking and Yaw Rate in the Cost Function

The DB-PTY controller adds a reference yaw rate based on the path curvature and vehicle velocity to the MPC formulation, similar to the SB-PTY controller. This will give the MPC a target yaw rate to follow and therefore improve the tracking and stability capabilities of the controller. The layout of this controller is the same as the DB-PT controller shown in figure 3.6 with the addition of a reference yaw rate.

DB-PTC: Differential braking and stability by Constraints

The DB-PTC controller uses two constraints to ensure the stability of the vehicle. The constraints used in this controller are the same ones as used in the SB-PTC controller and are defined in equations 3.48 and 3.49. The layout of this controller can be seen in figure 3.6.

DB-PTS: Differential braking and stability by VSC

The DB-PTS controller combines the DB-PT controller with the separate VSC. The MPC calculates the control outputs to follow the path, while the VSC can intervene using brake pressures when the vehicle goes outside of the stability bounds. In this case the MPC is now also able to output different brake torques, in contrast to the SB-PTS controller where only the VSC was able to have individual brake outputs. The total brake pressure on each wheel can thus be

defined as follows:

$$P_i = P_{MPC,i} + P_{VSC,i} \tag{3.51}$$

The layout of this controller is shown in figure 3.7.

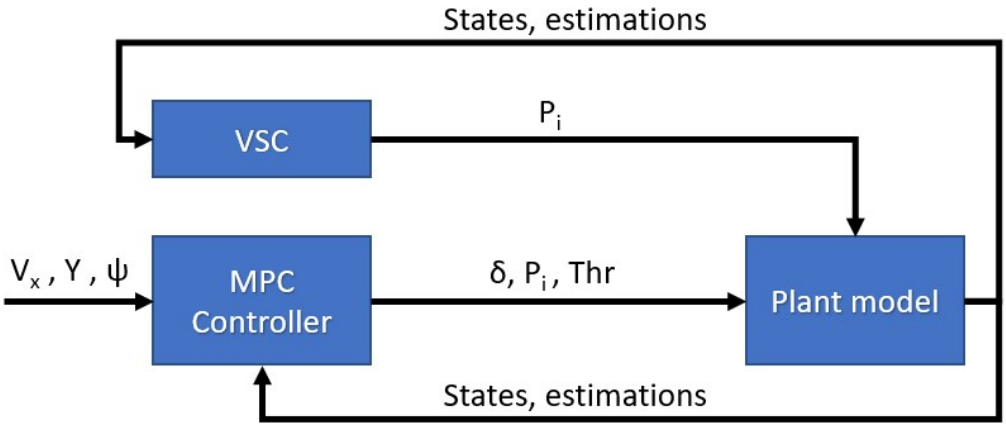

Figure 3.7: Layout of the DB-PTS Controller

Proposed controller

After comparing the initial eight controllers a final controller was created which integrated the stability control capabilities of the separate VSC more directly into the MPC controller. As the DB-PTY controller was found to have the overall best performance, it was chosen to use this controller to integrate the VSC in. Using this method, the goal was to obtain a controller with the tracking ability of the DB-PTY controller while having the stability of the SB-PTS and DB-PTS controllers. The layout of this new controller is shown in figure 3.8.

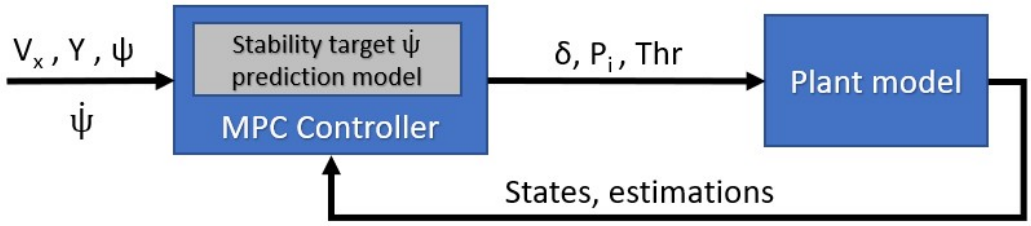

Figure 3.8: Layout of the proposed Controller

In order to integrate the VSC inside of the MPC, the MPC needs to be able to predict the stability of the vehicle. The equations that are used in this proposed controller are based on the equations that are used in the separate VSC. The separate VSC calculates the target yaw rate based on the lateral acceleration and steering angle (equations 3.45 and 3.46). For use in the MPC controller, these are modified such that the reference value for these equations to ensure stability is always close to 0. This is done by using the error between the stability equations ($\dot{\psi}_{GY}$ and $\dot{\psi}_{Ack}$) and the actual yaw rate of the vehicle. These equations are shown below:

$$\dot{\psi}_{GY,err} = \frac{a_y}{v_x} - r \tag{3.52}$$

$$\dot{\psi}_{Ack,err} = \frac{\delta v_x}{L(1 + K_h v_x^2)} - r \tag{3.53}$$

This means that in total there are three yaw rates that the MPC will optimise for, a yaw rate related to path curvature, a yaw rate related to the steering input and a yaw rate related to the lateral acceleration. The first yaw rate is related to path tracking, while the other two are related to vehicle stability. This also means that some trade-off is needed in the cost function weights to tune the controller between prioritising tracking and stability.

For the prediction, the MPC needs the time derivatives of these equations to be able to predict the future time steps in the optimisation. This is shown in the following equations:

$$\begin{aligned} \ddot{\psi}_{Ack,err} &= \frac{d}{dt}\left(\frac{\delta v_x}{L(1 + K_h v_x^2)} - r\right) \\ &= \frac{\left(L(1 + K_h v_x^2)\right)\left(v_x \dot{\delta} + \delta \dot{v}_x\right) - \delta v_x (2LK_h v_x \dot{v}_x)}{\left(L(1 + K_h v_x^2)\right)^2} - \dot{r} \end{aligned} \tag{3.54}$$

With this equation 3.54 it is possible to predict the evolution of the target yaw rate error between the YR_{Ack} and actual yaw rate r. All the derivatives in the equation (derivative of steering angle, derivative of longitudinal velocity and derivative of actual yaw rate) are already being calculated inside the MPC so it is trivial to use those inside of this equation.

For the YR_{GY} error this becomes a bit more complex. First start by calculating the update equation like in the above equation:

$$\begin{aligned} \ddot{\psi}_{GY,err} &= \frac{d}{dt}\left(\frac{a_y}{v_x} - r\right) \\ &= \frac{d}{dt}\left(\frac{\dot{v}_y + r v_x}{v_x} - r\right) \\ &= \frac{d}{dt}\left(\frac{\dot{v}_y}{v_x}\right) \\ &= \frac{v_x \ddot{v}_y - v_y \dot{v}_x}{v_x^2} \end{aligned} \tag{3.55}$$

The difficulty in equation 3.55 arises in the $\ddot{v}_y$ term. This second derivative of lateral velocity needs to be calculated from the equation of the derivative of lateral velocity, $\dot{v}_y$. This equation is given in equation 3.2. The derivation of the calculation of $\ddot{v}_y$ is shown below:

$$\begin{aligned} \ddot{v}_y &= \frac{d}{dt}\left(\frac{F_{x,f}\sin\delta + F_{y,f}\cos\delta + F_{y,r}}{m} - v_x r\right) \\ &= \frac{\dot{F}_{x,f}\sin\delta + F_{x,f}\dot{\delta}\cos\delta + \dot{F}_{y,f}\cos\delta - F_{y,f}\dot{\delta}\sin\delta + \dot{F}_{y,r}}{m} - v_x \dot{r} - \dot{v}_x r \end{aligned} \tag{3.56}$$

From this equation 3.56 a new difficulty arises. While most of the derivatives used in the equation are already available, the derivatives of the tire forces are not. Hence a new set of equations is required which gives the change in tire forces. The derivation for each of the

different tire forces is given below:

$$\begin{aligned}\dot{F}_x, f &= \frac{d}{dt}\left(\frac{GearRatio\left((Trq_{full} - Trq_{drag})Thr + Trq_{drag}\right) - (T_{b,fl} + T_{b,fr})}{R_{eff,f}}\right) \\ &= \frac{GearRatio(Trq_{full} - Trq_{drag})\dot{Thr} - (\dot{T}_{b,fl} + \dot{T}_{b,fr})}{R_{eff,f}}\end{aligned} \tag{3.57}$$

$$\begin{aligned}\dot{F}_y, f &= \frac{d}{dt}\left(Ca_{fl}\left(\delta - \frac{v_y + f_f r}{v_x - \frac{t_f}{2}r}\right) + Ca_{fr}\left(\delta - \frac{v_y + l_f r}{v_x + \frac{t_f}{2}r}\right)\right) \\ &= (Ca_{fl} + Ca_{fr})\dot{\delta} - Ca_{fl}\frac{(v_x - \frac{t_f}{2}r)(\dot{v}_y + l_f\dot{r}) - (v_y + l_f r)(\dot{v}_x - \frac{t_f}{2}\dot{r})}{(v_x - \frac{t_f}{2}r)^2} \\ &- Ca_{fr}\frac{(v_x + \frac{t_f}{2}r)(\dot{v}_y + l_f\dot{r}) - (v_y + l_f r)(\dot{v}_x + \frac{t_f}{2}\dot{r})}{(v_x + \frac{t_f}{2}r)^2}\end{aligned} \tag{3.58}$$

$$\begin{aligned}\dot{F}_y, r &= \frac{d}{dt}\left(Ca_{rl}\left(-\frac{v_y - l_r r}{v_x - \frac{t_r}{2}r}\right) + Ca_{rr}\left(-\frac{v_y - l_r r}{v_x + \frac{t_r}{2}r}\right)\right) \\ &= -Ca_{rl}\frac{(v_x - \frac{t_r}{2}r)(\dot{v}_y - l_r\dot{r}) - (v_y - l_r r)(\dot{v}_x - \frac{t_r}{2}\dot{r})}{(v_x - \frac{t_r}{2}r)^2} \\ &- Ca_{rr}\frac{(v_x + \frac{t_r}{2}r)(\dot{v}_y + l_r\dot{r}) - (v_y + l_r r)(\dot{v}_x + \frac{t_r}{2}\dot{r})}{(v_x + \frac{t_r}{2}r)^2}\end{aligned} \tag{3.59}$$

Where for equations 3.58 and 3.59 it is still assumed that the cornering stiffness remains constant throughout the prediction horizon. By combining all these equations, it is now possible for the MPC to calculate the stability yaw rates in the optimisation process.

Lastly, the cost function weights need to be tuned with these two extra states. As previously mentioned, there are now three yaw rates which the controller needs to track. One yaw rate based on the path curvature which is used for path tracking, and the two new yaw rates which are used for vehicle stability. These two sets are in conflict with each other, as when following a path there will always be some delay between the steering input and the yaw rate changing, as well as having some sideslip rate $\dot{\beta}$ when the vehicle is not in steady state. However, the two stability yaw rates will try to minimise this sideslip rate and steering delay, thus requiring a trade-off between tracking and stability.

This problem is solved by having the weights on the two stability yaw rates change depending on the vehicle sideslip angle and sideslip rate. The weight on the two stability yaw rates is multiplied by a factor between 0 and 1, with the factor being determined by the current state of the vehicle. This is visualised in figure 3.9. When the vehicle is in the low β and $\dot{\beta}$ region, the multiplication factor is close to 0. This means the weight on the two stability yaw rates is much lower than the weight on the tracking yaw rate. This in turn will make the MPC controller prioritise path tracking over vehicle stability. When the vehicle is in a region of high β or $\dot{\beta}$ (or a combination of both), the multiplication factor is close to 1. This will increase the weight in the

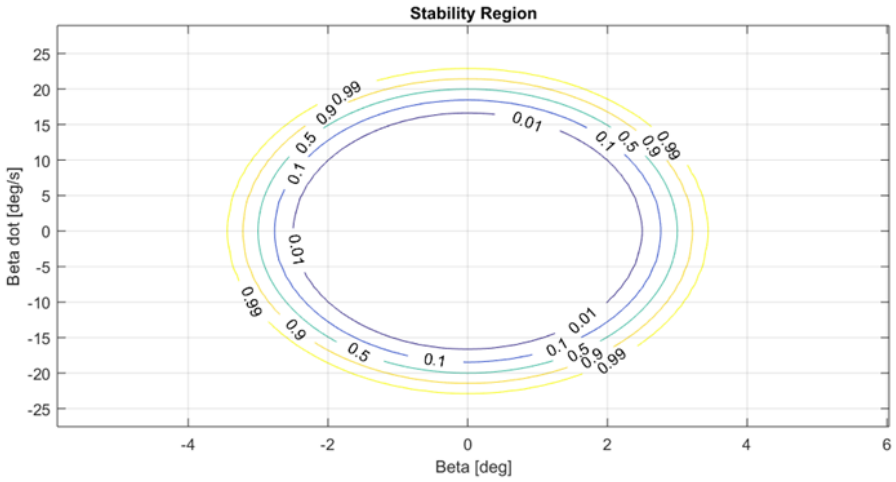

Figure 3.9: Weight Multiplication Factor depending on β and $\dot{\beta}$

two stability yaw rates in the cost function and thus make the MPC controller prioritise vehicle stability over path tracking.

The slope of the activation region as well as the values of β and $\dot{\beta}$ where the value would reach 1 needed to be tuned. The values where the multiplication factor becomes 1 was taken to be 5 degrees and 30 degrees/s. These are common values that are used to limit vehicle sideslip angle and sideslip rate. The slope was determined by iteratively checking controller performance with different values. When the slope was too low, the controller would prioritise stability too early. This lead to worse path tracking while the vehicle was still stable. When the slope was too high, the controller would prioritise stability too late. This caused the vehicle to spin in evasive manoeuvres, as the controller would only switch too prioritising stability when the vehicle was already close to the stability limit. By trial and error an intermediate value was found that gives good path following while still keeping the vehicle in the stable operating window.

3.8. Summary

In this chapter the design of all 9 different controllers that are used in this study have been shown. It started with the used vehicle and tire model, as well as the baseline constraints that are used inside the MPC formulation. Afterwards the separate VSC that is used in two controllers was explained. Highlighting the general working and used equations. Finally all the different controller variations were shown, explaining the differences between the controllers and giving a more detailed look into the specifics of each controller.

The used vehicle model as a planar model which is able to directly calculate tire forces for each wheel individually. The used control outputs are the steering wheel angle, brake torques for each wheel and throttle position. This means the vehicle is able to autonomously follow a predefined path. The tire model that is used is a Dugoff model, this Dugoff model is used to estimate the tire cornering stiffness for each iteration. The MPC is then able to use this estimated cornering stiffness in the calculation of the tire forces.

In order to keep the control inputs within reasonable bounds, some constraints have been imposed on the system. These constraints limit the vehicle's maximum speed, Throttle position and rate of change in throttle position, steering wheel angle and steering wheel rate and finally the brake torques and brake torque rates.

The separate VSC that is used in two controllers is a simplified model of a VSC that was built in-house at TME. This simplified model still captures the essence of the VSC that is necessary to stabilise the vehicle. It calculates two expected yaw rates based on the lateral acceleration and steering wheel angle, and compares those to the actual yaw rate of the vehicle. If the difference is outside the predefined bounds, the VSC will intervene using a PID control structure. The VSC will then output a braking torque to one side of the vehicle to stabilise it.

Lastly the 9 different controller configurations have been shown. The first 8 controllers can be divided into two groups of 4, where the MPC for the first group only calculates a single braking torque which is applied to all wheels, while for the second group the MPC is able to use differential braking. The first controller in these groups is a simple path follower without any further constraints. The second controller adds a target yaw rate based on the path curvature to the path following controller. The third controller has additional constraints in the MPC formulation to stabilise the vehicle. These constraints are a maximum error between the actual yaw rate of the vehicle and the expected yaw rates based on the lateral acceleration and steering wheel angle. The fourth controller in these two groups will stabilise the vehicle using a separate VSC. The MPC formulation in this controller is the same as in the first controller, but a separate VSC will stabilise the vehicle when necessary. Finally the last controller that was designed aims to incorporate the stability criteria that are used in the separate VSC into the MPC controller. This is done by adding two reference yaw rates. These reference yaw rates are the error between the actual yaw rate and the expected yaw rates based on the lateral acceleration and steering wheel angle. The value of this difference should be close to 0 for steady state cornering.

4

Simulation Environment

In this chapter an overview of the Simulink/CarMaker integration will be shown. It consists of an overview of the workflow, followed by a detailed explanation of the reference generator. Then the two manoeuvres that are used for evaluating the controllers will be shown, followed by the variations on these manoeuvres to evaluate the robustness. Then the KPIs that are used for an objective evaluation of the results will be given. Finally the process of tuning the weights of the MPC controllers will be shown.

4.1. Overview of Workflow

A general overview of the simulation workflow is shown in figure 4.1. The MPC outputs the controls, which are applied to the CarMaker vehicle model in Simulink. This model simulates the vehicle behaviour and calculates the state of the vehicle. These states are then used in the Reference Generator, Tuning of the MPC Weights and the OnlineData. The Reference Generator will be shown in depth in section 4.2. The OnlineData block calculates 7 vehicle parameters which are used inside of the MPC calculation. The first 4 of these values are the Cornering stiffnesses obtained from the Dugoff model, the other 3 values are used for the engine torque calculation. These values are the maximum and minimum torque at the current RPM as well as the current gear ratio.

This workflow between Simulink and CarMaker is similar to what is used in [28]. The main differences are that in this research not only the steering and brakes are controlled by the MPC, but also the throttle is now a controlled variable. This affects the outputs to the CarMaker environment as well as adding the torque and gear ratio values to the OnlineData block. Another difference is the way the reference path is being generated. In [28] the reference manoeuvre is based on a the distance and speed to an object in front of the vehicle, while in this study the reference generator uses a predefined manoeuvre that only requires the longitudinal position of the vehicle.

4.2. Reference Generator

The reference generator uses two consecutive sigmoid curves to create the Elk test manoeuvre and the Double Lane Change manoeuvre. The first sigmoid curve is used to create the change to the left lane, while the second sigmoid curve is used to create the curve from the left lane back to the original lane. The current global longitudinal position of the vehicle and its longitudinal velocity are used as inputs for the reference generator, while the output consists of the target lateral position, yaw angle, yaw rate and corresponding longitudinal position

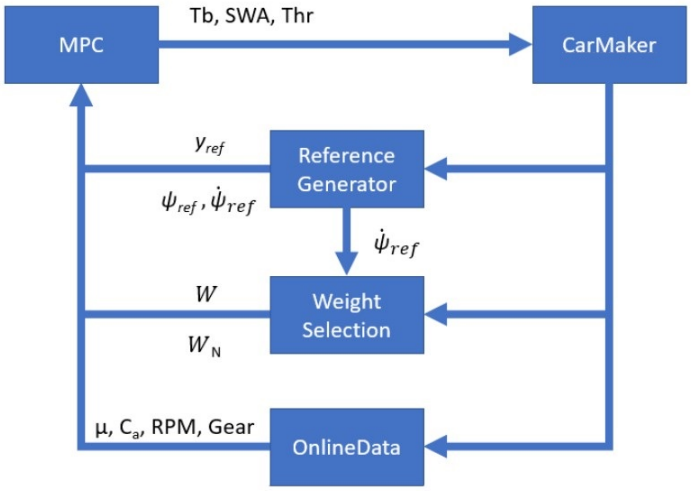

Figure 4.1: Overview of the Simulink Workflow

for the next 30 timesteps. The longitudinal position of these 30 timesteps are determined by taking the current global longitudinal velocity and calculating the vehicle position in those 30 timesteps assuming a constant velocity.

The equations that are used to calculate these target values are shown below, and are similar to what is used in [30]. These three equations (4.1 - 4.3) calculate the reference lateral position y_{ref}, reference yaw angle ψ_{ref} and reference yaw rate $\dot{\psi}_{ref}$. ψ_{ref} is based on the partial derivative of the lateral position with respect to the longitudinal position (equation 4.4), while the reference yaw rate is based on the path curvature (equation 4.5) and vehicle longitudinal speed. The sigmoid curve can be tuned by varying any of three parameters P_a, P_b and P_c. P_a changes the slope of the curve, P_b changes the amplitude of the curve and P_c changes the position of the center point of the curve. This effect of changing these parameters is shown in figure 4.2.

$$y_{ref}(x) = \frac{P_b}{1 + e^{-P_a(x-P_c)}} \tag{4.1}$$

$$\psi_{ref} = \tan^{-1}\left(\frac{\partial y_{ref}}{\partial x}\right) \tag{4.2}$$

$$\dot{\psi}_{ref} = \kappa v_x \tag{4.3}$$

$$\frac{\partial y_{ref}}{\partial x} = \frac{P_a P_b e^{-P_a(x-P_c)}}{\left(1 + e^{-P_a(x-P_c)}\right)^2} \tag{4.4}$$

$$\kappa = \frac{\left(\frac{\partial^2 y_{ref}}{\partial x^2}\right)}{\left(1 + \left(\frac{\partial y_{ref}}{\partial x}\right)^2\right)^{\frac{3}{2}}} \tag{4.5}$$

In the case of the Double Lane Change and Elk test, the amplitude was adjusted to match the predefined lane change width and the centre point was put in the centre longitudinal distance of the lane change. Finally, the slope was tuned such that the total length of the manoeuvre from the start to the end of the lane change were also the same as the predefined length. The dimensions of both the Elk test as well as the Double Lane Change are shown in more detail in section 4.3.

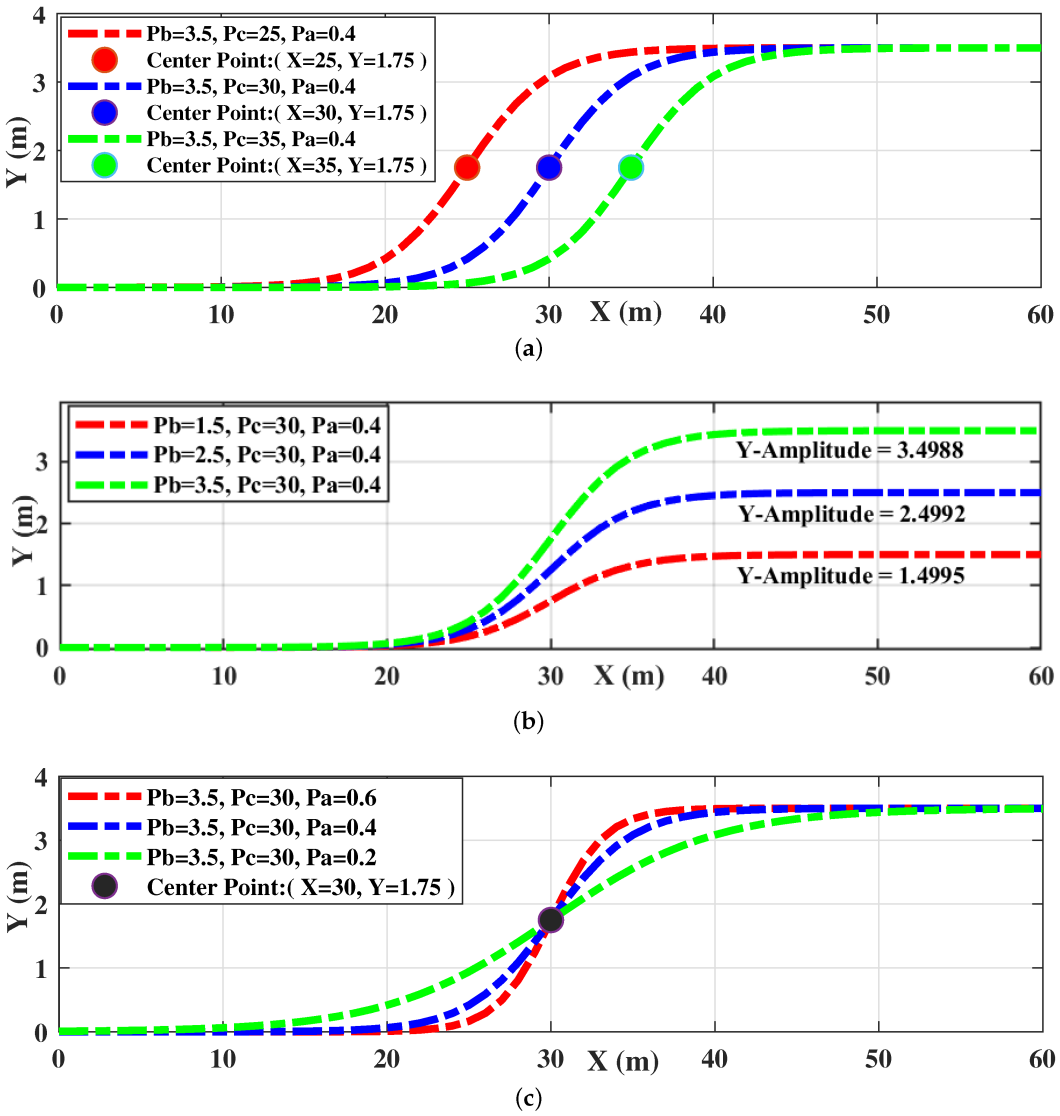

Figure 4.2: Sigmoid curve parameter variation [30]

4.3. Manoeuvres

This section will first cover the two different test manoeuvres that are used to evaluate the performance of the controllers, followed by some variations on these tests to assess the robustness. An overview of the test manoeuvres that have been used in literature is already given in section 2.3.1. These Elk test and Double Lane Change have been used in this research to evaluate the performance of the controllers.

The Elk test is shown in figure 2.4, it is a very aggressive manoeuvre used to test the vehicles capabilities to avoid an obstacle. It is defined in ISO: 3888-1. The vehicle should complete this manoeuvre at 72 km/h to pass the test. The Double Lane Change is defined in ISO 3888-2. It is similar to the Elk test, but it is a less aggressive manoeuvre. The vehicle should complete the manoeuvre at 80 km/h to pass the test. While the Double Lane Change is a less aggressive manoeuvre than the Elk test, it is useful to evaluate the robustness of the controllers in different conditions. As the Elk manoeuvre will already test the limit of the controllers in normal driving conditions. In the next section, the manoeuvre variations will be shown.

4.3.1. Manoeuvre Variations

In order to compare the performance of the controllers in different conditions, some variations have been applied to the manoeuvres. These variations include changes to the vehicle speed, road μ level (both overall and different levels in different lanes) as well as changes to the vehicle load. In this section, each of these variations will be shown.

Speed variation: The first variation is to complete the Double Lane Change manoeuvre at different speeds. For this variation it was chosen to select the predefined speed of the manoeuvre, 80 km/h as well as a speed slightly lower which would simulate a more natural driving condition and finally find the maximum speed for which the controller was still able to complete the manoeuvre without going out of the defined bounds. This is shown in table 4.1. The road μ for this variation was chosen to be 0.9, as this is close to a normal dry road condition.

Table 4.1: Speed variation

μ	Speed [km/h]
0.9	70
0.9	80
0.9	max

Road μ variation: The second variation is to have a lower road μ. This simulates a wet or snowy road and verifies the performance of the controllers in these non-ideal conditions. The high and medium road μ conditions was done at 80 km/h as this is the normal speed for which the Double Lane Change manoeuvre is taken. However, for the lowest road μ condition, the speed had to be lowered as upon inspection, no controller was able to complete the Double Lane Change at 80 km/h in this low μ condition. Therefore, the speed was reduced by 10 km/h such that the manoeuvre was able to be completed while staying within the predefined bounds. An overview of the conditions is shown in table 4.2.

Table 4.2: Road μ variation

μ	Speed [km/h]
0.3	70
0.6	80
0.9	80

Varying load: Another variation is the addition of extra mass to the vehicle. This is done in a similar way as in [28]. The added weight simulates occupants in the vehicle, and are added in sets of two at the locations shown in figure 4.3. For the first addition only the front two seats are occupied, while for the second weight addition all four occupants are in the car. This adds 150 kg and 300 kg respectively as each occupant adds 75 kg to the overall mass. The total vehicle mass therefore increases and the position of the occupants also moves the vehicle centre of gravity to a slightly different position, as well as giving it more inertia. The speed and road μ during these tests is taken to be the default values for the Double Lane Change, 80 km/h and 0.9 respectively. A complete overview of the variations is shown in table 4.3.

Road μ change: The fourth and final variation is to test a road μ change when the vehicle changes lanes. This is different from the μ level variation, as in this scenario the two lanes in the Double Lane Change manoeuvre now have different road μ values, instead of both lanes having the same, lowered value. This difference in road μ between the lanes is done to simulate a road in changing conditions. In this case one lane can still be wet or snowy while the other is already in a different condition and has a higher or lower grip level. The μ changes

Table 4.3: Weight variation

μ	Speed [km/h]	Weight [kg]
0.9	80	0 150 300

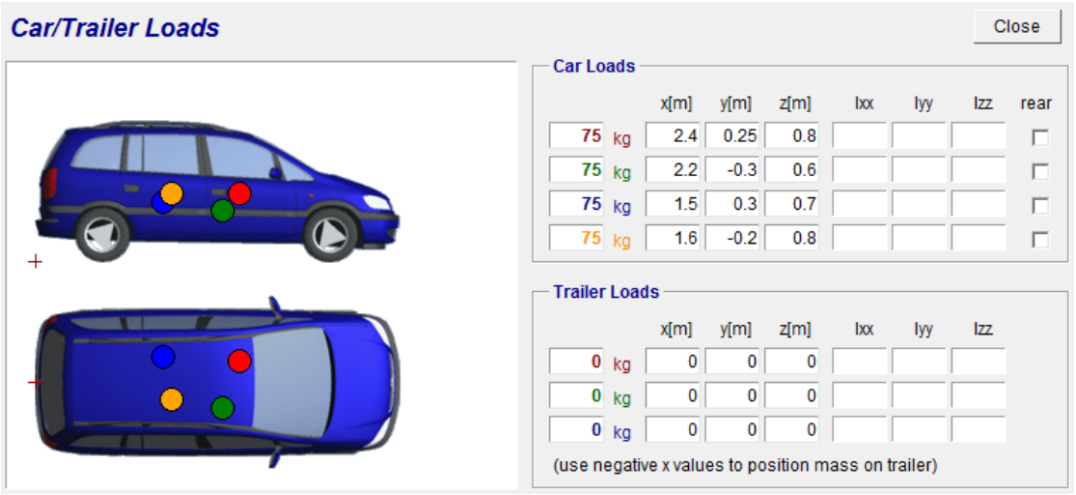

Figure 4.3: Passenger locations

that are being tested are 0.9 to 0.6, 0.6 to 0.3 and the other way around from low to high μ. The speed during the manoeuvre is taken to be 80 km/h for the change to and from 0.9 and 70 km/h for the change to and from 0.3. This is shown in table 4.4.

Table 4.4: Road μ change

μ	Speed [km/h]
0.9 → 0.6 0.6 → 0.9	80
0.6 → 0.3 0.3 → 0.6	70

4.4. KPIs

For proper evaluation of the performance of each controller, objective KPIs are needed. An overview of KPIs that are used in literature has been given in section 2.3.2. In this research, a selection of these KPIs are used. These KPIs evaluate the path following, vehicle stability, occupant comfort and controller computational time. The used KPIs are listed and explained below:

- NRMSE y, ψ and $\dot{\psi}$ [-]: Normalised Root Mean Square Error of the lateral position, yaw angle and yaw rate respectively. This shows the ability of the controller to follow the target reference lateral position, yaw angle and yaw rate. Better following will result in a lower value. The normalisation is done with respect to the maximum reference values.
- RMSE Ack_{err} [$\frac{rad}{s}$]: Root Mean Square Error between the expected $\dot{\psi}_{Ack}$ and the actual $\dot{\psi}$ of the vehicle. The equation for this error is given in section 3.7. A better match between the expected yaw rate and actual yaw rate will result in a lower value and

means the vehicle has better stability.

- RMSE GY_{err} [$\frac{rad}{s}$]: Root Mean Square Error of the difference between the expected $\dot{\psi}_{GY}$ and the actual $\dot{\psi}$ of the vehicle. The equation for this error is given in section 3.7. A better match between the expected yaw rate and actual yaw rate will result in a lower value and means the vehicle has better stability.
- Avg abs a_y [$\frac{m}{s^2}$]: The average of the absolute lateral acceleration. This gives an indication of the comfort during the manoeuvre. A lower value means lower average accelerations and better comfort.
- Avg abs jerk [$\frac{m}{s^3}$]: Similar to avg abs a_y but for jerk, the change in acceleration [$\frac{m}{s^3}$]. A lower value means better comfort for the occupants.
- ΔV_{end} [$\frac{m}{s}$]: The change between entry and exit velocity for the manoeuvre. A value of 0 means the vehicle has the same velocity at the end of the manoeuvre as at the start. A negative value means a loss in velocity and consequently more braking action was required to keep the vehicle to follow the path.
- MPC computational time [s]: The time it takes for the MPC to calculate the control output. This is dependent on the computer setup as well as the complexity of the MPC itself. A faster processor will be able to calculate the output faster, but a more complex model will take longer to compute. In this research all simulations were done on the same computer, hence the changes in computational time are purely due to differences between the MPC complexity.

4.5. Tuning of MPC controllers

The tuning of the MPC controllers is a time-consuming task. In order to find the best weights for the cost function, the following process is used: select the weights for the cost function, run the simulation, process KPIs from data, compare with the previous result and then try new weights. This iterative process is time-consuming as there is no ready-made guide available to find the optimum weights. Only a sensitivity analysis can be performed, which will give an indication of the influence of the parameters on the vehicle behaviour. If for example the data shows that the vehicle uses too much of a certain control input, a higher cost for that input could be set. However, there is no rule on how much higher the weight should then be set. Another additional difficulty is that each weight can also influence other weights indirectly. If for example the weight on the steering wheel input is increased, this will most likely also cause a decrease in tracking performance, as the controller will use lower steering inputs. Therefore, it is difficult to find the globally best set of weights. This is especially true when tuning the vehicle to perform in different scenarios. High control actions in a manoeuvre where a lot of grip is available may lead to great tracking and still have good stability. However, if those same weights are used in a lower grip scenario, the high control actions might cause instability.

After running an initial baseline test, the weights were changed systematically to optimise the path tracking and stability. This was done by looking at the KPIs, Position plot and Constraint plot. Where the main focus for the Position plot was such that the vehicle would complete the manoeuvre. This plot is shown in figure 4.4.

The red line indicates the reference path, the blue line the actual path of the vehicle, the orange squares the traffic cones marking the corridor width and the blue boxes are projections of the vehicle during the manoeuvre. This plot shows whether the vehicle passes the test and shows how close the vehicle is to the reference path. It was found that the initial lane width was very

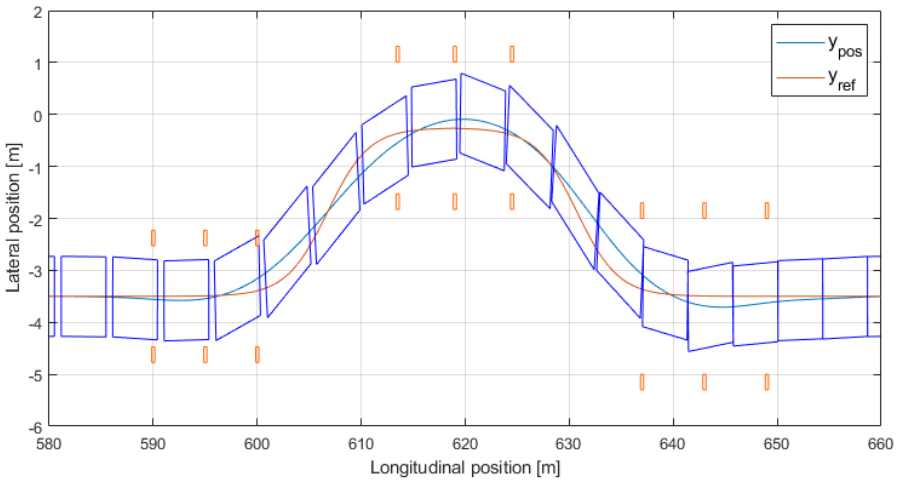

Figure 4.4: Position plot of the Elk manoeuvre

tight, and it was not possible to find a set of weights that would stop the vehicle from hitting the left cone at 600m. Therefore, only the 2nd and 3rd lanes were used in order to decide if the vehicle passed the test or not.

The main KPIs that were evaluated during the tuning were the Tracking KPIs consisting of the $NRMSE_\psi$ and $NRMSE_y$, and the Stability KPIs consisting of the $RMSE_{Ack}$ and $RMSE_{GY}$. Other KPIs like comfort were used only as an indication, as the manoeuvre is an evasive manoeuvre at the limit of handling. This means comfort for the occupants is less important than the safety ensured by the path following and vehicle stability.

The tuning of the MPC weights was done as follows: First a baseline run and an evaluation of the performance using the KPIs was done. Then one of the weights was changed in order to find an improvement in the performance. With the new weights a new simulation was done, the results were compared with the previous run. If the new weights resulted in an improved performance, these new weights were kept, if there was no improvement, the weights would be reverted to the previous version and another weight was changed. This was done until no significant improvement in the performance could be seen.

In figure 4.5 the progression of the KPIs for each iteration during the tuning of a controller is shown. Note that only the runs which resulted in a performance increase were kept. In the first iteration after the baseline run, the weights on ψ and y were increased, the tracking improved by around 15%, whereas the stability increased by about 10%. Overall this resulted in a net positive improvement of the controller. In the second iteration with better overall performance, the weight on brake control input was lowered. The stability improved, while the tracking reduced slightly. However, both are still lower than in the original baseline run. Finally, a small improvement in both tracking and stability can be seen in the final iteration, which was achieved by increasing the weight on the ψ further. After this iteration, no other change resulted in an overall improvement of the KPIs.

This method was used for the baseline SB-PT and DB-PT MPC controllers and controllers with added yaw rate reference SB-PTY and DB-PTY. The other controllers with stability constraints and added VSC used the same standard MPC controller and therefore the weights were kept the same as for the SB-PT and DB-PT controllers.

It is clear that this method to optimise the controllers consists of many iterations and trial and

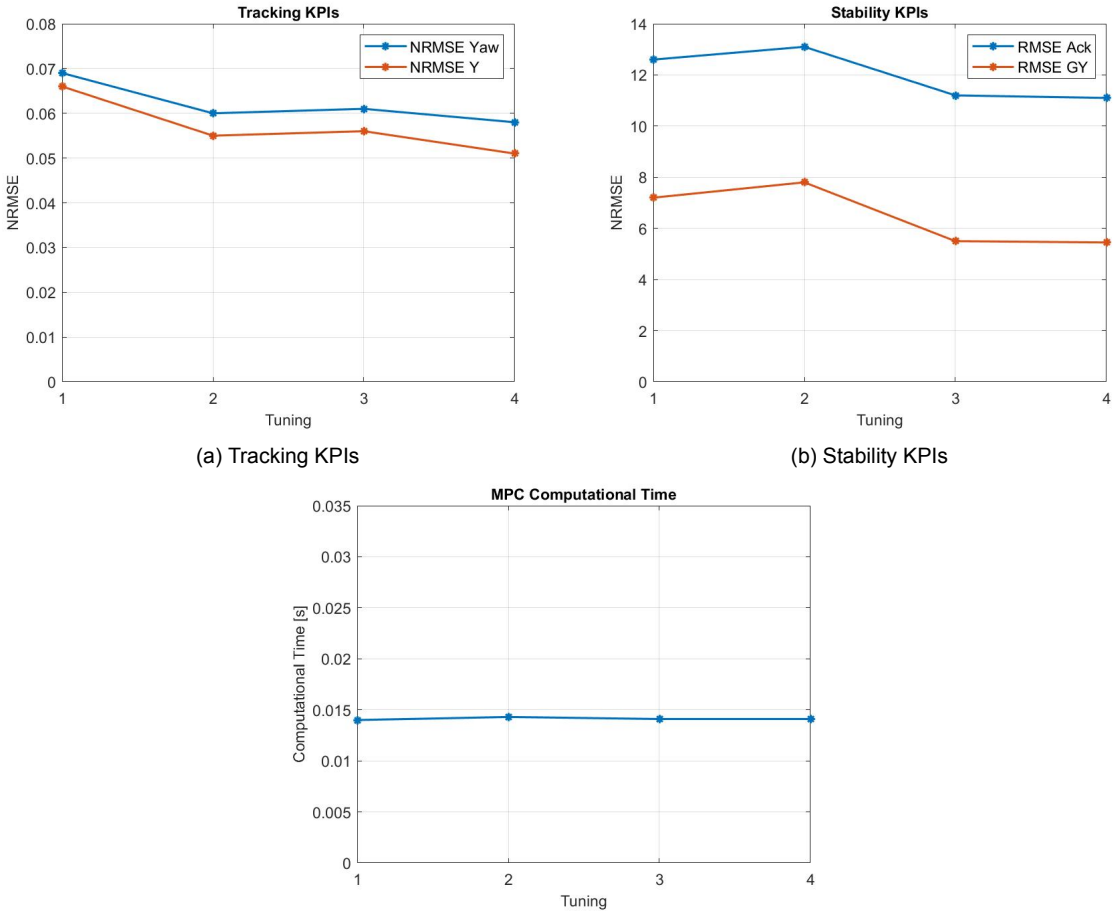

(a) Tracking KPIs

(b) Stability KPIs

(c) MPC computational time

Figure 4.5: Change in KPIs during MPC Tuning

error. There is no quick way to find the best possible set of weights for tracking or stability. There is also no way of knowing if the weights that are found after these iterations is also the global optimum. There could be an even better, completely different set of weights. An optimisation algorithm could be used as an improvement to find a set of weights that is potentially closer to the global optimum.

4.6. Summary

In this research the vehicle is simulated using the CarMaker + Simulink integration. The MPC controller outputs the throttle, brakes and steering input which are send to the CarMaker simulation. The new vehicle state which is calculated by the CarMaker simulation is then used for the Reference Generator, Weight Selection and calculation of OnlineData parameters. The output of these blocks is then used in the MPC for the calculation of new control inputs.

The Double Lane Change and Elk test are used for the evaluation of the controllers. These manoeuvres test the controller limits and can also be used for testing the robustness of the controllers. The robustness is tested by adding variations to the Double Lane Change manoeuvre. The longitudinal speed during the manoeuvre is changed to find the maximum speed for which the controllers can complete the manoeuvre. The overall road μ is changed to evaluate the performance in low grip conditions. Load is added to the vehicle to see how the MPC handles the addition of weight that is not present in the model of the MPC. Finally a different road μ is

implemented between the two different lanes to test how the controller behaves in changing conditions.

Some KPIs are used to get an objective metric in the evaluation of the controllers. These KPIs give a measure of how well the vehicle tracks the reference path, how well the controller is able to stabilise the vehicle and give an indication of the ride comfort for the occupants.

The tuning of the MPC controllers is a time-consuming process. The ideal weights for the cost function are obtained in an iterative process where one weight is changed at a time to see the effect on the performance. If the change had an overall positive impact on the KPIs, the weight change was kept. If there was no positive effect, the weight would be reverted to the previous value. Once no more improvement was found, the tuning was done. This is a very time consuming process as for each iteration the weights had to be selected and the simulation had to be run. This was then done for all 9 controllers.

5

Results

In this chapter the results of the different simulations will be shown. The analysis starts with the Elk test and DLC in standard conditions. The baseline speed for each manoeuvre will be used as well as the maximum speed for which each controller was able to complete the manoeuvre. Then the results for the speed variation will be shown, followed by the simulations where weight was added to the vehicle. Lastly the two scenarios where the road μ was lowered will be shown. Starting with the overall lowering of the μ level across the whole road surface area, followed by the μ change where one lane has a different μ level compared to the other lane.

Each section will be split into two parts, to keep the figures clear. In the first part the 8 baseline controllers will be compared to each other. In the second part the results of the proposed controller will be shown.

5.1. Elk Test

The Elk test was first run at 72 km/h, as this is the minimum speed for a vehicle to pass the test. Afterwards the manoeuvre was done at the maximum speed for which the vehicle would pass the test.

5.1.1. Baseline controllers

The KPIs for the 72 km/h run as well as the maximum speed for which each controller was able to pass the test are shown in table 5.1. In each column the best value is highlighted. It can be seen that the lowest tracking error is achieved by the DB-PTY controller, while the lowest stability KPIs are achieved by the DB-PTS and SB-PTC controller. The maximum speed for which the vehicle is able to pass the test is higher for the controllers which utilise differential braking than for the respective controllers that do not have this ability.

Table 5.1: KPIs for each controller in the Elk test at 72 km/h

	V_{max}	$NRMSE_Y$	$NRMSE_\psi$	$NRMSE_{\dot{\psi}}$	$RMSE_{Ack}$	$RMSE_{GY}$	Avg abs ay	Avg abs jerk	ΔV_{end}	MPC Time
SB-PT	75	0.0654	0.0669	0.1344	10.7307	6.1497	4.0778	11.4464	-9.5589	0.0027
SB-PTY	78	0.0513	0.0559	0.1186	12.5022	7.7037	3.9739	11.5790	-9.3270	0.0028
SB-PTC	74	0.0650	0.0688	0.1351	9.9781	5.3882	4.2469	11.7175	-10.3301	0.0084
SB-PTS	77	0.0529	0.0653	0.1298	9.5852	5.5835	3.8069	10.6862	-13.1965	0.0026
DB-PT	76	0.0589	0.0619	0.1268	11.7239	7.0851	3.9878	11.5234	-9.7455	0.0163
DB-PTY	78	0.0489	0.0564	0.1181	12.8846	8.1285	3.9442	11.5697	-9.6514	0.0163
DB-PTC	77	0.0568	0.0625	0.1274	10.8521	5.9614	4.0877	11.4841	-10.0188	0.0168
DB-PTS	78	0.0466	0.0628	0.1251	9.4946	5.6050	3.7595	10.6645	-13.3168	0.0160

The position plot of each controller is shown in figure 5.1. The SB-PTC controller has the high-

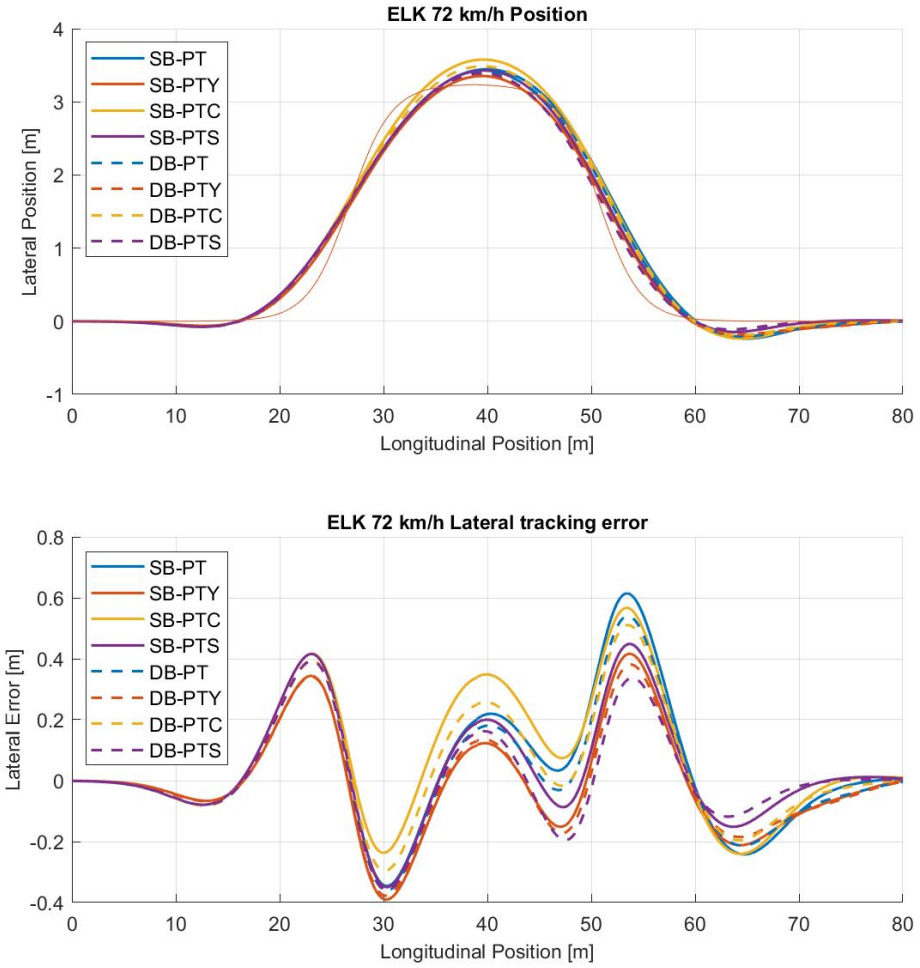

Figure 5.1: Position (top) and Lateral error (bottom) for the Elk test at 72 km/h

est overshoot when moving to the other lane. It can also be seen that the SB-PTY controller has to lowest overshoot when moving to the other lane, while the DB-PTS controller has to lowest overshoot when moving back towards the original lane. In general the controllers with differential braking have a lower overshoot and can make a tighter turn. This is due to the braking action which creates an additional yaw moment which helps to rotate the vehicle. The added brake action can be seen in figure 5.4 at 610m for the right side and 630m for the left side. The yaw rate can bee seen in figure 5.2. At the peak yaw rates at the 610m and 635m points, there is indeed a higher yaw rate for the controllers with differential braking. From this Yaw Rate plot it can also be seen that the two controllers with an additional reference yaw rate (SB-PTY and DB-PTY) have the highest peak yaw rates. The extra reference helps in the tracking during quick manoeuvres as the controller can rotate the vehicle more quickly. This can be seen in the tracking error plot of figure 5.1 where these two controllers are closest to the reference path during the turn between 610m and 640m.

The main KPIs, which are the two tracking KPIs and stability KPIs, have also been plotted in figure 5.3. The KPIs are visualised in a 2D plot to make the differences between the 8 controllers more clear. The dashed grey lines are circles centered around the origin, such that

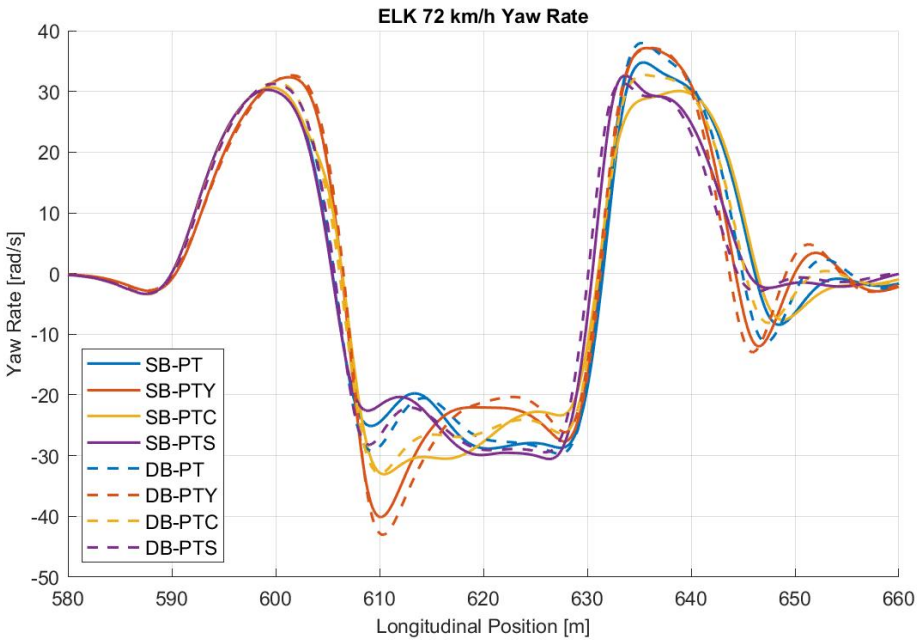

Figure 5.2: Yaw Rates for the Elk test at 72 km/h

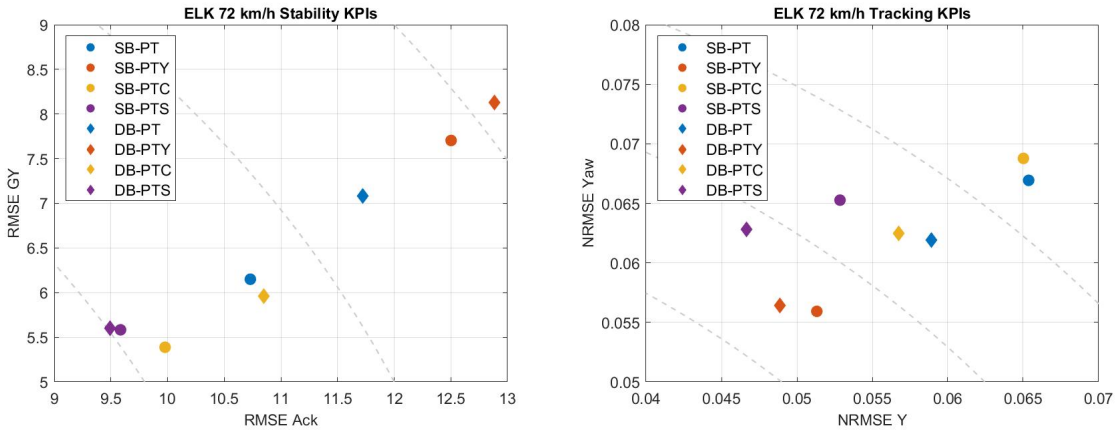

(a) Stability KPIs

(b) Tracking KPIs

Figure 5.3: Plots of the main KPIs for the Elk test at 72 km/h

the dot closest to the most inside dashed line can be seen as the best performing controller. For the stability KPIs it can indeed be seen that the DB-PTS and SB-PTS have the best performance followed by the SB-PTC controller. For tracking performance, the best performing controllers are the DB-PTY and SB-PTY controller followed by the DB-PTS controller. These plots also confirm that adding differential braking helps with tracking performance at the cost of worse stability.

The brake torques during the manoeuvre are shown in figure 5.4. The controllers with the separate VSC (SB-PTS and DB-PTS) use a lot more braking torque, which is where the VSC applies a corrective brake torque. This effect can also be seen in the KPI table 5.1 as these two controllers have the biggest speed loss at the end of the manoeuvre, indicating that a higher brake control action is used. The lower speed also helps in the tracking, as with a lower speed the vehicle has more time to complete the manoeuvre.

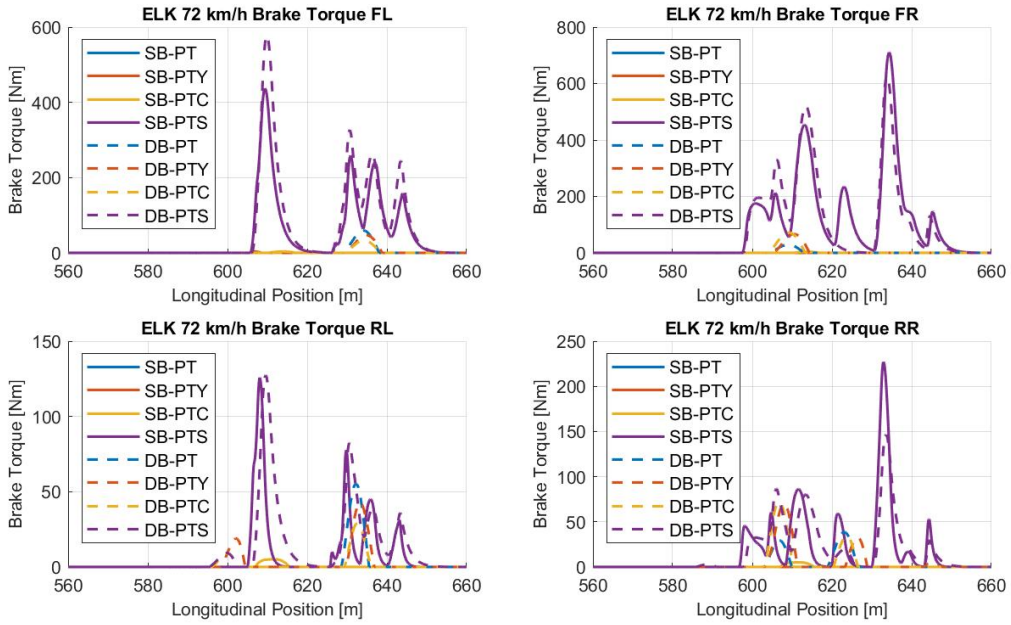

Figure 5.4: Braking Torques for the Elk test at 72 km/h

5.1.2. Proposed controller

The KPIs for the proposed controller, as well as the DB-PTY and DB-PTS controller are shown in table 5.2. From this table it can be seen that The stability of the proposed controller is indeed better than for the DB-PTY controller with also a slight improvement in tracking. This can also be seen by looking at the KPI plots in figure 5.6. It can indeed be seen that the proposed controller has the best tracking while the DB-PTS still has the best stability.

Table 5.2: KPIs for the proposed controller in the Elk test at 72 km/h

	V_{max}	$NRMSE_Y$	$NRMSE_\psi$	$NRMSE_{\dot{\psi}}$	$RMSE_{Ack}$	$RMSE_{GY}$	Avg abs ay	Avg abs jerk	ΔV_{end}	MPC Time
DB-PTY	78	0.0489	0.0564	0.1181	12.8846	8.1285	3.9442	11.5697	-9.6514	0.0163
DB-PTS	78	0.0466	0.0628	0.1251	9.4946	5.6050	3.7595	10.6645	-13.3168	0.0160
Proposed	79	0.0510	0.0532	0.1117	12.2207	7.8533	3.8023	11.2329	-11.1281	0.0166

However, looking at the position plot and the lateral tracking error during the manoeuvre in figure 5.5. It can be seen that the proposed controller has a lower overshoot when changing to the second lane, while having the largest overshoot when returning to the original lane. The DB-PTS controller has the opposite where it has the lowest overshoot in the return lane, while it has the biggest overshoot when changing to the second lane. Overshooting on the lane change could be considered a bigger problem, as this has the risk of overshooting into the oncoming lane.

When performing the Elk test at the maximum speed for each controller, the relative performance between the controllers changes. Figure 5.7 shows the main KPIs for the controllers at the maximum speed for which each controller can complete the manoeuvre. The proposed controller has the best tracking as well as stability, even though the speed for which it could complete the manoeuvre was 1 km/h faster than for the other two controllers. The DB-PTS controller now has the 2nd best stability and the worst tracking, while the DB-PTY controller has the worst stability and 2nd best tracking. The performance improvement for the stability KPIs of the proposed controller over the DB-PTS controller is 11%. While the improvement for the tracking KPIs over the DB-PTY controller is 8 % in the maximum speed scenario.

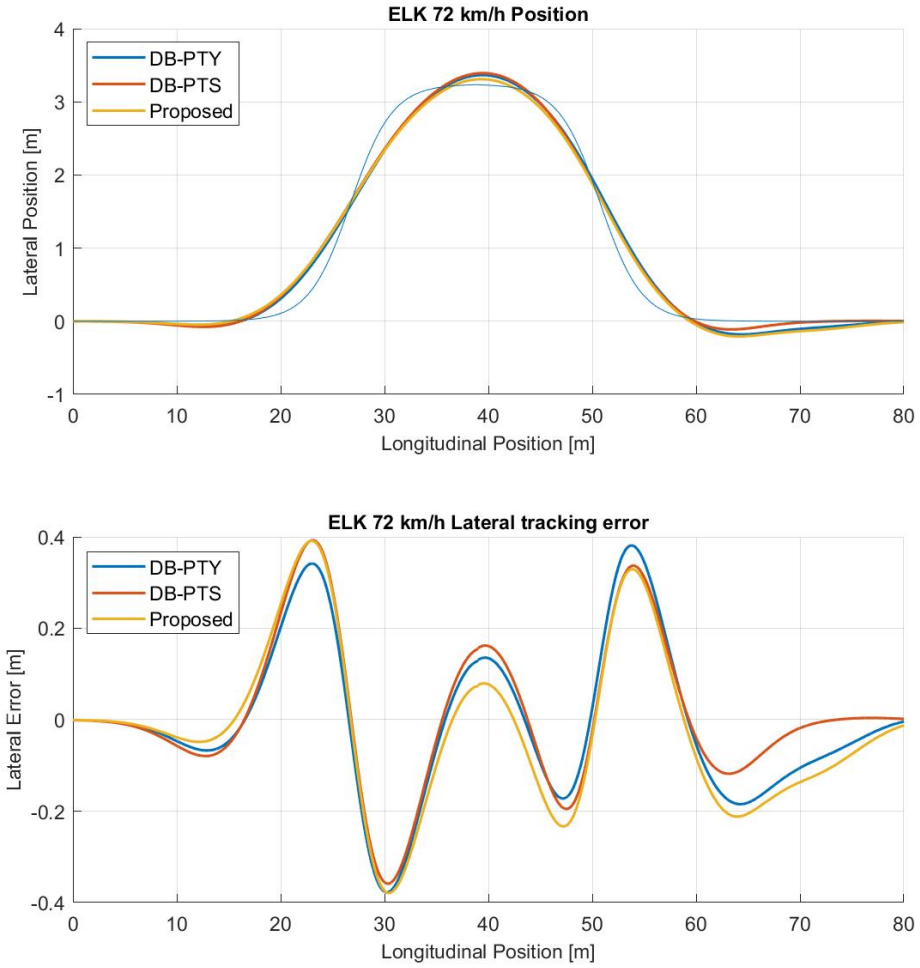

Figure 5.5: Position plot for the proposed controller in the Elk test at 72 km/h

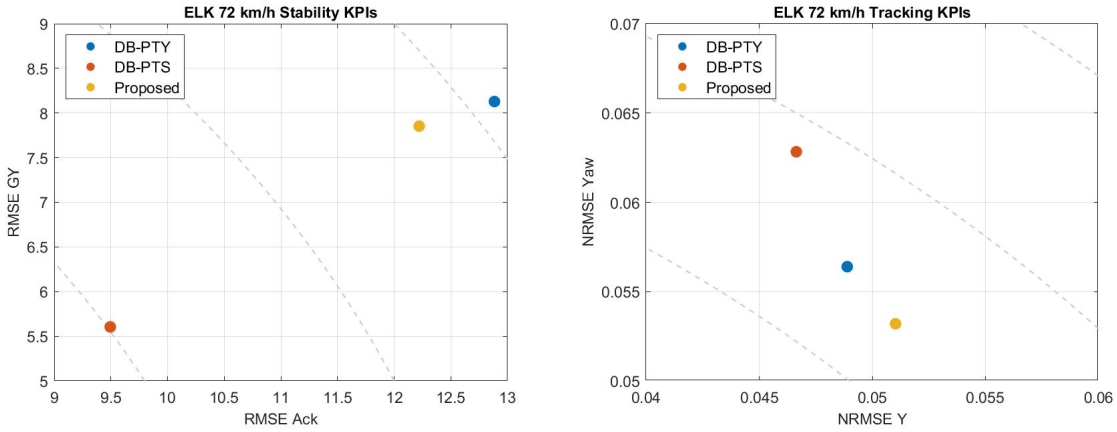

(a) Stability KPIs

(b) Tracking KPIs

Figure 5.6: Plots of the main KPIs for the Elk test at 72 km/h

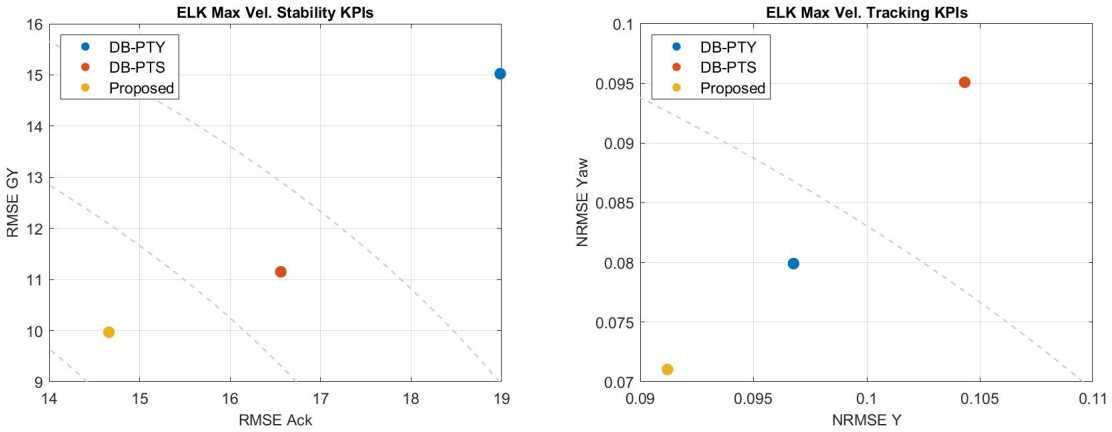

(a) Stability KPIs (b) Tracking KPIs

Figure 5.7: Plots of the main KPIs for the Elk test at max km/h

The stability can also be compared by looking at the β,$\dot{\beta}$ plot, as shown in figure 5.8. This figure shows a 2D plot of the sideslip angle and sideslip rate of the vehicle during the manoeuvre. There is a clear difference between the proposed controller and the other two controllers. The proposed controller has significantly lower β and $\dot{\beta}$ values, with maximum β of 6 deg and maximum $\dot{\beta}$ of 30 deg/s. These values also coincide with the activation of the stability yaw rates in the proposed controller. Combining this information with the KPI plots at the maximum speed, shows that the proposed controller can switch between prioritising tracking and stability depending on the state of the vehicle.

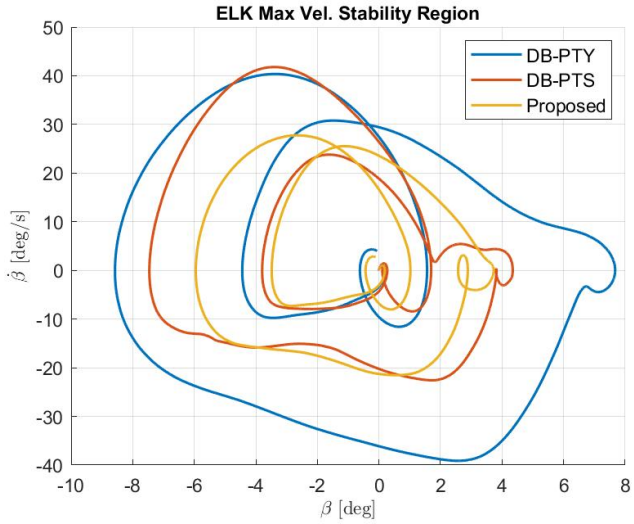

Figure 5.8: β $\dot{\beta}$ for the proposed controller in the Elk test at max km/h

Comparing the vehicle position and lateral error at the maximum speeds in figure 5.9 shows that the proposed controller has the lowest overshoot in the lane change as well as in the return to the original lane. The reason the proposed controller could not reach a higher speed was because it would hit the left hand side cone on the exit lane. The DB-PTS controller has the highest overshoot in both the lane change as well as the return to the original lane. This high return overshoot is also the reason why the speed couldn't be increased further, as the vehicle would overshoot the lane too much. Finally the DB-PTY controller follows a

similar path to the proposed controller, but it would become unstable at higher speeds. Here the benefit of the proposed controller becomes clear, as this controller was able to stabilise the vehicle at even higher speeds. At these high speeds the vehicle would cut across the previously mentioned left hand side cones when returning to the original lane. However, the controller was still able to keep the vehicle stable during the manoeuvre. For the other two controllers, the higher speed resulted in a spin as the controller was not able to stabilise the vehicle in such an aggressive manoeuvre.

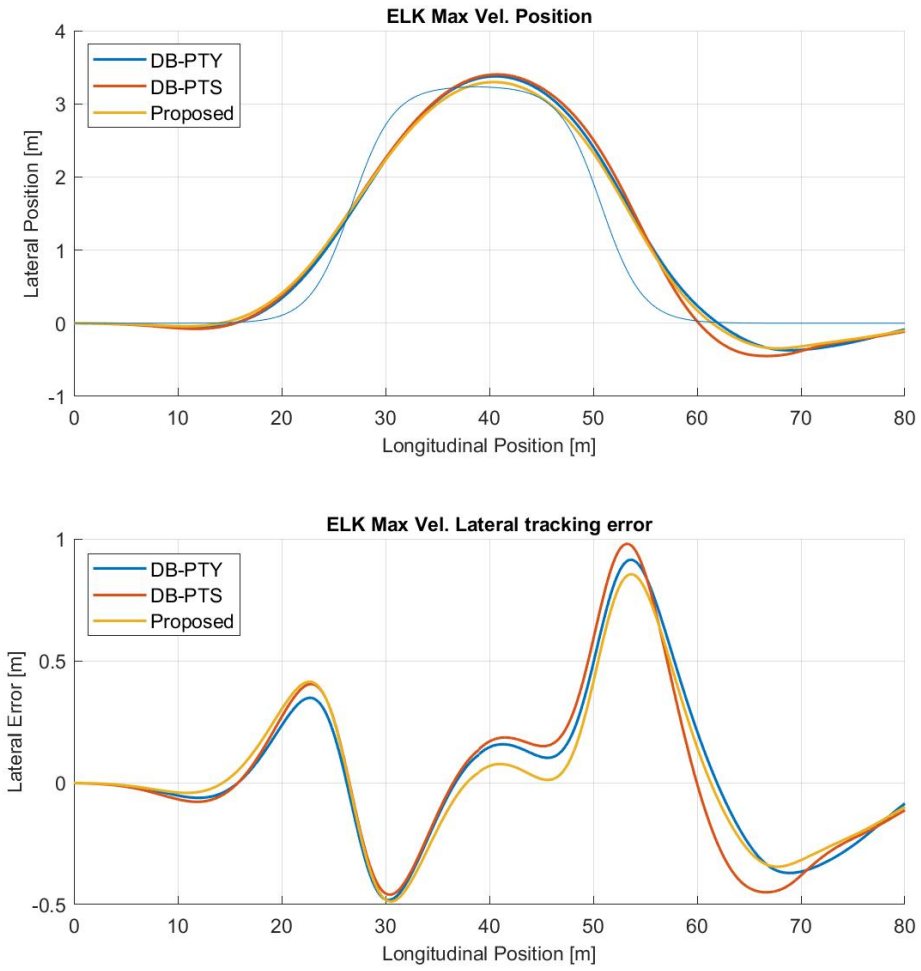

Figure 5.9: Position plot for the proposed controller in the Elk test at max km/h

5.2. Double Lane Change

The DLC test was first performed at 80 km/h, as this is the minimum speed required for a vehicle to pass the test. Afterwards the speed was increased to find the maximum speed for which the vehicle would pass the test, similar to the method used in the Elk test manoeuvre of the previous section.

5.2.1. Baseline controllers

In Table 5.3 the KPIs for the 80 km/h run are shown, as well as the maximum speed for which each controller was able to pass the test. In each column the best value is highlighted for

clarity.

Table 5.3: KPIs for baseline controllers in the DLC test at 80 km/h

	V_{max}	$NRMSE_Y$	$NRMSE_\psi$	$NRMSE_{\dot{\psi}}$	$RMSE_{Ack}$	$RMSE_{GY}$	Avg abs ay	Avg abs jerk	ΔV_{end}	MPC Time
SB-PT	110	0.0313	0.0510	0.1114	6.2687	3.5841	2.6173	8.3163	-8.9360	0.0026
SB-PTY	110	0.0284	0.0431	0.0877	7.0449	4.3816	2.5952	8.5179	-9.1501	0.0027
SB-PTC	94	0.0313	0.0510	0.1114	6.2697	3.5857	2.6175	8.3179	-89514	0.0048
SB-PTS	110	0.0302	0.0497	0.1096	6.1505	3.3468	2.5399	8.1019	-11.5223	0.0026
DB-PT	112	0.0299	0.0482	0.1038	6.5079	3.8310	2.6126	-9.1669	-9.7455	0.0158
DB-PTY	111	0.0280	0.0415	0.0826	7.2632	4.6018	2.5802	8.5371	-9.3203	0.0161
DB-PTC	99	0.0299	0.0482	0.1038	6.5079	3.8310	2.6126	8.3973	-9.1669	0.0161
DB-PTS	110	0.0285	0.0461	0.0998	6.4896	3.6703	2.5474	8.2191	-12.1508	0.0158

At this relatively low speed, there are only small differences between the controllers as the vehicle is able to complete the manoeuvre easily. The best performing controller for tracking at this speed is the DB-PTY controller. For stability the SB-PTS controller has the best performance.

Looking at the KPI plots in figure 5.10 shows that there is even some overlap between the SB-PT and SB-PTC controllers as well as the DB-PT and DB-PTC controllers. This is because the imposed stability constraints on the SB-PTC and DB-PTC controllers are not reached and thus their performance is the same as the original SB-PT and DB-PT controllers.

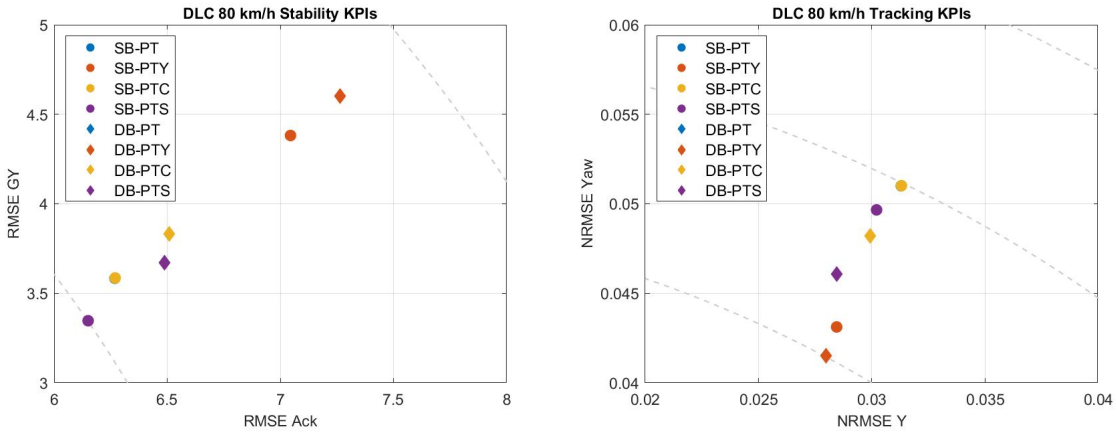

(a) Stability KPIs (b) Tracking KPIs

Figure 5.10: Plots of the main KPIs for the DLC at 80 km/h

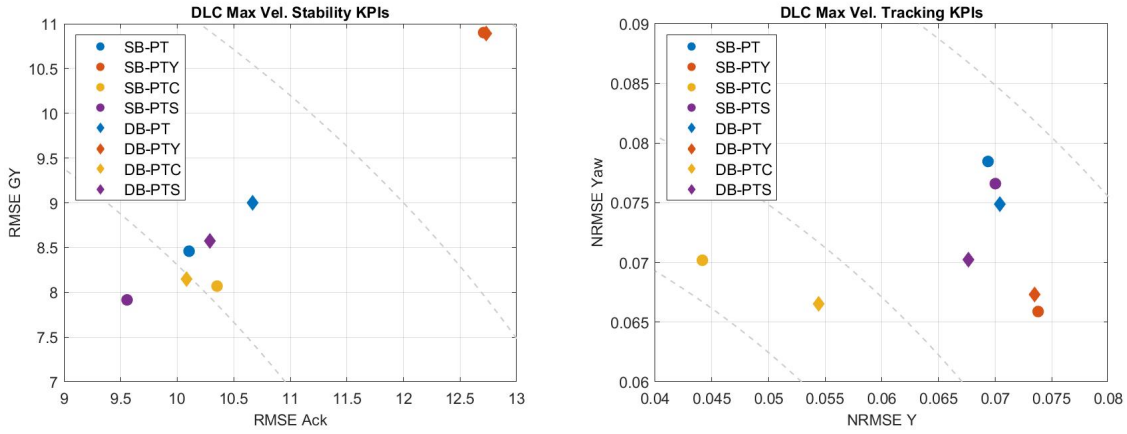

(a) Stability KPIs (b) Tracking KPIs

Figure 5.11: Plots of the primary KPIs

When plotting the results for the maximum km/h test it should be noted that the different controllers have different maximum speeds. The highest maximum speed was attained by the SB-PTS controller at 112 km/h with most other controllers reaching 111 or 110 km/h. Only the SB-PTC and DB-PTC controllers ad a significantly lower maximum speed at 94 km/h and 99 km/h respectively.

Looking at the position plot for the baseline controllers at their maximum speed in figure 5.12, indeed an instability in the SB-PTC controller can clearly be seen between 620 and 660m where the vehicle doesn't follow a smooth curve like the other controllers, but instead shows an oscillation when moving to the second lane. A similar path can be seen on the DB-PTC controller as well. This can be explained by the vehicle exceeding the constraint due to a model mismatch. The controller will then attempt to keep the vehicle within the bounds, thereby over correcting.

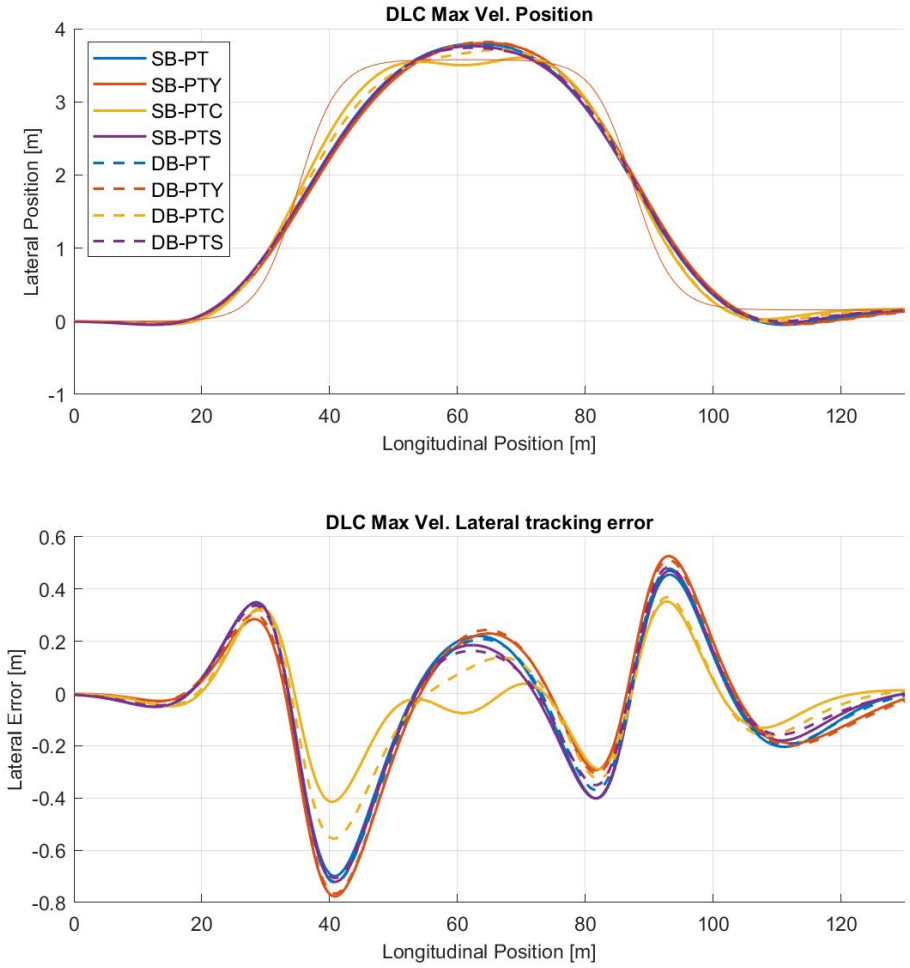

Figure 5.12: Position plot for the baseline controllers in the DLC test at max km/h

When analysing the results from the two Stability and Tracking KPIs in figure 5.11 it should again be noted that most vehicles have a different speed. Therefore, the difference in KPIs is not only due to the difference in controllers, but also partly due to a small difference in speed. Some controllers have the same maximum speed of 110 km/h. These can be com-

pared directly with each other. These controllers are the SB-PT SB-PTY DB-PT and DB-PTS controller. Comparing the SB-PT and DB-PTY controller it can be seen that adding the reference yaw rate results in better tracking of path, but worse stability. Comparing the SB-PT and DB-PT controller a similar trade-off can be seen for adding differential braking. Finally comparing the DB-PT and DB-PTS controller it can be seen that the VSC improves both tracking as well as stability.

5.2.2. Proposed controller

At 80km/h, the proposed controller adds stability to the vehicle at the cost of some tracking performance, as seen in table 5.4 and figure 5.13. However, at this speed the differences between the controllers are low, similar to the previous comparison between the baseline controllers. Especially the tracking performance is very similar. This can also be seen in the position plot in figure 5.14. The biggest difference can be seen between the proposed controller and the other two in the lane change to the other lane, where the proposed controller has a more smooth path, resulting in the better stability and comfort at the cost of some tracking.

Table 5.4: KPIs for proposed controller in the DLC test at 80 km/h

	V_{max}	$NRMSE_Y$	$NRMSE_\psi$	$NRMSE_{\dot{\psi}}$	$RMSE_{Ack}$	$RMSE_{GY}$	Avg abs ay	Avg abs jerk	ΔV_{end}	MPC Time
DB-PTY	111	0.0280	0.0415	0.0826	7.2632	4.6018	2.5802	8.5371	-9.3203	0.0161
DB-PTS	110	0.0285	0.0461	0.0998	6.4896	3.6703	2.5474	8.2191	-12.1508	0.0158
Proposed	113	0.0325	0.0449	0.0947	5.8221	3.1889	2.4413	7.7026	-10.3227	0.0163

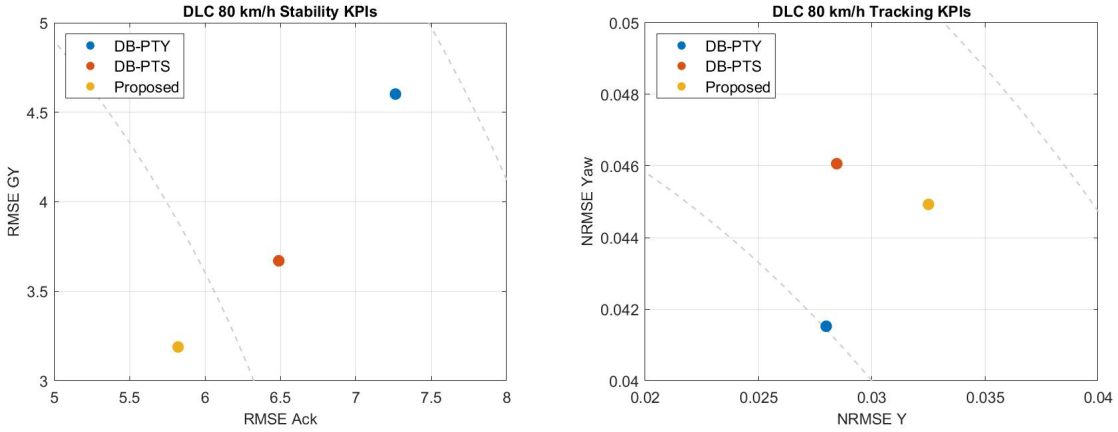

(a) Stability KPIs

(b) Tracking KPIs

Figure 5.13: Plots of the primary KPIs

5.3. Speed Variation

After simulating the DLC at the minimum and maximum speed, a simulation at an intermediate speed was done. This intermediate speed was chosen to be 99 km/h as this was the highest speed for which all but one of the controllers were able to complete the manoeuvre. It is also closer to the maximum speeds of most vehicles, such that differences at the limit of handling can be more clearly seen.

5.3.1. Baseline controllers

In figure 5.15 the KPIs for the baseline controllers at different speeds is shown. Most controllers have a steady increase in KPI when longitudinal speed gets increased. The two controllers which stand out the most are the SB-PTC and DB-PTC controllers. These controllers have the lowest maximum speed and also the steepest increase in KPIs. Furthermore it can be

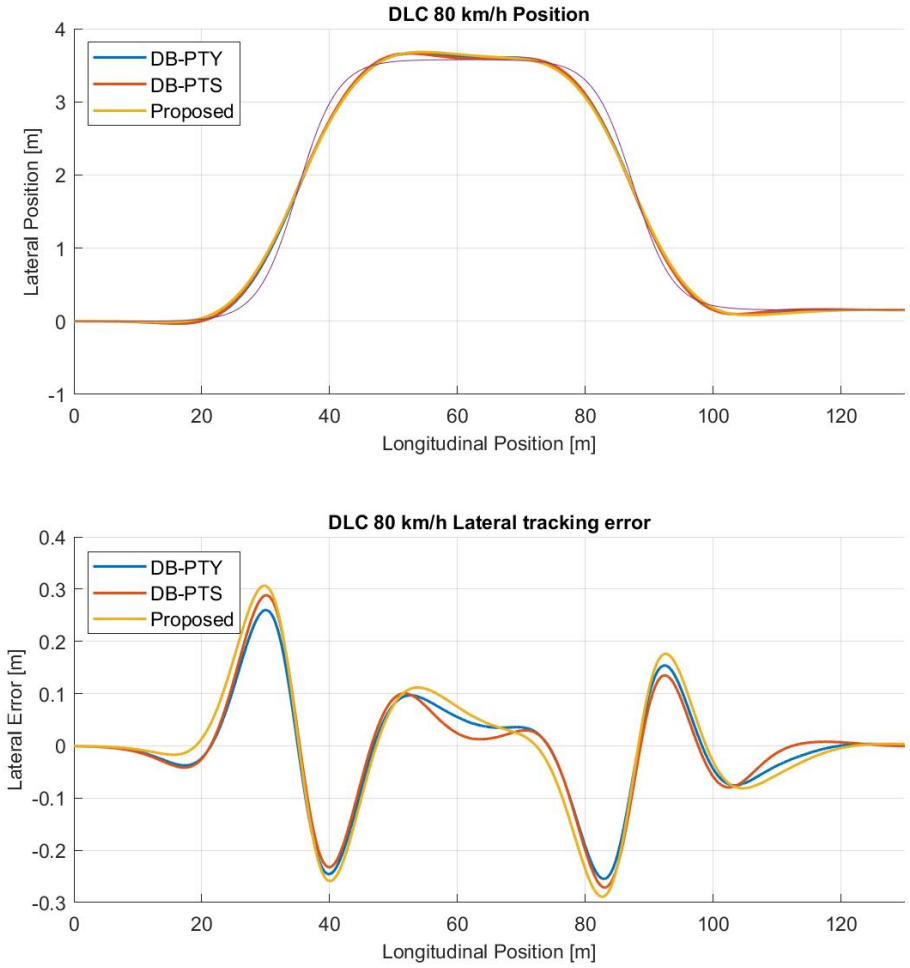

Figure 5.14: Position plot for the proposed controller in the DLC test at 80 km/h

seen that the controllers with differential braking have improved tracking performance (5.15a-5.15b) at the cost of lower stability performance (5.15c-5.15d).

5.3.2. Proposed controller

The proposed controller has the highest speed for which it is still able to complete the manoeuvre within the bounds. When looking at the results in figure 5.16a, the lateral tracking performance of the proposed controller is slightly worse than the DB-PTY and DB-PTS controller in low speed, but the slope is lower resulting at better performance at higher speeds compared to those other two. The yaw tracking performance (figure 5.16b) at higher speeds is worse than for the two other controllers. This can be explained by looking at the two stability KPI plots, 5.16c and 5.16d. From these plots it is clear that the proposed controller has better stability than the other two controllers. At these higher speeds the target yaw rate, which is based on the path curvature, is difficult to achieve without compromising stability. Another point that can be seen is that the stability KPIs for the proposed controller increase at a lower rate than for the other two controllers, especially at higher speeds. This was also confirmed by the fact that the proposed controller was able to stabilise the vehicle at speeds higher than 113 km/h. Even though the manoeuvre would fail as the vehicle would not return to the original

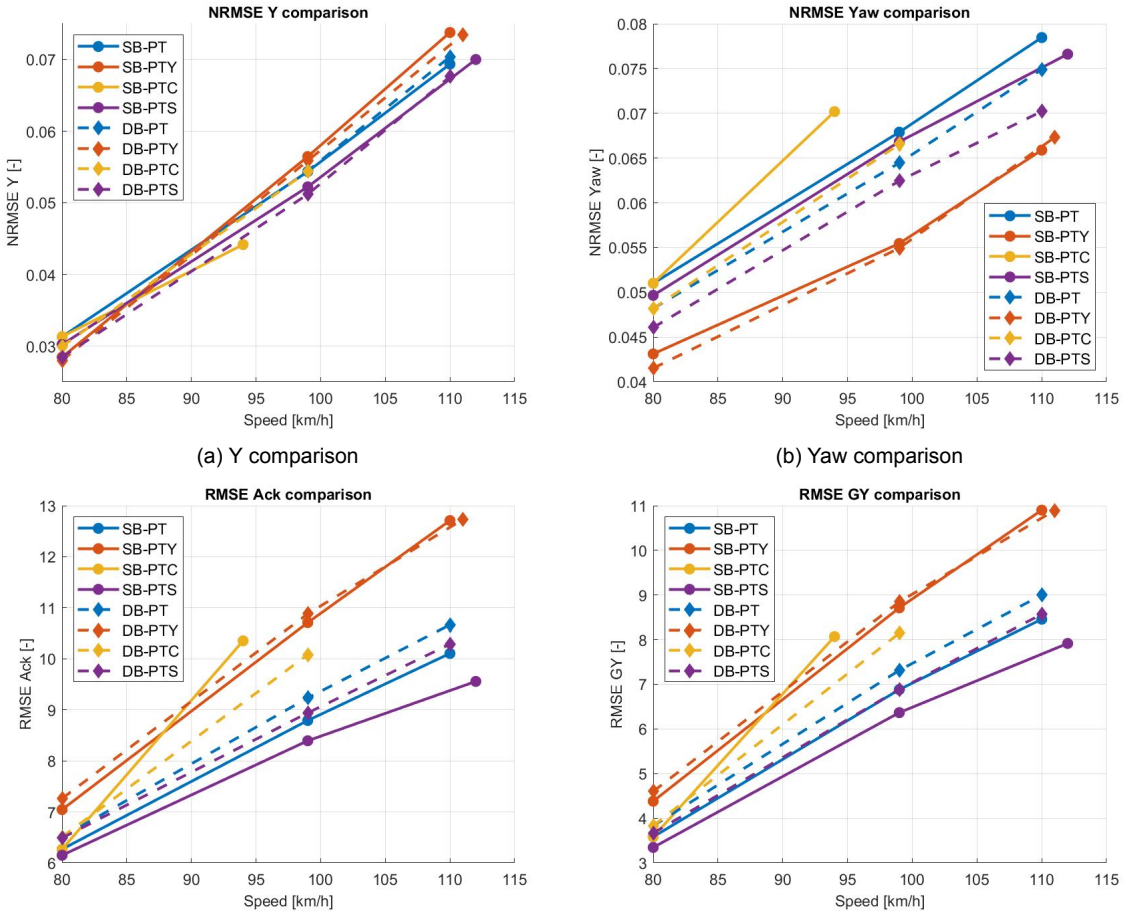

(a) Y comparison

(b) Yaw comparison

(c) Ack comparison

(d) GY comparison

Figure 5.15: KPIs for the baseline controllers when varying speed

lane in time, the controller was able to stabilise the vehicle during the manoeuvre. The other two controllers were only able to go slightly faster before becoming unstable.

5.4. Adding Weight

Weight is added to the vehicle to simulate extra occupants which are not modeled in the MPC controllers. In this case there is an extra error between the model inside the MPC and the actual vehicle. This model mismatch of the weight and inertia of the vehicle will likely deteriorate the performance of the controller. This is due to the vehicle now having a slower response than expected in the MPC calculations.

5.4.1. Baseline controllers

The results from the baseline controllers can be seen in figure 5.17. The added weight indeed causes worse performance for all controllers in tracking and stability. However, some controllers are more affected than others. The tracking performance of the controllers with differential braking is less effected than the controllers without differential braking, as seen in figures 5.17a and 5.17b. The controllers with differential braking have a lower slope compared to their counterparts without differential braking. For stability generally the opposite is true, as we've seen in previous sections where there was a trade-off between tracking and stability. However, there are some outliers. The DB-PTY controller has a better RMSE Ack with 300kg

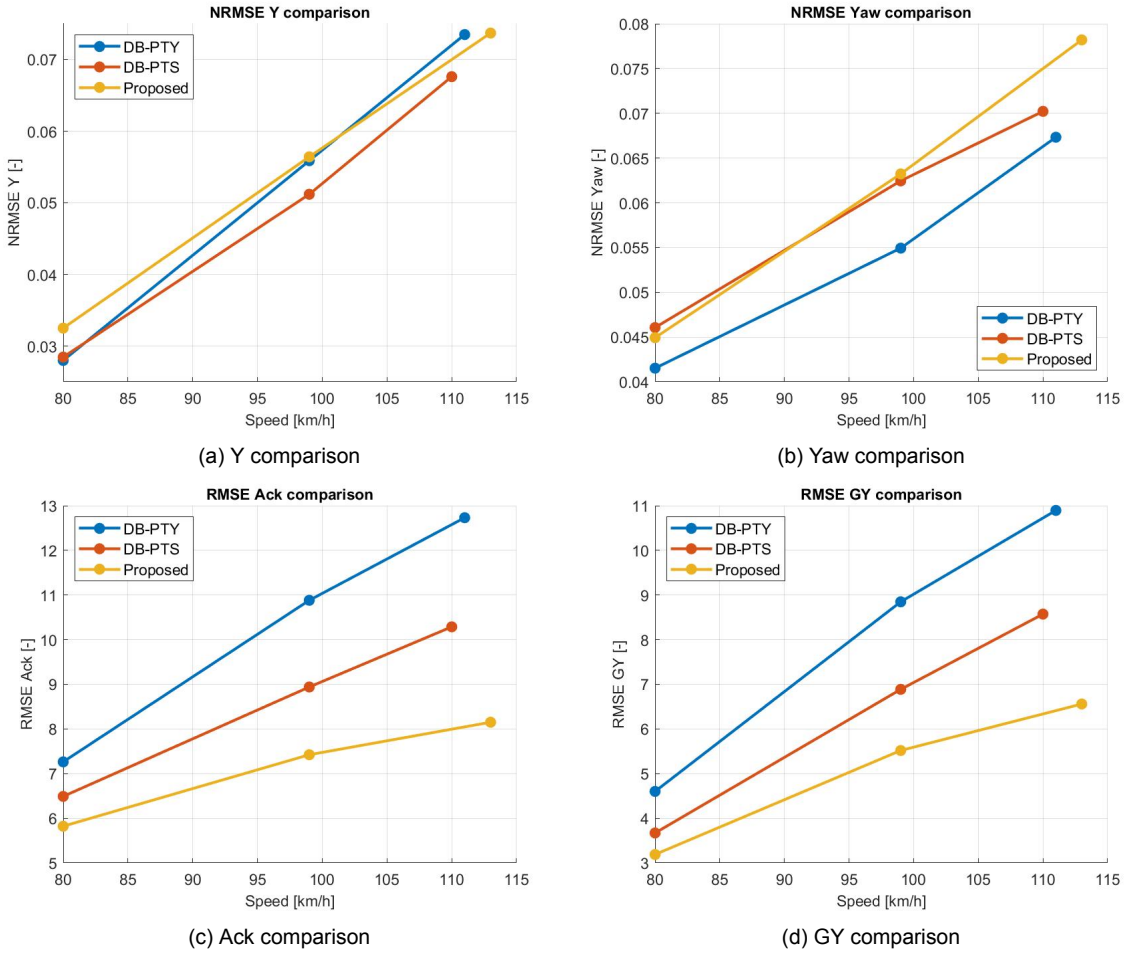

(a) Y comparison

(b) Yaw comparison

(c) Ack comparison

(d) GY comparison

Figure 5.16: KPIs for the proposed controller when varying speed

than with 150kg, seen in figure 5.17c. While the 1,1 controller has a better RMSE GY at 150kg than for the simulation with no extra weight (figure 5.17d). No clear reason has been found for these outliers. Although in general the performance still deteriorates when looking at the combination of RMSE Ack and RMSE GY for these controllers.

Furthermore, the SB-PT and DB-PT controllers are more affected then the other controllers in both tracking and stability. The SB-PTY and DB-PTY controllers still have the best tracking, while the SB-PTS controller has the best stability, with the DB-PTS controller increasing the tracking ability at the cost of some stability. These two controllers also have the best comfort KPIs by a large margin.

5.4.2. Proposed controller

For the proposed controller the most noticeable observation when looking at the KPIs in figure 5.18, is that almost all KPIs have a drop when going from 150-300 kg. This indicates a better performance for this controller when 300kg is added as opposed to only adding 150kg. The other controllers all have an increase in KPIs as more weight is added. The relative performance between the controllers therefore changes, as the proposed controller has the best performance for almost all KPIs in the 300kg scenario.

The DB-PTS controller has the worst stability performance deterioration of these controllers. This could be explained by the fact that the DB-PTS controller not only has a mismatch in the

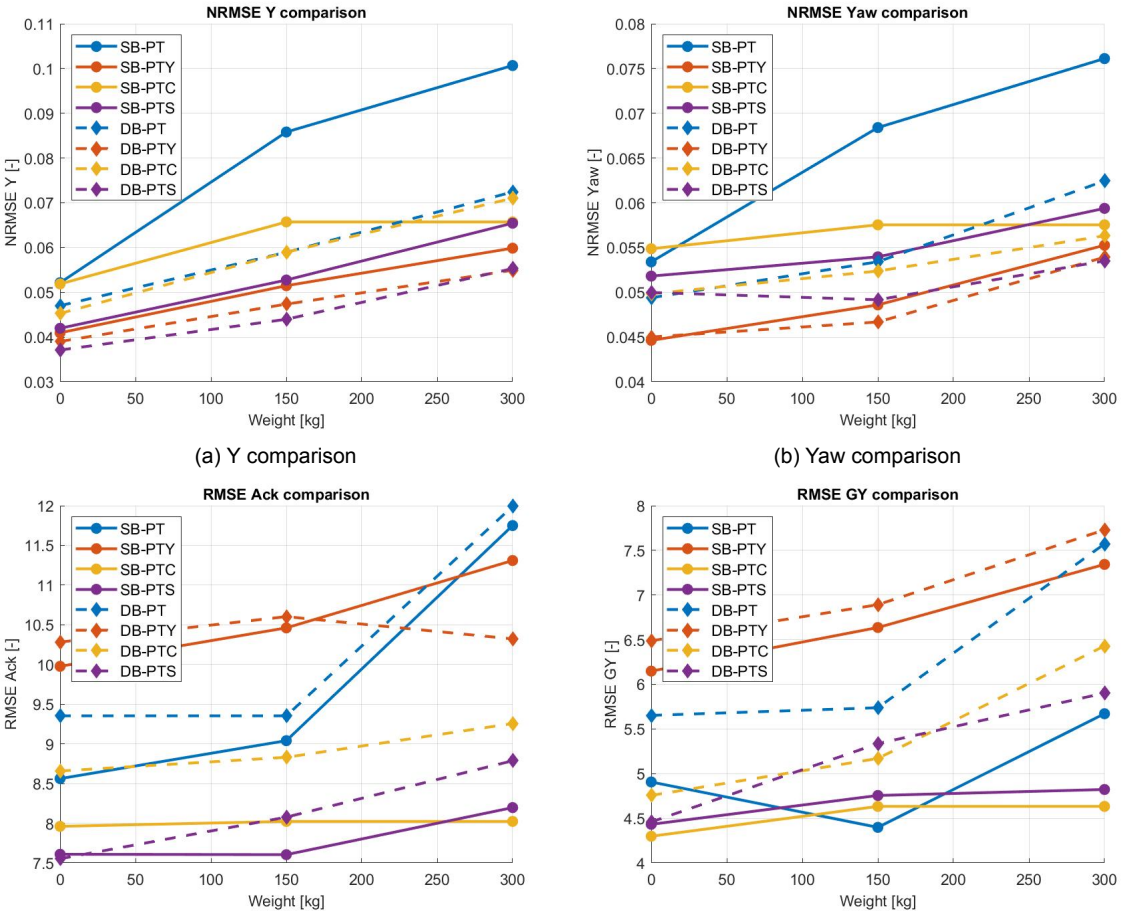

(a) Y comparison

(b) Yaw comparison

(c) Ack comparison

(d) GY comparison

Figure 5.17: KPIs for the baseline controllers when varying weight

MPC controller, but also in the separate VSC. When the VSC intervenes, the control output will be less optimal than what the controller was tuned for. This further decreases performance compared to only having a mismatch in the MPC.

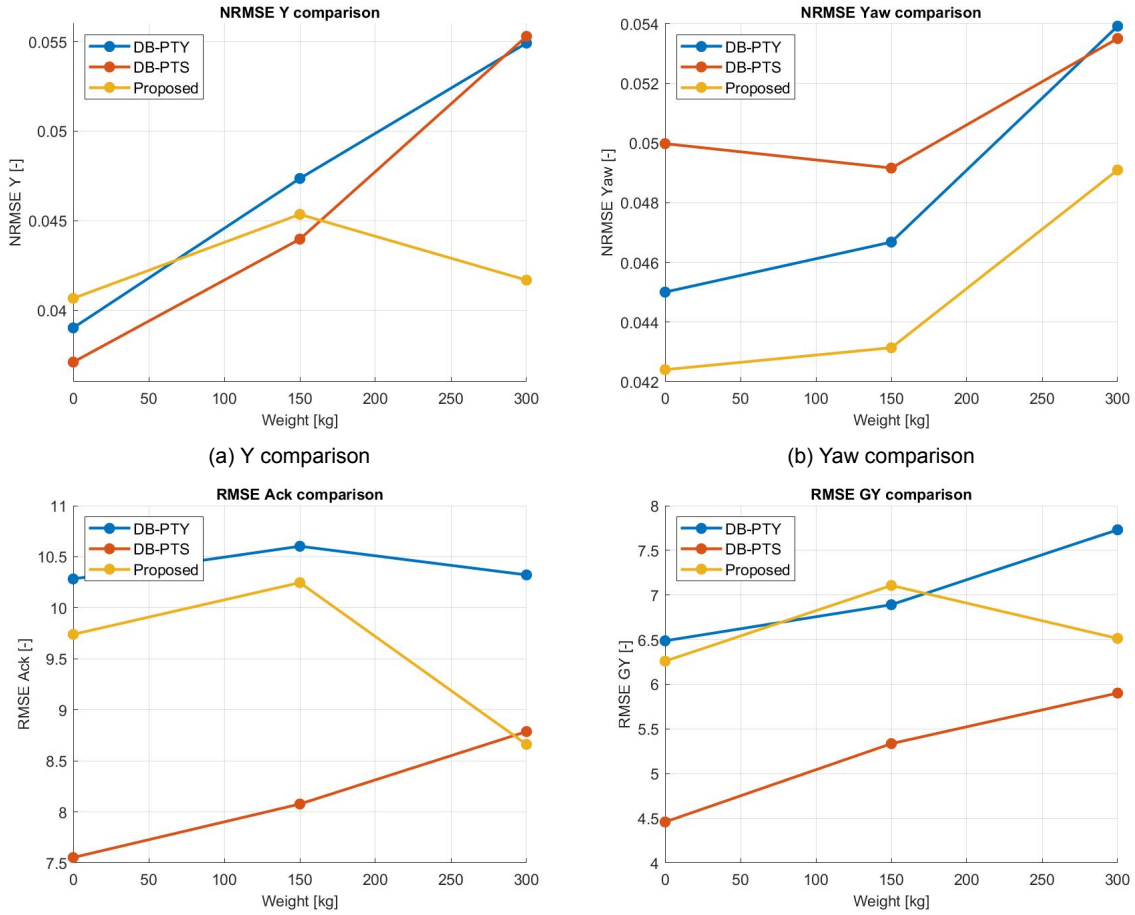

(a) Y comparison

(b) Yaw comparison

(c) Ack comparison

(d) GY comparison

Figure 5.18: KPIs for the proposed controller when varying weight

5.5. Low μ

In the low μ scenarios the complete road surface μ is lowered. The simulation was performed with three different μ levels, 0.9, 0.6 and 0.3. The respective speeds at these μ levels was 80 km/h, 80 km/h and 70 km/h. The speed was lowered for the 0.3μ case, as none of the controllers was able to complete the manoeuvre at 80 km/h.

5.5.1. Baseline controllers

The results for the baseline controllers are shown in figure 5.19. When lowering μ the controllers will in general have worse tracking performance. For the stability there is a clear difference between the controllers that can use differential braking and those that can not (figures 5.19c and 5.19d). The controllers that have differential braking have better stability in the 0.6μ case compared to the 0.9μ case. On the other hand, the controllers without differential braking have worse stability in the 0.6μ case. However, in the lowest μ case of 0.3, the controllers without differential braking have slightly better performance than those that do have differential braking. note that the decrease in RMSE values in the 0.3μ case is partly due to the lower speed for this scenario.

In the tracking KPIs there is again a difference between the controllers that can and can not use differential braking. The controllers with differential braking have lower performance deterioration in the lower μ conditions. This is because in these low grip scenarios, the front

wheels quickly reach the maximum level of available grip. The use of differential braking can then aid in adding an extra yaw moment to rotate the vehicle.

5.5.2. Proposed controller

The results for the proposed controller are shown in figure 5.20. For the proposed controller there is a bigger deterioration in tracking performance than for the other two controllers. However, the stability of the vehicle is also increased the most. In this scenario the trade-off between tracking and stability performance is again visualised. With a different controller tuning for low μ scenarios the tracking could be improved, at the cost of stability. In this case the tuning was done such that the overall performance was the best.

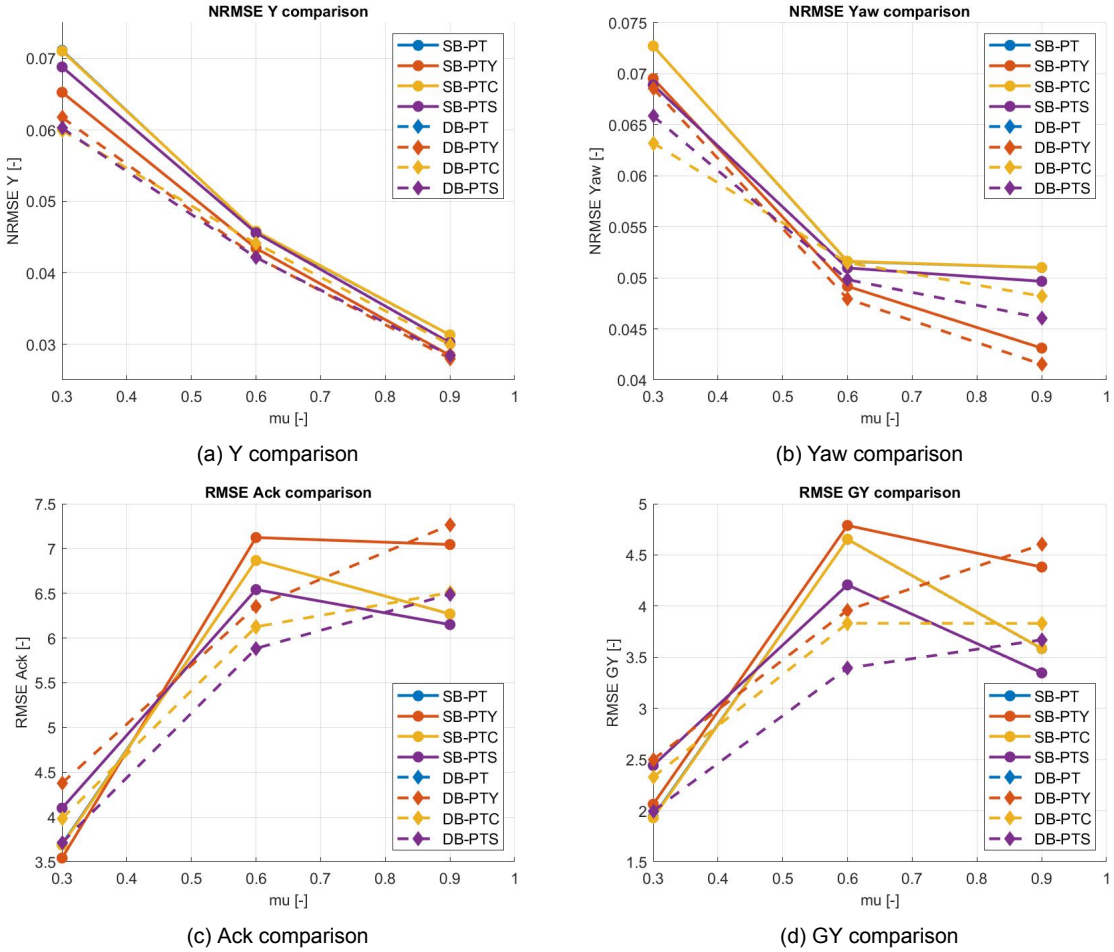

(a) Y comparison

(b) Yaw comparison

(c) Ack comparison

(d) GY comparison

Figure 5.19: KPIs for the baseline controllers when varying μ

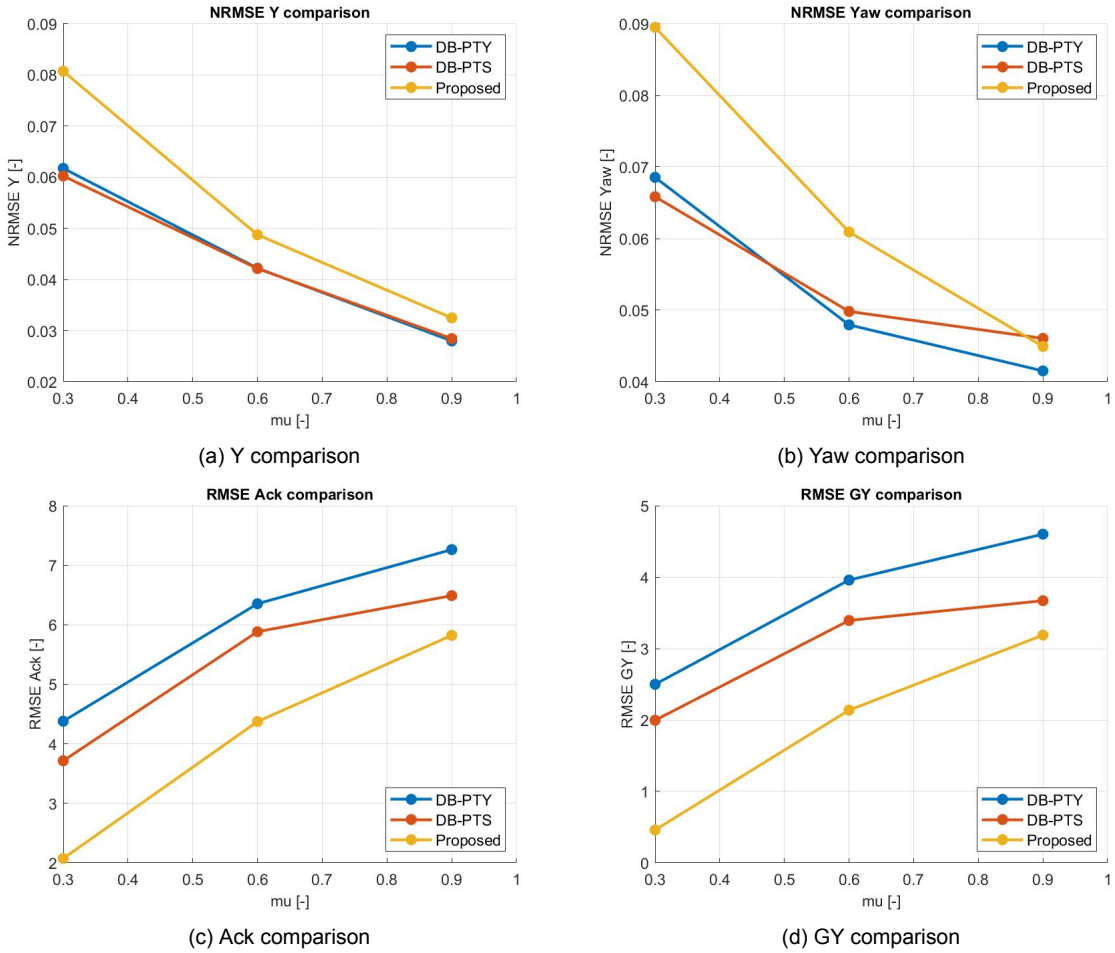

(a) Y comparison

(b) Yaw comparison

(c) Ack comparison

(d) GY comparison

Figure 5.20: KPIs for the proposed controller when varying μ

5.6. μ change

The μ change scenario's were performed in both directions with one μ step between the lanes. This was done to test realistic driving scenarios. As going from a snowy 0.3μ road to a wet 0.6μ road will have a higher occurrence than going from a 0.3μ road to a 0.9μ road surface.

5.6.1. Baseline controllers

Figure 5.21 shows the results for the baseline controllers for the different μ level changes. In all conditions the controllers with differential braking have better performance in the lower μ conditions than the controllers that do not have differential braking. This can be seen in the stability KPIs and tracking KPIs. This is again due to the fact that the controllers with differential braking have an extra control input available to control the vehicle. In the low μ conditions the front tires quickly reach the maximum available grip level. By utilising differential braking, the controller is able to control the vehicle more effectively when the steering input limit is reached.

It can also be seen that the performance for all controllers is better in the scenario where the original lane has a lower mu than the second lane has. In this case the controller predicts a certain input while expecting the lower μ level. When the μ level suddenly increases, there is more grip available making the path more easy to follow. In the opposite direction the reverse is true. When the μ level suddenly lowers, there is less grip available, which the controller could not previously predict. The vehicle will then be more difficult to control which reduces

tracking and stability.

5.6.2. Proposed controller

The results for the proposed controller are shown in figure 5.22. For most KPIs the relative performance between the controllers remains similar for the different scenarios. One exception that can be seen is in the tracking KPIs where the proposed controller has a much larger decrease in performance in the $0.3 \rightarrow 0.6\mu$ scenario. In these scenarios the same trend as in the previous low μ scenarios can be seen. The proposed controller has better stability in the low μ conditions, at the cost of worse tracking.

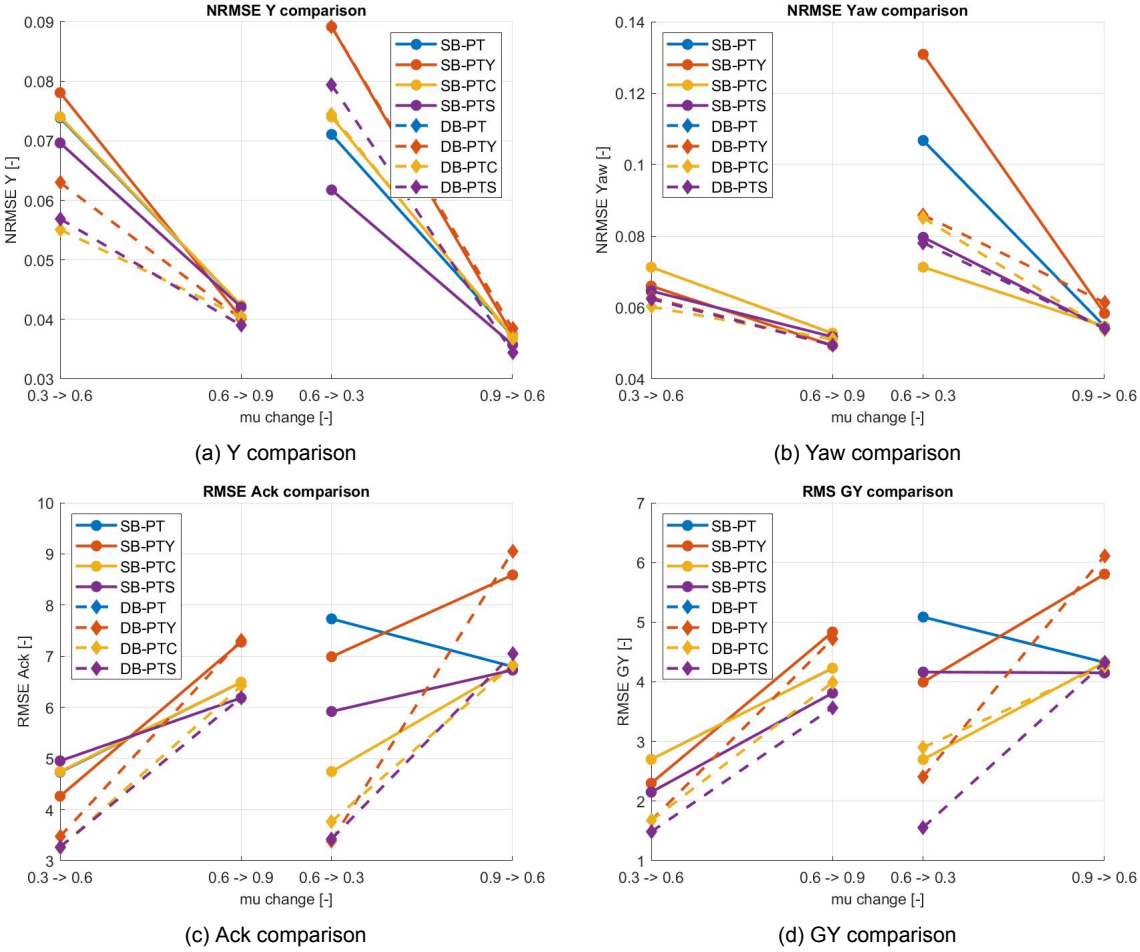

(a) Y comparison

(b) Yaw comparison

(c) Ack comparison

(d) GY comparison

Figure 5.21: KPIs for the baseline controllers when driving across a μ change

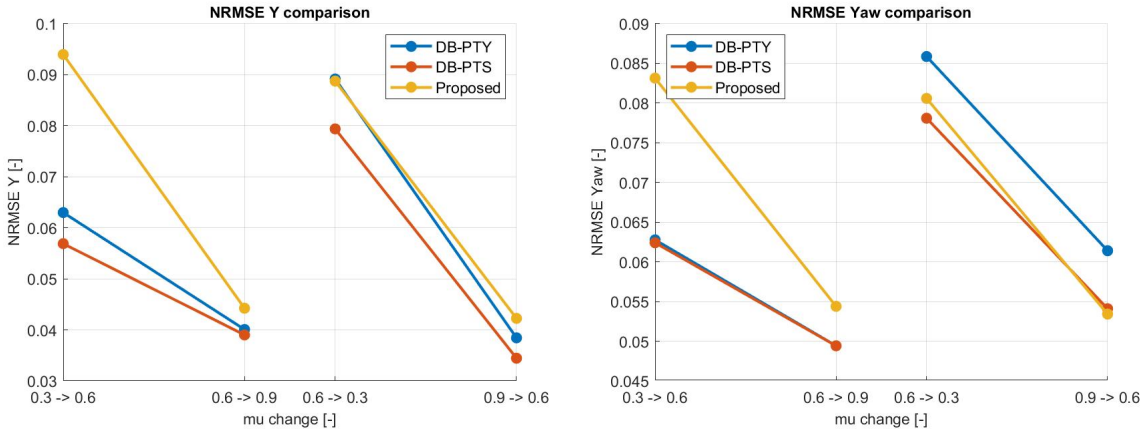

(a) Y comparison

(b) Yaw comparison

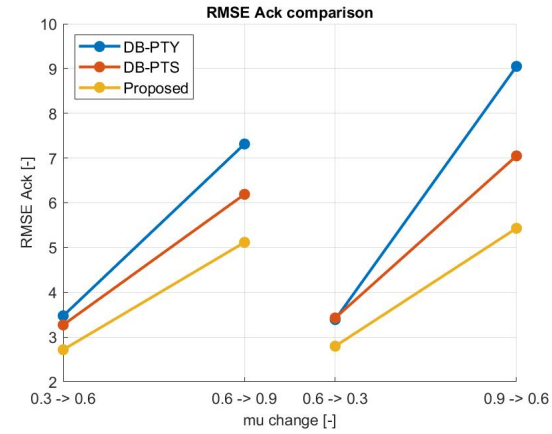

(c) Ack comparison

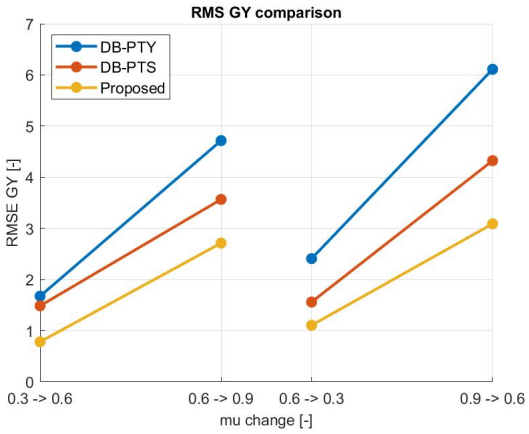

(d) GY comparison

Figure 5.22: KPIs for the proposed controller when driving across a μ change

6

Discussion

In this chapter the results of the previous chapter will be discussed. First the trade off between the tracking performance and stability of the vehicle will be discussed. Secondly the difference in computational time between the different controllers will be highlighted including the performance benefits. Then a comparison between the results and results from literature will be made. Finally some recommendations for future work will be given.

6.1. Tracking vs Stability

In all scenarios there is a clear trade off between tracking and stability performance. In general a higher vehicle stability KPI leads to lower path tracking capabilities, as the vehicle is more limited in the yaw response. This is seen the best in the proposed controller, where the trade off between tracking and stability is made directly in the cost function. A higher weight on the stability will make the MPC prioritise vehicle stability over path following, thereby reducing the tracking KPIs. An increase on the path following weights will have the opposite effect. In this case the MPC prioritises following the reference path over vehicle stability. This allows for more vehicle sideslip and a higher sideslip rate at the cost of potentially resulting in a loss of control at too high speeds.

For the other controllers the trade off between tracking and stability is not as direct. The extra reference yaw rate adds both stability and tracking performance when the cost function weight is kept relatively low. When the weight on the reference yaw rate is increased too much it will lead to instability of the vehicle. This is because the reference yaw rate is based on the curvature of the reference path, which does not take the vehicle handling limits into account. If the weight on the reference yaw rate is therefore too high, the controller will attempt to follow a yaw rate that is outside the physical limits of the vehicle.

The controllers with stability constraints should keep the vehicle within stable bounds. In practice it was found that due to modelling inaccuracies these bounds were exceeded in aggressive manoeuvres, which lead to the controller overcompensating in an attempt to keep the vehicle within the constraints. This is why both controllers have a much lower maximum speed for which they were able to complete the Elk test and Double Lane Change.

When a separate VSC is used to stabilise the vehicle, the stability KPIs are better than for the controllers with a reference yaw rate at the cost of worse tracking. This is due to the VSC intervening when the vehicle is too close to the stability limits. This intervention is done outside of the MPC and therefore the MPC can not predict this intervention, deteriorating

tracking performance.

The application of differential braking in the controller also has an effect on the tracking and stability KPIs. In all scenario's the addition of differential braking to a controller lead to increased tracking performance and a decrease in stability performance. The added yaw rate caused by the difference in braking pressure on each side of the car makes the vehicle more agile, but also creates a higher sideslip rate. Overall the increased tracking by including differential braking was more beneficial than the decrease in stability.

6.2. Comparison to Literature

In this section the results for the Elk test and Double Lane Change will be compared to other literature. However, a direct comparison is difficult to make. This is due do differences in vehicle speed, road μ and the used manoeuvre. The manoeuvres that are used in the literature below are often close to the ISO definition of the Elk test or Double Lane Change, but do not have the exact same dimensions. Often the length of the manoeuvre is somewhere in between the ISO definition of the Elk test and Double Lane Change. Therefore, a direct comparison can not be made but this comparison can still serve as an indication if the performance corresponds to the found literature.

Table 6.1 shows the results from the proposed controller for mu levels of 1, 0.9, 0.6 and 0.3 as well as the results from literature. The papers that are shown all use MPC for control with the steering wheel and yaw control as controlled variables. The manoeuvres in these papers are not identical, the length and width of the Double Lane Changes as well as the speed and μ level have been included to give an indication of the manoeuvre conditions. The last three columns show the KPIs for the manoeuvre.

Table 6.1: Proposed Controller compared to literature

Source	Length [m]	Width [m]	$V[m/s]$	μ	Y_{RMSE}	ψ_{RMSE}
Comb. Contr.	40	3.2	19.44	1	0.0510	0.0532
	80	3.5	22.22	0.9	0.0325	0.0449
	80	3.5	22.22	0.6	0.048	0.061
	80	3.5	19.44	0.3	0.081	0.089
Rokonuzzaman M. [31]	35	4	16.66	1	0.05	-
Katriniok A. [32]	50	3.2	17	1	0.12	-
Ge L. Zao [33]	70	4.4	18	0.85	0.085	-
B. Zhang [34]	65	4	15	0.75	0.2704	0.0343
	65	4	30	0.75	0.3317	0.0262
Yakub F. [11]	125	3.5	25	1	0.0908	0.0524
	100	3.5	20	0.3	0.1394	0.0268

As already stated a direct comparison can not be made, however some insights into the performance of the proposed controller relative to earlier papers can still be given. Comparing the first row of the proposed controller to the controller presented by Rokonuzzaman [31], a similar performance can be seen. The vehicle speed for the proposed controller is higher (72km/h vs 60km/h), but the manoeuvre is also less agressive (longer length and smaller width). The Y_{RMSE} of these controllers is very similar at around 0.05. Comparing to the controller by Katriniok A. [32], the proposed controller performs significantly better. The manoeuvre during the proposed controller test is more aggressive as it is completed in a shorter distance, while the vehicle speed is also higher. Nevertheless the Y_{RMSE} is still lower at 0.051 compared to the

0.12 in the literature.

The controller by Ge L. can be compared to the second row of the proposed controller. The μ level is similar, however the manoeuvre in the paper by Ge L. is more aggressive, while the speed is higher in the proposed controller. The length and width are both around 20% shorter and wider, while the speed is around 20% slower. However, the final Y_{RMSE} value for the controller by Ge L. is over 2.5 times higher than for the proposed controller, indicating a better overall performance.

The controllers by B. Zhang are tested using a μ of 0.75. These can be compared to an interpolation of the second and third row of the proposed controller. However, the manoeuvre in the paper by B.Zhang is more aggressive, with the vehicle speed being higher in the tests for the proposed controller. Comparing to the first row of the controller by B. Zhang should give an idea of the relative performance. The Y_{RMSE} value of the controller by B. Zhang is 0.27, while the Y_{RMSE} value of the proposed controller in this case is around 0.04. However the ψ_{RMSE} of the controller by B. Zhang is 0.0343, while the ψ_{RMSE} for the proposed controller is around 0.053. The controller by B. Zhang has better yaw tracking performance, while the proposed controller has better lateral position tracking performance.

Finally comparing the the controller by Yakub F. The closest test conditions is found by comparing the second test of Yakub F. to the fourth row of the proposed controller. The μ value is the same, while the speed is almost equal. The only difference is the length of the manoeuvre which is longer in the test of Yakub F. In this case the Y_{RMSE} value for the proposed controller is lower than that of the controller by Yakub F. The ψ_{RMSE} value is higher for the proposed controller. The result is therefore similar to the previous case, where the proposed controller has better lateral position tracking, with lower yaw tracking.

Note that in the comparison only the tracking performance is compared. In the cited literature there was no mention of stability KPIs and as such, they could not be compared.

6.3. Recommendations

In this research the tuning of the weights for the MPC controller was all done manually by trial and error. While the KPIs were used to find the optimum weights, there is still a possibility that a better set of weights exists for a controller. This method is also labour-intensive as for each iteration the KPIs have to be analysed, new weights need to be selected and the simulation needs to be run. Another method for tuning the controllers is using an optimisation strategy which would find a (local) optimum set of weights. Automating the tuning of the controllers using this method should give an overall improvement of the controller. This was done in by Rokonuzzaman, where they used a Genetic Algorithm to tune the different controllers [31]. The optimiser was used in order to ensure an equal tuning effort between the different controllers. The cost function for this optimisation consisted of the sum of the used KPIs. A similar method could be utilised here, however the MPC models used in this research have more states and control outputs than the controllers used by [31]. Therefore the optimisation will be more computational intensive, although the optimisation for the weights can be done offline and does not change once the best set has been found.

A second improvement could be made by having the weights be dependent on the driving conditions. Currently the weights change depending on the road μ level. At lower μ levels the weights will change to keep the vehicle stable in these conditions where there is less grip available. However, there are more factors which influence the performance and requirements of the controller. As an example, the weights that would give the best stability during the Elk test would lead to too much stabilisation in the Double Lane Change. Having weights that can

change depending on the driving scenario would mean less trade-off is required and a better overall performance could be obtained.

Finally a last point of future work would be an implementation in a real vehicle in order to assess the real world performance. Currently all controllers have only been tested in simulation. Even though this is a state of the art simulation environment, a real world test is essential in testing and confirming of the conclusions obtained from simulation.

7

Conclusion

In this research a total of nine different controllers have been designed and evaluated. All controllers had some unique combination of features like differential braking, target states, constraints and stability control methods. These controllers were evaluated using industry standard tests like the Elk test and Double Lane Change. To test the robustness of the controllers, some variations were added like different speeds, road μ level, vehicle load level and changing between lanes of different mu. After the simulations were completed the controllers were compared using KPIs regarding the trajectory tracking, stability, comfort and computational time, in order to get a good understanding of the performance of each controller.

Adding differential braking to the control strategy gives better performance in all cases. Tracking and stability is improved, as well as robustness and performance in low μ conditions. The added differential braking allows for a more complex control strategy by giving the freedom of selecting individual brake torques, aiding in both reference tracking and stability. However, this more complex control also comes at the cost of a higher computational load demand. The extra states required to compute the individual brake torques naturally need more computational effort to be solved. The controllers with differential braking needed around six times more time to compute, but this was still well within the update rate of the MPC so in this case that caused no issue.

From the results it can be concluded that adding a reference yaw rate for the controller to follow greatly improves the tracking and stability of the vehicle. Both the SB-PTY and DB-PTY controllers performed better in tracking and stability than the SB-PT and DB-PT controllers without the reference yaw rate.

The controllers with stability constraints SB-PTC and DB-PTC, did improve stability. However, due to the model mismatch between the MPC model and the actual vehicle, the vehicle sometimes exceeds the predefined constraints. The MPC was often unable to return the vehicle within the bounds when this occurred, resulting in a loss of control.

The controllers with a separate VSC added, SB-PTS and DB-PTS had better tracking and stability than the controllers without the added VSC. However, the SB-PTY and DB-PTY with a reference yaw rate had even better tracking, but a slightly worse stability. One problem with the separate VSC was that there is no feedback to the MPC regarding the VSC operation. Therefore, when the MPC output exceeded the stability conditions of the VSC, there was a sudden change in vehicle behaviour that the MPC did not predict. This mismatch between the predicted trajectory and actual trajectory resulted in a worse performance.

The proposed controller was made in an attempt to solve this problem. This was done by calculating the stability equations of the VSC within the MPC itself. This method has promising results as the tracking is better than the DB-PTS controller with the separate VSC, while the stability is better than both the DB-PTS and the DB-PTY controller. It also has the highest passing speed for the Elk test and is able to stabilise the vehicle at much higher speeds than the other two controllers. One difficulty with this controller is the added complexity introduced by the two extra states and multiple extra equations needed to calculate those states. This increases the computational load slightly and makes the tuning of the weights more complex, as there are more weights to tune.

In conclusion the controllers with differential braking were the better performing controllers. Of these controllers the DB-PTY controller with a yaw rate reference had the best tracking, while the DB-PTS controller with a separate VSC had better stability. The combination of these two in the proposed controller gives an increased performance in both as well as stability. The new controller improves path tracking by 8% compared to the pure path tracking controller. While the stability is improved by 11% compared to the controller with a separate VSC. Furthermore the new controller was able to keep the vehicle stable at higher speeds and was more robust to varying conditions. There are still points where this controller can be improved, primarily in the selection of the weights, but overall this controller has the best performance of all tested controllers.

A

Vehicle Parameters

Table A.1: Vehicle Parameters

Parameter	Explanation	Value
$C_{r,f}$	Front roll stiffness	$42307[Nm/rad]$
$C_{r,r}$	Rear roll stiffness	$36039[Nm/rad]$
h_{cg}	Height of CoG	$0.673[m]$
h_f	Front roll height	$0.27[m]$
h_r	Rear roll height	$0.28[m]$
I_z	Moment of Inertia around z-axis	$3386[kgm^2]$
K_h	Stability factor	$0.004[s^2/m^2]$
l_f	Distance between front axle and CoG	$1.093[m]$
l_r	Distance between rear axle and CoG	$1.570[m]$
m	Vehicle mass	$1712[kg]$
$R_{eff,f}$	Front effective tire radius	$0.359[m]$
$R_{eff,r}$	Rear effective tire radius	$0.353[m]$
S_{rat}	Steering ratio	$15.8[-]$
t_f	Front track width	$1.628[m]$
t_r	Rear track width	$1.635[m]$

B

Cost Function Weights

Table B.1: Weights for the SB-PT, SB-PTC and SB-PTS Controllers

Tuning Parameter	Value	Tuning Parameter	Value
Q_v	$1 * 10^1 \mu^5$	$Q_{N,v}$	$1 * 10^2 \mu^5$
$Q_{\dot{\psi}}$	-	$Q_{N,\dot{\psi}}$	-
Q_{ψ}	$3 * 10^2/\mu$	$Q_{N,\psi}$	$5 * 10^5/\mu^5$
Q_y	$5 * 10^3/\mu$	$Q_{N,y}$	$5 * 10^5/\mu^5$
R_{st}	$5 * 10^3/\mu^3$	$R_{N,st}$	$5 * 10^3/\mu^6$
R_{Tb}	$1 * 10^{-2}/\mu^6$	$R_{N,Tb}$	$1/\mu^6$
R_{Thr}	$1 * 10^3/\mu^3$	$R_{N,Thr}$	$1 * 10^4/\mu^3$
$P_{\Delta st}$	$5 * 10^3/\mu^6$		
$P_{\Delta Tb}$	$5 * 10^{-4}/\mu^4$		
$P_{\Delta Thr}$	$1 * 10^3/\mu^3$		

Table B.2: Weights for the SB-PTY Controller

Tuning Parameter	Value	Tuning Parameter	Value
Q_v	$1 * 10^1 \mu^5$	$Q_{N,v}$	$1 * 10^2 \mu^5$
$Q_{\dot{\psi}}$	$3 * 10^3/\mu$	$Q_{N,\dot{\psi}}$	$3 * 10^4/\mu$
Q_{ψ}	$3 * 10^2/\mu$	$Q_{N,\psi}$	$5 * 10^5/\mu^5$
Q_y	$5 * 10^3/\mu$	$Q_{N,y}$	$5 * 10^4/\mu^5$
R_{st}	$5 * 10^2/\mu^3$	$R_{N,st}$	$5 * 10^3/\mu^6$
R_{Tb}	$1 * 10^{-2}/\mu^6$	$R_{N,Tb}$	$1/\mu^6$
R_{Thr}	$1 * 10^3/\mu^3$	$R_{N,Thr}$	$1 * 10^4/\mu^3$
$P_{\Delta st}$	$5 * 10^3/\mu^6$		
$P_{\Delta Tb}$	$5 * 10^{-4}/\mu^4$		
$P_{\Delta Thr}$	$1 * 10^3/\mu^3$		

Table B.3: Weights for the DB-PT, DB-PTC and DB-PTS Controllers

Tuning Parameter	Value	Tuning Parameter	Value
Q_v	$1 * 10^1 \mu^5$	$Q_{N,v}$	$1 * 10^2 \mu^6$
$Q_{\dot{\psi}}$	-	$Q_{N,\dot{\psi}}$	-
Q_{ψ}	$3 * 10^4/\mu$	$Q_{N,\psi}$	$5 * 10^5/\mu^4$
Q_y	$5 * 10^3/\mu$	$Q_{N,y}$	$5 * 10^5/\mu^4$
R_{st}	$5 * 10^3/\mu^3$	$R_{N,st}$	$5 * 10^3/\mu^6$
R_{Tb}	$1 * 10^{-2}/\mu^4$	$R_{N,Tb}$	$1 * 10^{-2}/\mu^3$
R_{Thr}	$1 * 10^3/\mu^3$	$R_{N,Thr}$	$1 * 10^4/\mu^3$
$P_{\Delta st}$	$5 * 10^3/\mu^6$		
$P_{\Delta Tb}$	$5 * 10^{-5}/\mu^3$		
$P_{\Delta Thr}$	$1 * 10^3/\mu^3$		

Table B.4: Weights for the DB-PTY Controller

Tuning Parameter	Value	Tuning Parameter	Value
Q_v	$1 * 10^1 \mu^5$	$Q_{N,v}$	$1 * 10^2 \mu^6$
$Q_{\dot{\psi}}$	$3 * 10^3/\mu$	$Q_{N,\dot{\psi}}$	$1 * 10^3/\mu^2$
Q_{ψ}	$3 * 10^4/\mu$	$Q_{N,\psi}$	$5 * 10^5/\mu^4$
Q_y	$5 * 10^3/\mu$	$Q_{N,y}$	$5 * 10^4/\mu^4$
R_{st}	$5 * 10^3/\mu^3$	$R_{N,st}$	$5 * 10^3/\mu^6$
R_{Tb}	$1 * 10^{-2}/\mu^4$	$R_{N,Tb}$	$1 * 10^{-2}/\mu^3$
R_{Thr}	$1 * 10^3/\mu^3$	$R_{N,Thr}$	$1 * 10^4/\mu^3$
$P_{\Delta st}$	$5 * 10^3/\mu^6$		
$P_{\Delta Tb}$	$5 * 10^{-5}/\mu^3$		
$P_{\Delta Thr}$	$1 * 10^3/\mu^3$		

Table B.5: Weights for the Proposed Controller

Tuning Parameter	Value	Tuning Parameter	Value
Q_v	$1 * 10^1 \mu^5$	$Q_{N,v}$	$1 * 10^2 \mu^6$
$Q_{\dot{\psi}}$	$3 * 10^3/\mu$	$Q_{N,\dot{\psi}}$	$1 * 10^3/\mu^2$
Q_{ψ}	$3 * 10^4/\mu$	$Q_{N,\psi}$	$5 * 10^5/\mu^4$
Q_y	$5 * 10^3/\mu$	$Q_{N,y}$	$5 * 10^4/\mu^2$
Q_{Ack}	$AF * 1 * 10^4/\mu^{4.75}$	$Q_{N,Ack}$	$AF * 1 * 10^4/\mu^{4.75}$
Q_{GY}	$AF * 1 * 10^6/\mu^{2.5}$	$Q_{N,GY}$	$AF * 1 * 10^6/\mu^{2.5}$
R_{st}	$5 * 10^3/\mu^3$	$R_{N,st}$	$5 * 10^3/\mu^6$
R_{Tb}	$1 * 10^{-3}/\mu^3$	$R_{N,Tb}$	$1 * 10^{-2}/\mu^3$
R_{Thr}	$1 * 10^3/\mu^3$	$R_{N,Thr}$	$1 * 10^4/\mu^3$
$P_{\Delta st}$	$5 * 10^3/\mu^6$		
$P_{\Delta Tb}$	$5 * 10^{-5}/\mu^5$		
$P_{\Delta Thr}$	$1 * 10^3/\mu^3$		

Where AF is the value of the Activation Factor as described in section 3.7

C

Paper

20XX-01-XXXX

Combined Path Following and Vehicle Stability Control using Model Predictive Control

Author, co-author (Do NOT enter this information. It will be pulled from participant tab in MyTechZone)

Affiliation (Do NOT enter this information. It will be pulled from participant tab in MyTechZone)

Abstract

This paper presents an innovative combined control using Model Predictive Control to enhance the stability of automated vehicles. It integrates path tracking and vehicle stability control into a single controller to satisfy both objectives. The stability enhancement is achieved by computing two expected yaw rates based on the steering wheel angle and on lateral acceleration into the MPC model. The vehicle's stability is determined by comparing the two reference yaw rates to the actual one. Thus, the MPC controller prioritises path tracking or vehicle stability by actively varying the cost function weights depending on the vehicle states. Using two industrial standard manoeuvres, i.e. moose test and double lane change, we demonstrate a significant improvement in path tracking and vehicle stability of the proposed MPC over eight benchmark controllers in the high-fidelity simulation environment. The numerous benchmark controllers use different path tracking and stability control methods to assess each performance benefit. They are split into two groups: the first one uses differential braking in the control output, while the second group can only provide an equal brake torque for the wheels in the same axle. Furthermore, the controller's robustness is evaluated by changing various parameters, e.g. initial vehicle speed, mass and road friction coefficient. The proposed controller keeps the vehicle stable at higher speeds even with varying conditions.

Introduction

Following a target path and keeping the vehicle stable is a crucial property for active vehicle safety systems in automated driving. Vehicle stability control has reduced fatal single-vehicle accidents by about 30-50% for passenger cars and up to 50-70% for sport utility vehicles [1]. Despite this, the considerable uncertainty in the road friction coefficient and the potential conflicts between path tracking and stability performances make this problem particularly challenging [2]. If separate controllers perform each task, potential conflict between tracking and stability can happen. Thus, we focus on the combined control to mediate possible conflicting objectives with the primary goal to enhance vehicle safety. MPC allows the simultaneous optimisation of the steering angle and the braking signal to perform evasive manoeuvres, and it improves the general performance of the controller [3]. For this reason, a vehicle driven at 10 m/s during an evasive manoeuvre can be stabilised by developing a nonlinear Model Predictive Control based on a 10 Degrees of Freedom (DoF) planar vehicle model. However, its high complexity does not allow a real-time application because 12 s manoeuvres require a 15 min long simulation [4]. The complex 10 DoFs planar vehicle is substituted by an extended bicycle model, which has a better trade-off between simplicity and accuracy. It allows the computation of the yaw moment generated by the different tyre longitudinal forces in the same axle. Thus, it admits the application of differential braking as further control input together with the steering angle. The controller stabilises the vehicle in every situation, but its robustness to different vehicle masses and parameters is not assessed. Recently, a controller based on an integrated NMPC allowed direct computation of the control actions for each of the four wheels, assuring vehicle stability through constraints [2]. The controller robustness performance is extensively assessed by applying various disturbances, e.g. lateral wind, and varying the rod friction coefficient. However, the stability and tracking objectives can clash during manoeuvres at the limit of the handling. In such a situation, assuring stability through constraints does not allow priorities stability over tracking or vice versa. Thus, we propose a combined approach covering path tracking and stability control into a single controller, using the steering wheel, throttle and brakes as actuation. The controller evaluates the vehicle's stability when deciding on the control inputs to follow the path. This leads to increased path tracking and stability compared to a control structure where separate controllers achieve these tasks. The combination is feasible thanks to the computation of two extra desired yaw rates on the steering wheel angle and on lateral acceleration. The actual yaw rate is compared with the two references, and the MPC controller prioritises path tracking or vehicle stability, varying the cost function weights. These parameters in the cost function differ depending on the vehicle state. A moose test and a double lane change in high-fidelity simulation environment are used to evaluate the performance of the proposed controller. Furthermore, its robustness is tested by varying the vehicle speed, the vehicle mass and the road friction coefficient.

The main contribution of this paper is twofold. The first is the combined path tracking and vehicle stability controller, which improves the tracking performance by 8% and enhances the vehicle stability by 11% compared with the baseline controllers. The second contribution is the improved robustness of the vehicle stability to the variation of vehicle speed, mass and road friction coefficient.

Proposed Controller

The following section explains the development of the proposed combined controller. It describes the nominal vehicle model, the

reference generation, the stability assessment and the cost function weights tuning.

Vehicle Model

The vehicle motion is described by a planar vehicle model, see Figure 1. The model states are the longitudinal v_x and the lateral velocity v_y in the vehicle's body frame, the yaw rate $\dot{\psi}$, the longitudinal position X_p, the lateral position Y_p and the heading angle ψ in the global reference frame, the steering angle δ, the throttle position T_{hr} and the brake torque T_b. The model's inputs are the steering angle rate $\dot{\delta}$, the throttle rate $\dot{T}_{hr}$ and the brake torque rate $\dot{T}_b$. The dynamic equations of the vehicle model are represented as follows:

$$\dot{x} = \begin{bmatrix} \dot{v}_x = \dfrac{\left(F_{x,fl}+F_{x,fr}\right)\cos(\delta) - F_{drag} - \left(F_{y,fl}+F_{y,fr}\right)\sin(\delta)}{m} + \\ + \dfrac{\left(F_{x,rl}+F_{x,rr}\right)}{m} + v_y\dot{\psi} \\ \dot{v}_y = \dfrac{\left(F_{x,fl}+F_{x,fr}\right)\sin(\delta) + \left(F_{y,fl}+F_{y,fr}\right)\cos(\delta)}{m} + \\ + \dfrac{\left(F_{y,rl}+F_{y,rr}\right)}{m} - v_x\dot{\psi} \\ \ddot{\psi} = \dfrac{\left(F_{x,fl}+F_{x,fr}\right)\sin(\delta)l_f + \left(F_{y,fl}+F_{y,fr}\right)\cos(\delta)l_f + \left(F_{y,rl}+F_{y,rr}\right)l_r}{I_{zz}} + \\ + \dfrac{0.5t_f\left(F_{x,fl}-F_{x,fr}\right)\cos(\delta) + 0.5t_f\left(F_{y,fl}-F_{y,fr}\right)\sin(\delta) + 0.5t_r\left(F_{x,rl}-F_{x,rr}\right)}{I_{zz}} \\ v_x\sin(\psi) + v_y\cos(\psi) \\ v_x\sin(\psi) - v_y\sin(\psi) \\ \dot{\psi} \\ \dot{\delta} \\ \dot{T}_{hr} \\ \dot{T}_b \end{bmatrix} \tag{1}$$

where $F_{x,ij}$ are the longitudinal tyre forces, i stands for front (f) or rear (r), while j stands for left (l) or right (r). $F_{y,ij}$ are the lateral tyre forces and F_{drag} is the aerodynamic drag force, which has quadratic relationship with the vehicle speed. The other parameters are reported in Table 1.

The longitudinal tyre forces are computed according to the following equations:

$$F_{x,f} = \frac{G_R\left(\left(T_{rq,full} - T_{rq,\min}\right)T_{hr} + T_{rq,\min}\right) - \left(T_{b,fl} + T_{b,fr}\right)}{\mathrm{R}_{eff,f}} \tag{2}$$

$$F_{x,r} = -\frac{T_{b,rl} + T_{b,rr}}{\mathrm{R}_{eff,r}} \tag{3}$$

where G_R is the total gear ratio between the engine and the wheels, $T_{rq,full}$ and $T_{rq,min}$ the maximum and minimum engine torque at the corresponding engine speed, $T_{b,ij}$ the braking torque on each wheel and $R_{eff,i}$ the effective tire radius at the front and rear axle of the vehicle. The engine torque map is defined as a look-up table.

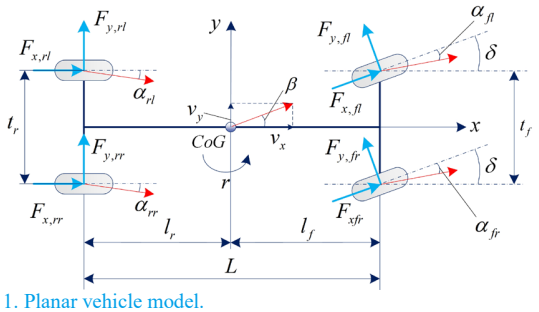

Figure 1. Planar vehicle model.

Table 1. Vehicle parameters used in the nominal model.

Symbol	Explanation	Value [Unit of measure]
l_f	Distance between the centre of gravity and the front axle	1.093 [m]
l_r	Distance between the centre of gravity and the rear axle	1.570 [m]
t_f	Front track width	1.628 [m]
t_r	Rear track width	1.635 [m]
m	Vehicle mass	1712 [kg]
I_{zz}	Vehicle inertia moment around the vertical axes	3386 [kg m^2]
$C_{l,fj}$	Cornering stiffness of front tyre	93468 [N rad]
$C_{l,rj}$	Cornering stiffness of rear tyre	76084 [N rad]
$C_{x,fj}$	Longitudinal stiffness of front tyre	211156 [N]
$C_{x,rj}$	Longitudinal stiffness of rear tyre	137764 [N]

The lateral tyre forces are computed as follow:

$$F_{y,fl} = C_{y,fl}\left(\delta - \frac{v_{y,fl}}{v_{x,fl}}\right) = C_{y,fl}\left(\delta - \frac{v_y + l_f\dot{\psi}}{v_x - 0.5t_f\dot{\psi}}\right) \tag{4}$$

$$F_{y,fr} = C_{y,fr}\left(\delta - \frac{v_{y,fr}}{v_{x,fr}}\right) = C_{y,fr}\left(\delta - \frac{v_y + l_f\dot{\psi}}{v_x + 0.5t_f\dot{\psi}}\right) \tag{5}$$

$$F_{y,rl} = C_{y,rl}\left(\delta - \frac{v_{y,rl}}{v_{x,rl}}\right) = C_{y,rl}\left(-\frac{v_y - l_r\dot{\psi}}{v_x - 0.5t_r\dot{\psi}}\right) \tag{6}$$

$$F_{y,rr} = C_{y,rr}\left(\delta - \frac{v_{y,rr}}{v_{x,rr}}\right) = C_{y,rr}\left(-\frac{v_y - l_r\dot{\psi}}{v_x + 0.5t_r\dot{\psi}}\right) \tag{7}$$

where $C_{y,ij}$ are the adaptive tyres cornering stiffness's computed at every time step according to the Dugoff tyre model, see Eq. 8. The Dugoff model is not differentiable, so it cannot be used during the MPC optimisation. Thus, the adaptive cornering stiffness is assumed to be constant over the prediction horizon in the MPC inner model [5]. The adaptive cornering stiffness allows to capture the non-linearities of the tire behaviour, so it increases the accuracy of the prediction, but it behaves such as linear tire model in the MPC inner model. The added complexity of a non-linear tyre model does not affect the optimisation time.

$$C_{y,ij} = C_{l,ij} f(\lambda_{ij}) \tag{8}$$

$C_{l,ij}$ are the tyre constant tyre cornering stiffness that are adapted at every time step by $f(\lambda)$, the weighting function of the Dugoff tyre model, see Eq. 9, which depends on the vehicle speed, road friction coefficient μ and the vertical force applied to the tyre $F_{z,ij}$ according to Eq. 10 and Eq. 11.

$$f(\lambda) = \begin{cases} \lambda(2-\lambda), & \lambda \le 1 \\ 1, & \lambda > 1 \end{cases} \tag{9}$$

$$\lambda = \frac{\mu F_{z,ij}\left(1-\kappa_{ij}\right)}{2\sqrt{\left(C_{x,ij}\kappa_{ij}\right)^2 + \left(C_{y,ij}\tan\left(\alpha_{ij}\right)\right)^2}} \tag{10}$$

$$\mu = \mu_0\left(1 - e_r v_{x,ij}\sqrt{\kappa^2{}_{ij} + \tan^2\left(\alpha_{ij}\right)}\right) \tag{11}$$

where κ_{ij} is the longitudinal slip of the front/rear left/right wheel, $C_{x,ij}$ is the longitudinal tyre stiffness, μ_0 is the peak friction coefficient and e_r is the friction reduction coefficient according to wheel longitudinal velocity.

Cost Function

The controller's objective is to follow a reference trajectory, keeping the desired speed and maintaining the vehicle inside the stability region. The proposed cost function is represented in Eq. 12. The number of equally spaced optimisation steps in the prediction horizon *N* is 30. All the symbols with foot N are related to the terminal stage of the MPC optimisation. R and R_r are the quadratic weights on the input and the input rate to reduce actuator's usage. Q_{V_X}, $Q_{\dot{\psi}}$, Q_y and Q_{ψ} are the quadratic weights for, respectively, longitudinal speed, yaw rate, lateral position and heading angle error. Their values ensure accurate path tracking to the controller but do not consider vehicle stability.

$$\begin{aligned} J = &\sum_{k=1}^{N-1} \begin{pmatrix} \left(V_{xi} - V_{xi,des}\right)^2 Q_{V_x} + \left(\dot{\psi}_i - \dot{\psi}_{i,des}\right)^2 Q_{\dot{\psi}} \\ + \left(y_i - y_{i,des}\right)^2 Q_y + \left(\psi_i - \psi_{i,des}\right)^2 Q_{\psi} \\ + \left(GY_{err,i}\right)^2 Q_{GY_{err}} + \left(Ack_{err,i}\right)^2 Q_{Ack_{err}} \\ + u_i{}^2 R + \dot{u}_i{}^2 R_r \end{pmatrix} + \\ &+ \begin{pmatrix} \left(V_{xN} - V_{xN,des}\right)^2 Q_{N,V_x} + \left(\dot{\psi}_N - \dot{\psi}_{N,des}\right)^2 Q_{N,\dot{\psi}} \\ + \left(y_N - y_{N,des}\right)^2 Q_{N,y} + \left(\psi_N - \psi_{N,des}\right)^2 Q_{N,\psi} \\ + \left(GY_{err,N}\right)^2 Q_{N,GY_{err}} + \left(Ack_{err,N}\right)^2 Q_{N,Ack_{err}} \\ + u_N{}^2 R_N \end{pmatrix} \end{aligned} \tag{12}$$

$Q_{GY_{err}}$ and $Q_{Ack_{err}}$ are, respectively, the quadratic weights on the error between the actual yaw rate and two expected steady state yaw rates, one based on the vehicle lateral acceleration GY_{err} and the other one based on steering wheel angle Ack_{err}. The first error is computed according to the following equation:

$$GY_{err} = \frac{a_y}{v_x} - \dot{\psi} \tag{13}$$

The second one is computed according to the following:

$$Ack_{err} = \frac{\delta v_x}{L\left(1 + k_h v_x{}^2\right)} - \dot{\psi} \tag{14}$$

where k_h is the stability factor [6], computed according to:

$$k_h = \frac{m}{L}\left(\frac{\frac{l_f C_{y,f} - l_r C_{y,r}}{-C_{y,f} - C_{y,r}}}{-l_f C_{y,f} - \frac{l_f C_{y,f} - l_r C_{y,r}}{C_{y,f} + C_{y,r}} C_{y,f}}\right) \tag{15}$$

GY_{err} and Ack_{err} aim to keep the vehicle in a steady state condition, enhancing its stability. Thus, there are three yaw rates that the MPC will optimise for: i) yaw rate related to path curvature, ii) yaw rate related to the steering input and iii) yaw rate related to the lateral acceleration. The first one, associated tuning weight $Q_{\dot{\psi}}$, is related to path tracking, and its mathematical definition is provided in Eq. 19, while the other two are related to vehicle stability. However, clashes between tracking and stability occur during manoeuvres at the limit of handling. Thus, $Q_{GY_{err}}$, $Q_{Ack_{err}}$ and $Q_{\dot{\psi}}$ are varied along the vehicle manoeuvre to prioritise tracking or stability. The weights associated with GY_{err} and Ack_{err} change depending on the vehicle's sideslip angle β and sideslip angle rate $\dot{\beta}$. The vehicle sideslip angle cannot be measured through the sensors currently installed in the commercial vehicle, so it is estimated [7, 8]. $Q_{GY_{err}}$, $Q_{Ack_{err}}$ are multiplied by the factor between 0 and 1, computed according to Figure 2. When the vehicle has low β and $\dot{\beta}$ values, the multiplication factor is close to 0 because the vehicle is already stable, hence, $Q_{GY_{err}}$, $Q_{Ack_{err}}$ are much lower than $Q_{\dot{\psi}}$. Thus, the MPC controller prioritises path tracking over vehicle stability. Vice versa, when the vehicle has a high β and $\dot{\beta}$ values, the multiplication factor is close to 1 because the vehicle is

close to the unstable region. Thus, the MPC controller prioritises vehicle stability over path tracking. The circular shape of the multiplication factor correspond to the circle circumscribed in the stability trapezoid, usually associated with the phase-plot analysis [9, 10]. This assumption is conservative, but it further prioritises stability over path tracking, reducing the chances that the controller brings the vehicle into an unstable region. All the tuned weight coefficient are reported in the Appendix.

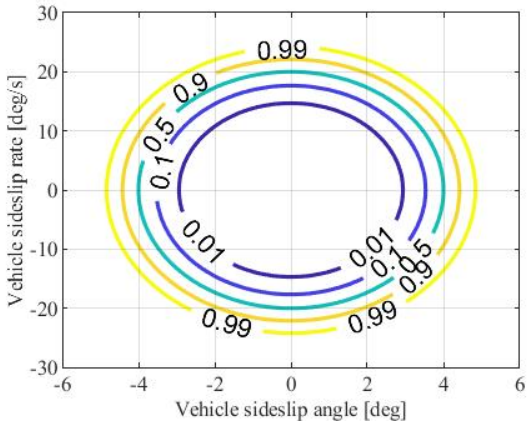

Figure 2. $Q_{GY_{err}}$ and $Q_{Ack_{err}}$ multiplication factor based on the vehicle state β-$\dot{\beta}$ phase plot.

Constraints

The implemented constraints are:

$$\begin{aligned} 0 \le v_x \le \frac{170}{3.6} \\ 0 \le T_{hr} \le 1 \\ -1 \le \dot{T}_{hr} \le 1 \\ -2.76\frac{360\pi}{180S_{rat}} \le \delta \le 2.76\frac{360\pi}{180S_{rat}} \\ -\frac{800\pi}{180S_{rat}} \le \dot{\delta} \le \frac{800\pi}{180S_{rat}} \\ 0 \le T_b \le 4886 \\ -7023 \le \dot{T}_b \le 7023 \end{aligned} \tag{16}$$

The equality constraint ensures that the optimisation follows the dynamics of the planar vehicle model. The goal of the inequality constraints is to limit the maximum values and the maximum rates of the control outputs. From top to bottom, the first constraint limits the velocity to the vehicle's top speed. The second and third constraints limit the throttle input and throttle rate, respectively. The throttle input is limited between 0 and 1, where 0 means the throttle is closed, while 1 corresponds to a fully open throttle. The throttle rate is limited to ensure smooth driving. Furthermore, the steering wheel angle and steering wheel angle rate are also constrained, and their values depend on the steering ratio S_{rat} (18.8). The final two constraints limit the brake torque and the brake torque rate.

Benchmark Controllers, KPIs and Manoeuvres

This section describes the baseline methods, selected KPIs and manoeuvres.

Benchmark

The proposed solution is compared with eight industrial benchmark controllers, representing different baselines for path tracking, stability control and a cascade of the two. Furthermore, every baseline is designed with or without differential braking. They are mainly split into two sets. The first one, called Single Brake (SB), is a control architecture where the braking input is a single brake command to all wheels. The second set, called Differential Braking (DB), is formed by controllers that apply differential braking and thus independently send different brake pressure to each wheel. This makes the controller more complex but gives the ability to induce an extra yaw moment to the vehicle. Every control set is further split into four groups:

- Path Tracking (PT): it performs path tracking without considering vehicle stability. The controller uses the lateral position, the yaw angle and the vehicle speed as references.
- Path Tracking and Yaw Rate (PTY): it adds to the simple path tracking controller a reference yaw rate, based on the path curvature and vehicle speed, in the cost function to develop the stability control capabilities.
- Path Tracking & Stability Constraints (PTC): it is a path tracking controller which adds two constraints to the MPC formulation to ensure vehicle stability. The combination of path tracking and stability constraints aims to develop a controller capable of correctly following a path, even in emergency manoeuvres, keeping the vehicle stable in every situation. The further constraint limits the error between the actual vehicle yaw rate and the expected yaw rate.
- Path Tracking & Stability Controller (PTS): a cascade controller in which the path tracking MPC, from the first configuration, is followed by a separate stability controller. The latter is a simplified version of industrial vehicle stability controller.

KPIs

The performance of every controller is assessed using five KPIs, commonly used for path tracking and vehicle stability controllers [4, 11, 12]. The proposed KPIs are:

- To evaluate the tracking performance, the Normalised Root Mean Square Error (NRMSE) of the lateral position $NRMSE_y$, heading angle $NRMSE_\psi$, and yaw rate $NRMSE_{\dot{\psi}}$. They of the controller.
- To assess vehicle stability, the Root Mean Square Error (RMSE) of the difference between the expected yaw rate, based on the steering angle $RMSE_{Ack}$, and the actual vehicle yaw rate.
- Also, to analyse vehicle stability, the RMSE of the difference between the expected yaw rate, based on the lateral acceleration $RMSE_{GY}$, and the actual vehicle yaw rate.

Manoeuvres

Two manoeuvres used to evaluate the performance of the proposed controller: i) Double Lane Change, and ii) Moose test, designed following ISO 3888-1 and ISO 3888-2. Both represent evasive manoeuvres when the vehicle has to avoid an object crossing the

vehicle's path [11, 13]. The main differences between the two tests are the road's length and the lanes' width. While the vehicle drives for 125 m to complete a double lane change, the length of a moose test is only 61 m. Thus, the track's width is slightly wider in a moose manoeuvre. Furthermore, the initial velocity in Double Lane Change test is 80 km/h, while it is 72 km/h in the Moose test. However, the Moose test is a more challenging manoeuvre [14]. The reference velocity is considered constant along all the trajectory. For both manoeuvres, the path is generated using two consecutive sigmoid curves that relate the longitudinal position to a lateral offset [15]. The following equation gives the desired lateral position:

$$y_{des}(x) = \frac{P_b}{1 + e^{-P_a(x - P_c)}} \tag{17}$$

where P_a, P_b and P_c are parameters used to define the curve. Two sigmoid curves in opposite directions generate the two sequential corners. The generated manoeuvres are used to compute the reference yaw angle ψ_{des}, see Eq. 17, and the reference yaw rate $\dot{\psi}_{des}$, see Eq.19.

$$\psi_{des} = \arctan\left(\frac{\partial y_{des}}{\partial x}\right) \tag{18}$$

Where $\frac{\partial y_{des}}{\partial x}$ is the derivative of the lateral reference position over the derivative of the longitudinal vehicle position, computed according to:

$$\frac{dy_{des}}{dx} = \frac{P_a P_b e^{-P_a(x - P_c)}}{\left(1 + e^{-P_a(x - P_c)}\right)^2} \tag{19}$$

$$\dot{\psi}_{des} = k v_x \tag{20}$$

Where k is the curvature of the road, which is computed according to the following equation:

$$k = \frac{\left(\frac{\partial^2 y_{ref}}{\partial x^2}\right)}{\left(1 + \left(\frac{\partial y_{ref}}{\partial x}\right)^2\right)^{\frac{3}{2}}} \tag{21}$$

Double Lane Change Variations

Several variations are applied to the Double Lane Change test, to evaluate the robustness of the controllers, such as road friction coefficient, initial vehicle speed, and vehicle weight variation. The summary of all the simulated conditions is summarized in Table 2.

Three different initial velocities are considered: 70 km/h, 80 km/h and the maximum speed for which the controller is capable of keeping the vehicle inside the road boundaries.

Two additional weights are added to the vehicle: 150 kg and 300 kg. In the case of 150 kg, the extra weight is equally split between the driver and passenger locations. While in the case of 300 kg, the weight is added also to the left- and right-rear passenger locations. These variations aim to analyse how additional passengers influence the controller's performance.

The road friction coefficient variations are considered for two different scenarios. In the first one, the μ level of the whole road changes. It emulates different road conditions such as ice or snow ($\mu = 0.3$), rain ($\mu = 0.6$) and dry ($\mu = 0.9$). The icy road's initial velocity is reduced to 70 km/h because none of the controllers complete the manoeuvre with a higher initial speed. The second scenario shows a difference in μ level between the two lanes. The initial velocity is set up to 70 km/h whenever the road has a friction coefficient of 0.3 because it represents the highest speed for which all controllers successfully pass the manoeuvre.

Table 2. Summary of the different initial conditions for a double lance change manoeuvre.

Number of variations	Friction Coeff. [-]	Initial Vehicle Velocity [km/h]	Added Weight [kg]
1	0.9	70	0
2	0.9	80	0
3	0.9	Max	0
4	0.9	80	150
5	0.9	80	300
6	0.3	70	0
7	0.6	80	0
8	0.9 to 0.6	80	0
9	0.6 to 0.9	80	0
10	0.6 to 0.3	70	0
11	0.3 to 0.6	70	0

Simulation Results

Experiments are conducted with a passenger vehicle modelled in IPG/Carmaker using a high-fidelity Toyota vehicle model. The model has been parametrized based on mass-inertia parameters obtained from vehicle inertia measuring facility, suspension kinematics and compliance obtained by measurement on a Kinematics & Compliance test rig for wheel suspension characterization, and finally, validated by field tests on the proving ground. This section demonstrates the performance of the proposed controller concerning the benchmark methods. The analysis is performed by simulating the Moose test. Furthermore, it studies the robustness of the proposed controller using different vehicle and road conditions in the Double Lane Change test.

Moose Test

The vehicle's trajectory obtained by different controllers configuration in the Moose test is shown in Figure 3. All the controllers allow the vehicle to pass the test successfully but with different performance levels. Thus, a focus on the vehicle lateral tracking error is reported in Figure 4. It shows that the SB-PTC controller has the highest overshoot

when moving to the offset lane, while the proposed controller has the lowest one. Interestingly, the DB-PTS controller shows the lowest overshoot when returning to the original lane. In general, Figure 3 and Figure 4 prove that controllers with differential braking have a lower overshoot and allow a tighter turn to the vehicle. This is due to the extra yaw moment generated by the different braking torque of the left and right tyres.

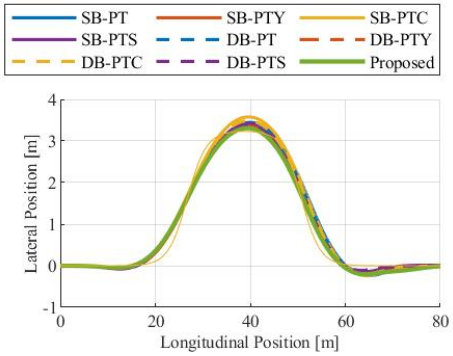

Figure 3. Vehicle trajectory for the Moose test at 72 km/h.

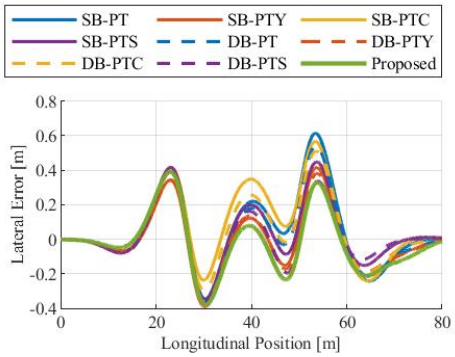

Figure 4. Lateral tracking error for the Moose test at 72 km/h.

A further analysis of the path tracking capabilities is reported in Figure 5. It evaluates the controller performance by comparing the $NRMSE_y$ and $NRMSE_\psi$. Both values are better when they are minimised. It can be seen that the controllers with the best performance are the proposed controller and DB-PTY, closely followed by SB-PTY. It is necessary to investigate the vehicle's stability properties with tracking capabilities (see Figure 6). The cascaded controller configuration with and without differential braking achieves higher stability properties, closely followed by the SB-PTC controller. By analysing Figure 5 and Figure 6, differential braking helps the controller achieve higher tracking performance at the cost of stability.

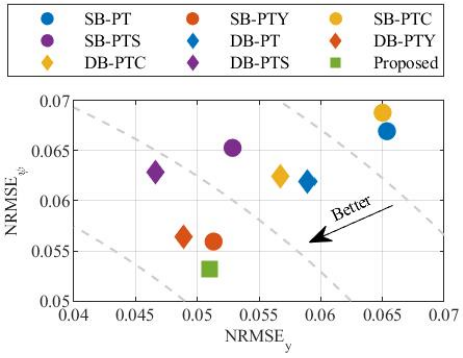

Figure 5. Comparison of the controllers path tracking capabilities using $NRMSE_y$ and $NRMSE_\psi$ (Moose test, 72 km/h).

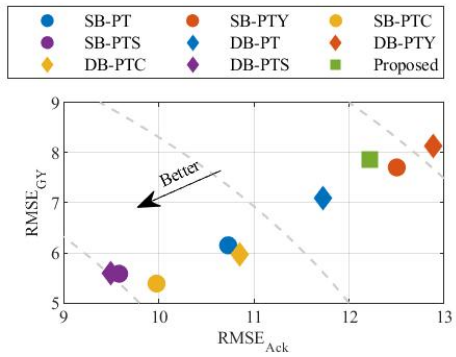

Figure 6. Comparison of the controllers stability capabilities using $RMSE_{Ack}$ and $RMSE_{GY}$ (Moose test, 72 km/h).

However, the relative performance changes when performing the Moose test at the maximum speed for which each controller still completes the manoeuvre. Figure 7 and Figure 8 show, respectively, the controller path tracking and stability performance in the Moose test driven at the maximum velocity. In this scenario, it can be seen that the proposed controller achieves the best performance for both path tracking and stability compared with DB-PTY and DB-PTS. The performance improvement for the stability KPIs of the proposed controller is 11% over the DB-PTS. While the improvement for the tracking KPIs is 8% over the DB-PTY in the maximum speed scenario.

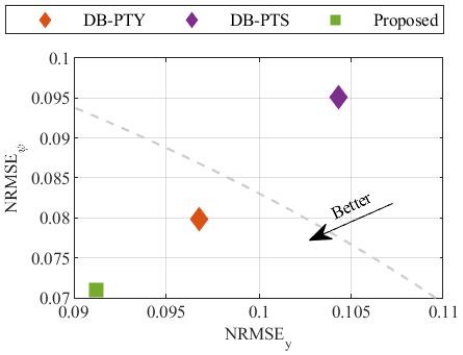

Figure 7. Comparison of the controllers path tracking capabilities using $NRMSE_y$ and $NRMSE_\psi$ (Moose test, maximum speed).

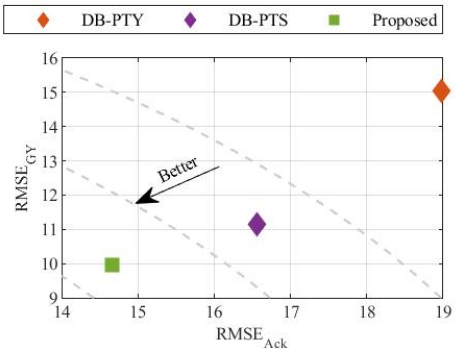

Figure 8. Comparison of the controllers stability capabilities using $RMSE_{Ack}$ and $RMSE_{GY}$ (Moose test , maximum speed).

The stability properties can also be compared considering the sideslip angle and sideslip angle rate phase portrait, see Figure 9. The proposed controller has significantly lower β and $\dot{\beta}$ values, with a maximum β of 6 deg and a maximum $\dot{\beta}$ of 30 deg/s. These values coincide with the stability prioritisation in the proposed controller. It highlights the ability of the proposed controller to prioritise tracking or stability depending on the state of the vehicle.

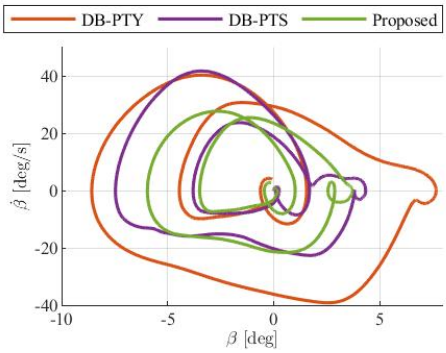

Figure 9. $\beta - \dot{\beta}$ phase portrait for the proposed controller, DB-PTC and DB-PTS (Moose test, maximum speed).

Double Lange Change

This section focuses on the robustness of the proposed controller showing how the tracking and stability KPIs change at the variations of initial speed, mass and friction coefficient in the Double Lane Change manoeuvre.

Initial Velocity Variation

Figure 10 shows the variation of the tracking KPIs in the Double Lane Change test with a different velocity. All the controllers have a linear increase in the KPIs when the velocity increases. SB-PTC and DB-PTC show the steepest KPIs increase, and they have the lowest maximum speed at which the vehicle successfully performs the manoeuvre. Furthermore, the controllers with differential braking improved tracking performance at the cost of stability, see Figure 11. At lower speeds, the lateral tracking performance of the proposed controller is slightly worse than the other controllers, but at higher speeds, it outperforms all the others. Furthermore, it allows the vehicle to be driven with the highest speed within the road bounds of the Double Lane Change manoeuvre. Figure 10b shows the tracking of the heading angle. The path-tracking performance of the proposed controller deteriorates more at higher speeds than the other controllers. This can be explained by looking at the two stability KPIs (Figure 11). The proposed controller has better stability performance at all speeds, with a lower performance deterioration at higher speeds as well. The reference yaw rate, based on the path curvature, is challenging to track at higher speeds without compromising stability. Therefore better stability KPIs will result in overall lower yaw tracking KPIs.

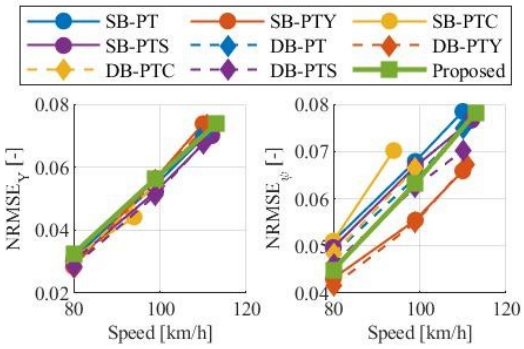

Figure 10. Tracking KPIs variation according to initial velocity.

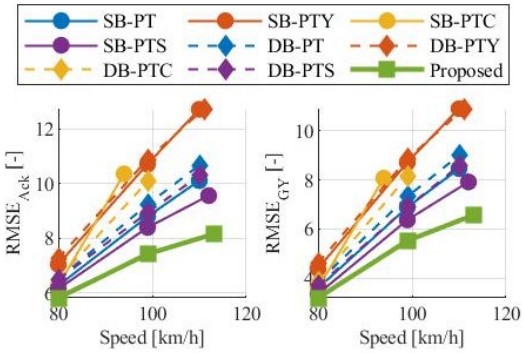

Figure 11. Stability KPIs variation according to initial velocity.

Vehicle Weight Variations

The variation of the tracking and stability KPIs due to adding weight is shown in Figure 12 and Figure 13. The added weight causes worse performance for all controllers. However, the tracking performance of the controllers with differential braking is less affected than the ones without it. Considering vehicle stability, the opposite trend is noticeable. Nevertheless, there are some outliers. For instance, the DB-PTY controller has a better $RMSE_{ack}$ with further mass of 300 kg than 150 kg. Another example is the SB-PT controller, which has a better $RMSE_{Gy}$ at 150kg than with no extra weight. However, the overall performance of DB-PTY and SB-PT still deteriorates when looking at the combined $RMSE_{ack}$ and $RMSE_{Gy}$ performance. The most notable observation about the proposed controller is that almost all KPIs have a drop when going from 150 kg to 300 kg. This indicates a better performance when 300 kg is added instead of only 150 kg. All the other controllers show the opposite trend.

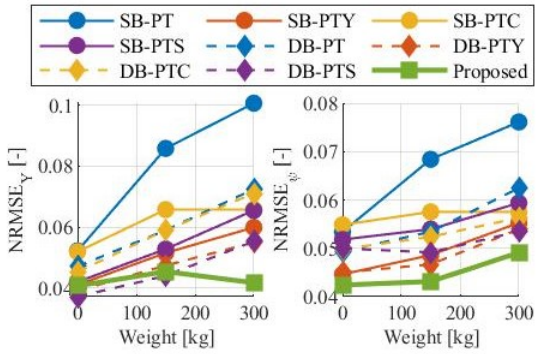

Figure 12. Tracking KPIs variation due vehicle weight.

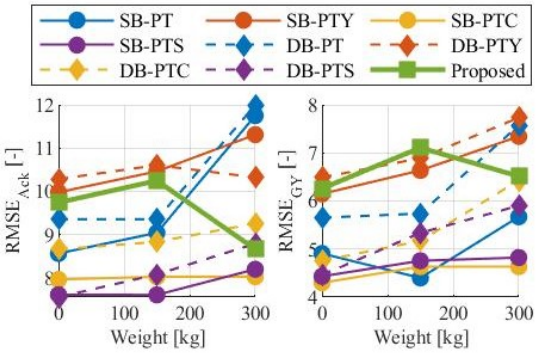

Figure 13. Stability KPIs variation due vehicle weight.

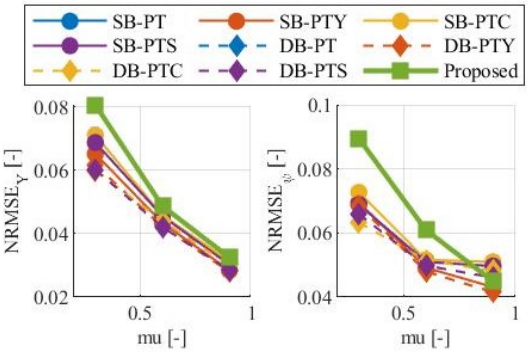

Figure 14. Tracking KPIs variation due to friction coefficient.

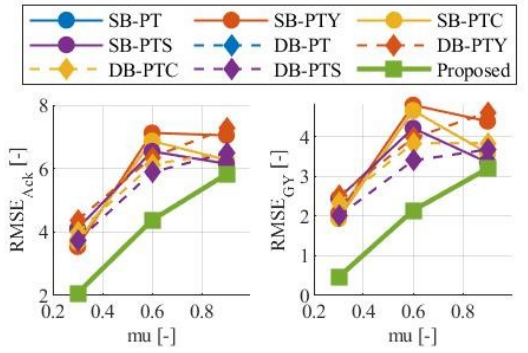

Figure 15. Stability KPIs variation due to friction coefficient.

Friction Coefficient

Figure 14 and Figure 15 show, respectively, the tracking and stability KPIs variation when the manoeuvre is simulated with various friction coefficient. When lowering μ, the controllers generally have worse tracking performance. Regarding stability, there is a clear performance gap between the controllers that can use differential braking and those that cannot. The controllers with differential braking have better stability in the 0.6μ case compared to the 0.9μ case, while those without DB have worse stability in the 0.6μ case. However, when μ is equal to 0.3, the controllers without differential braking have slightly better stability performance than the others. It is essential to highlight that the worst stability KPIs in the 0.3μ case is partly due to the lower initial speed for this scenario, see Figure 15. Analysing the tracking KPIs, there is a difference between the controllers with and without differential braking. The controllers with DB have lower tracking performance deterioration in the lower μ conditions, see Figure 14. A possible explanation is that the front wheels quickly reach the saturation region at the low friction scenario. There is a more significant deterioration in tracking performance for the proposed controller than for the other controllers. However, the stability of the vehicle also increased the most. It is important to highlight that with a different controller tuning for low μ scenarios, the tracking could be improved at the cost of stability. For safety reasons, it is preferred to insure vehicle stability.

Split Friction Coefficient

Figure 16 and Figure 17 show the results for the split friction coefficient scenario. The controllers with differential braking perform better than the controllers without it in all cases. A possible explanation is that DB controllers have an extra control input available to control the vehicle. Furthermore, the performance for all controllers is better in the scenario where the original lane has a lower μ than the second lane. A possible explanation is that the controller predicts a particular input expecting a low friction coefficient μ, but when the μ level suddenly increases, more grip is available, making the path easier to follow. In the opposite scenario, the reverse is true. When the μ level suddenly lowers, there is less grip available, which the controller could not previously predict. The vehicle is more difficult to control and reduces tracking and stability. For most KPIs, the relative performance between the controllers remains similar for the different scenarios. One exception happens in the tracking KPIs where the proposed controller has a much more significant decrease in performance in the $0.3 \rightarrow 0.6\mu$ scenario. In this situation, the proposed controller has better stability at the cost of worse tracking, as it happens when the entire road has a low friction coefficient.

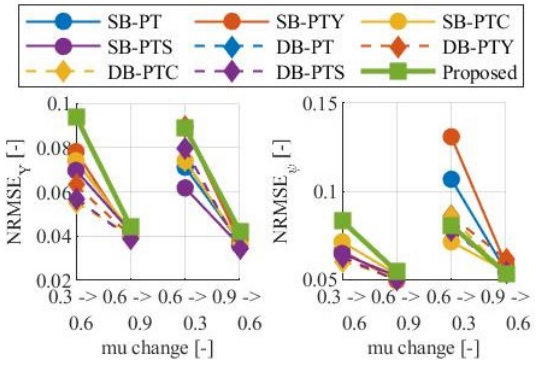

Figure 16. Tracking KPIs variation when the road has a split friction coefficient.

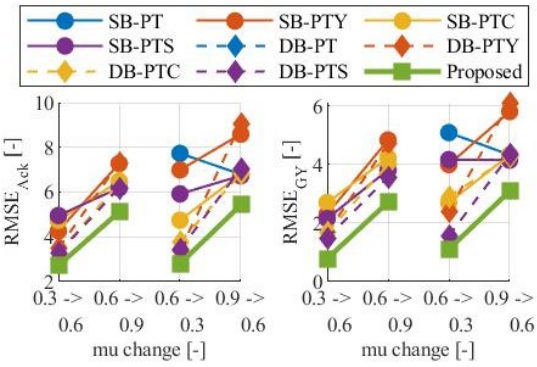

Figure 17. Stability KPIs variation when the road has a split friction coefficient.

Conclusions

This paper presents a novel MPC controller which combines path tracking and vehicle stability into a single controller. It includes two additional reference yaw rates to the cost function, indicating the vehicle's stability. The performance of the proposed control is compared with eight industrial benchmarks designed to evaluate the benefits of different path tracking and stability controllers. Their performance is assessed through two industry-standard tests, i.e. Moose test and Double Lane Change. Furthermore, the controller's robustness is tested by changing various vehicle and road parameters in the Double Lane Change manoeuvre. Using the high-fidelity simulation environment, we show that adding differential braking increases the overall performance of the controllers. The path tracking performance is increased at the cost of a slight decrease in stability performance. Additionally, the controllers with differential braking are more robust in varying conditions. Primarily, we prove an 8% improvement in tracking capability and an 11% improvement in stability performance than a cascaded controller path tracking and vehicle stability with differential braking. Furthermore, it also has the best robustness to the considered variations. Future works involve the implementation of the proposed controller in the vehicle demonstrator to verify its benefit in a real scenario.

References

[1] S. A. Ferguson, "The effectiveness of electronic stability control in reducing real-world crashes: a literature review," *Traffic injury prevention,* vol. 8, no. 4, pp. 329-338, 2007.

[2] N. Chowdhri, L. Ferranti, F. S. Iribarren, and B. Shyrokau, "Integrated nonlinear model predictive control for automated driving," *Control Engineering Practice,* vol. 106, p. 104654, 2021.

[3] P. Falcone, F. Borrelli, J. Asgari, E. Tseng, and D. Hrovat, "Predictive Active Steering Control for Autonomous Vehicle Systems," *Control Systems Technology, IEEE Transactions on,* vol. 15, pp. 566-580, 06/01 2007, doi: 10.1109/TCST.2007.894653.

[4] P. Falcone, H. Eric Tseng, F. Borrelli, J. Asgari, and D. Hrovat, "MPC-based yaw and lateral stabilisation via active front steering and braking," *Vehicle System Dynamics,* vol. 46, no. S1, pp. 611-628, 2008.

[5] A. Bhoraskar and P. Sakthivel, "A review and a comparison of Dugoff and modified Dugoff formula with Magic formula," in *2017 International Conference on Nascent Technologies in Engineering (ICNTE)*, 27-28 Jan. 2017 2017, pp. 1-4, doi: 10.1109/ICNTE.2017.7947898.

[6] W. Milliken, D. Milliken, E. Kasprzak, and L. Metz, "Race car vehicle dynamics: Problems, answers and experiments," *Dynamics,* vol. 265, p. 5Control267, 1995.

[7] A. Bertipaglia, D. de Mol, M. Alirezaei, R. Happee, and B. Shyrokau, "Model-based vs Data-driven Estimation of Vehicle Sideslip Angle and Benefits of Tyre Force Measurements," *arXiv preprint arXiv:2206.15119,* 2022.

[8] A. Bertipaglia, B. Shyrokau, M. Alirezaei, and R. Happee, "A Two-Stage Bayesian Optimisation for Automatic Tuning of an Unscented Kalman Filter for Vehicle Sideslip Angle Estimation," *Proc. of 33rd IEEE Intelligent Vehicles Symposium , Aachen, Germany,* 2022.

[9] B. Shyrokau and D. Wang, "Control allocation with dynamic weight scheduling for two-task integrated vehicle control," in *Proc. 11th Int. Symp. Adv. Vehicle Control*, 2012, pp. 1-6.

[10] B. Shyrokau, D. Wang, D. Savitski, K. Hoepping, and V. Ivanov, "Vehicle motion control with subsystem prioritization," *Mechatronics,* vol. 30, pp. 297-315, 2015.

[11] L. Li, Y. Lu, R. Wang, and J. Chen, "A three-dimensional dynamics control framework of vehicle lateral stability and rollover prevention via active braking with MPC," *IEEE Transactions on Industrial Electronics,* vol. 64, no. 4, pp. 3389-3401, 2016.

[12] W. Zhang, Z. Wang, L. Drugge, and M. Nybacka, "Evaluating model predictive path following and yaw stability controllers for over-actuated autonomous electric vehicles," *IEEE Transactions on Vehicular Technology,* vol. 69, no. 11, pp. 12807-12821, 2020.

[13] H. Lu, Y. Shi, D. He, and F. Yu, "Model-based vehicle stability control with tyre force and instantaneous cornering stiffness estimation," *Proceedings of the Institution of Mechanical Engineers, Part D: Journal of Automobile Engineering,* vol. 230, no. 6, pp. 754-770, 2016.

[14] R. Q. Guo, L. Yuan, and J. Z. Xie, "Implement of handling and stability road test of passenger vehicle for ISO standards," in *Applied Mechanics and Materials*, 2014, vol. 568: Trans Tech Publ, pp. 1869-1874.

[15] B. Lu *et al.*, "Hybrid path planning combining potential field with sigmoid curve for autonomous driving," *Sensors,* vol. 20, no. 24, p. 7197, 2020.

Contact Information

Alberto Bertipaglia is with the Department of Cognitive Robotics, Delft University of Technology

Acknowledgments

The Dutch Science Foundation NWO-TTW supports the research within the EVOLVE project (nr. 18484).

Abbreviation

MPC	Model Predictive Control
KPI	Key Performance Indicator
NRMSE	Normalised Root Mean Squared Error
RMSE	Root Mean Squared Error
DB	Differential Braking
SB	Single Braking
PT	Path Tracking
PTY	Path Tracking and Yaw Rate
PTC	Path Tracking & Stability Constraints
PTS	Path Tracking & Stability Controller

Appendix

Tuning coefficient	Value	Tuning coefficient	Value
Q_V	$1e1 / \mu^5$	$Q_{N,V}$	$1e2 / \mu^6$
Q_y	$5e3 / \mu$	$Q_{N,y}$	$5e4 / \mu^2$
Q_ψ	$3e4 / \mu$	$Q_{N,\psi}$	$5e5 / \mu^4$
Q_r	$3e3 / \mu$	$Q_{N,r}$	$1e3 / \mu^2$
Q_{st}	$5e3 / \mu^3$	$Q_{N,st}$	$5e3 / \mu^6$
Q_{Br}	$1e-3 / \mu^3$	$Q_{N,Br}$	$1e-2 / \mu^3$
Q_{Thr}	$1e3 / \mu^3$	$Q_{N,Thr}$	$1e4 / \mu^3$
$R_{\Delta st}$	$5e3 / \mu^6$	$R_{N,\Delta st}$	-
$R_{\Delta Br}$	$5e-5 / \mu^5$	$R_{N,\Delta Br}$	-
$R_{\Delta Thr}$	$1e3/\mu^3$	$R_{N,\Delta Thr}$	-
$Q_{Ack,err}$	$AF * 1e4 / \mu^{4.75}$	$Q_{N,Ack,err}$	$AF * 1e4 / \mu^{4.75}$
$Q_{GY,err}$	$AF * 1e6 / \mu^{2.5}$	$Q_{N,GY,err}$	$AF * 1e6 / \mu^{2.5}$

Bibliography

[1] *A Brief History of Electronic Stability Controls and their Applications - Safety Research & Strategies, Inc.* URL: https://www.safetyresearch.net/a-brief-history-of-electronic-stability-controls-and-their-applications/.

[2] Susan A Ferguson. “The Effectiveness of Electronic Stability Control in Reducing Real-World Crashes: A Literature Review”. In: *Traffic Injury Prevention* 8 (4 2007), pp. 329–338. ISSN: 1538-9588. DOI: 10.1080/15389580701588949. URL: https://www.tandfonline.com/action/journalInformation?journalCode=gcpi20.

[3] NHTSA. “FINAL REGULATORY IMPACT ANALYSIS FMVSS No . 126”. In: (126 2007), p. 169. URL: http://www.nhtsa.gov/DOT/NHTSA/Rulemaking/Rules/Associated%20Files/ESC_FRIA_%2003_2007.pdf.

[4] Euro NCAP. *Electronic Stability Control | Euro NCAP*. URL: https://www.euroncap.com/en/vehicle-safety/the-ratings-explained/safety-assist/previous-tests/esc/ (visited on 05/16/2022).

[5] Shaosong Li et al. “Vehicle Stability Control Based on Model Predictive Control Considering the Changing Trend of Tire Force Over the Prediction Horizon”. In: *IEEE Access* 7 (2019), pp. 6877–6888. DOI: 10.1109/ACCESS.2018.2889997.

[6] Mooryong Choi and Seibum B. Choi. “Model Predictive Control for Vehicle Yaw Stability With Practical Concerns”. In: *IEEE Transactions on Vehicular Technology* 63.8 (2014), pp. 3539–3548. DOI: 10.1109/TVT.2014.2306733.

[7] Hui Lu et al. “Model-based vehicle stability control with tyre force and instantaneous cornering stiffness estimation”. In: *Proceedings of the Institution of Mechanical Engineers, Part D: Journal of Automobile Engineering* 230.6 (2016), pp. 754–770. DOI: 10.1177/0954407015594926. eprint: https://doi.org/10.1177/0954407015594926. URL: https://doi.org/10.1177/0954407015594926.

[8] Stefano Di Cairano et al. “Vehicle Yaw Stability Control by Coordinated Active Front Steering and Differential Braking in the Tire Sideslip Angles Domain”. In: *IEEE Transactions on Control Systems Technology* 21.4 (2013), pp. 1236–1248. DOI: 10.1109/TCST.2012.2198886.

[9] Craig Earl Beal and J. Christian Gerdes. “Model Predictive Control for Vehicle Stabilization at the Limits of Handling”. In: *IEEE Transactions on Control Systems Technology* 21.4 (2013), pp. 1258–1269. DOI: 10.1109/TCST.2012.2200826.

[10] Hengyang Wang et al. “Path Tracking Control for Autonomous Vehicles Based on an Improved MPC”. In: *IEEE Access* 7 (2019), pp. 161064–161073. ISSN: 21693536. DOI: 10.1109/ACCESS.2019.2944894.

[11] Fitri Yakub and Yasuchika Mori. “Comparative study of autonomous path-following vehicle control via model predictive control and linear quadratic control”. In: *Proceedings of the Institution of Mechanical Engineers, Part D: Journal of Automobile Engineering* 229.12 (2015), pp. 1695–1714. DOI: 10.1177/0954407014566031. eprint: https://doi.org/10.1177/0954407014566031. URL: https://doi.org/10.1177/0954407014566031.

[12] Hongliang Zhou, Levent Guvenc, and Zhiyuan Liu. “Design and evaluation of path following controller based on MPC for autonomous vehicle”. In: *Chinese Control Conference, CCC* (Sept. 2017), pp. 9934–9939. ISSN: 21612927. DOI: 10.23919/CHICC.2017.8028942. URL: https://ieeexplore-ieee-org.tudelft.idm.oclc.org/document/8028942.

[13] Paolo Falcone et al. “MPC-based yaw and lateral stabilisation via active front steering and braking”. In: *Vehicle System Dynamics* 46.sup1 (2008), pp. 611–628. DOI: 10.1080/00423110802018297. URL: https://doi.org/10.1080/00423110802018297.

[14] Wenliang Zhang et al. “Evaluating Model Predictive Path Following and Yaw Stability Controllers for Over-Actuated Autonomous Electric Vehicles”. In: *IEEE Transactions on Vehicular Technology* 69.11 (2020), pp. 12807–12821. DOI: 10.1109/TVT.2020.3030863.

[15] R. Brach. “Tire Models for Vehicle Dynamic Simulation and Accident Reconstruction”. In: 2009. DOI: https://doi-org.tudelft.idm.oclc.org/10.4271/2009-01-0102.

[16] Hans B. Pacejka. “Chapter 4 - Semi-Empirical Tire Models”. In: *Tire and Vehicle Dynamics (Third Edition)*. Ed. by Hans B. Pacejka. Third Edition. Oxford: Butterworth-Heinemann, 2012, pp. 149–209. ISBN: 978-0-08-097016-5. DOI: https://doi.org/10.1016/B978-0-08-097016-5.00004-8. URL: https://www.sciencedirect.com/science/article/pii/B9780080970165000048.

[17] Shaosong Li et al. “Vehicle Yaw Stability Control at the Handling Limits Based on Model Predictive Control”. In: *International Journal of Automotive Technology* 21 (Apr. 2020), pp. 361–370. DOI: 10.1007/s12239-020-0034-7.

[18] Akshay Bhoraskar and Sakthivel Palanivelu. “A review and a comparison of Dugoff and modified Dugoff formula with Magic formula”. In: Jan. 2017, pp. 1–4. DOI: 10.1109/ICNTE.2017.7947898.

[19] *Passenger Cars – Test track for a severe lane-change manoeuvre – Part 2: Obstacle Avoidance*. Standard. Geneva, CH: International Organization for Standardization, Mar. 2011.

[20] VEHICO”. *VEHICO - ISO Lane Change Test*. british. URL: https://www.vehico.com/index.php/en/applications/iso-lane-change-test.

[21] Run Qing Guo, Lin Yuan, and Jin Zhong Xie. “Implement of Handling and Stability Road Test of Passenger Vehicle for ISO Standards”. In: *Measurement Technology and its Application III*. Vol. 568. Applied Mechanics and Materials. Trans Tech Publications Ltd, Aug. 2014, pp. 1869–1874. DOI: 10.4028/www.scientific.net/AMM.568-570.1869.

[22] Liang Li et al. “A Three-Dimensional Dynamics Control Framework of Vehicle Lateral Stability and Rollover Prevention via Active Braking With MPC”. In: *IEEE Transactions on Industrial Electronics* 64.4 (2017), pp. 3389–3401. DOI: 10.1109/TIE.2016.2583400.

[23] S Angelis et al. “Optimal Steering for Double-Lane Change Entry Speed Maximization”. In: *Proceedings of AVEC’14 International symposium on advanced vehicle control, 22-26 September 2014,Tokyo, Japan*. 2014.

[24] Euro NCAP. “EUROPEAN NEW CAR ASSESSMENT PROGRAMME (Euro NCAP) THE DYNAMIC TEST OF CAR ELECTRONIC STABILITY CONTROL (ESC) SYSTEMS PROTOCOL”. In: (2011).

[25] A. Linder et al. “Methods for the Evaluation of Traffic Safety Effects of Antilock Braking System (ABS) and Electronic Stability Control (ESC) – A Literature Review”. In: 2007.

[26] Lin Zhang et al. “Model predictive control for integrated longitudinal and lateral stability of electric vehicles with in-wheel motors”. In: *IET Control Theory & Applications* 14 (Aug. 2020). DOI: 10.1049/iet-cta.2020.0122.

[27] Basilio Lenzo et al. “On the experimental analysis of single input single output control of yaw rate and sideslip angle”. In: *International Journal of Automotive Technology* 18 (Oct. 2017). DOI: 10.1007/s12239-017-0079-4.

[28] Nishant Chowdhri. *Model Predictive Control For Automated Driving and Collision Avoidance Design of an integrated NMPC with simultaneous lateral and longitudinal control via steering and braking*. 2021. URL: http://repository.tudelft.nl/..

[29] Heemels M. *MPC and constrained systems*. 2013. URL: https://heemels.tue.nl/research/mpc-and-constrained-systems.

[30] Bing Lu et al. “Hybrid Path Planning Combining Potential Field with Sigmoid Curve for Autonomous Driving”. In: *Sensors* 20.24 (2020). ISSN: 1424-8220. DOI: 10.3390/s20247197. URL: https://www.mdpi.com/1424-8220/20/24/7197.

[31] “Review and performance evaluation of path tracking controllers of autonomous vehicles”. In: *IET Intelligent Transport Systems* 15 (5 May 2021), pp. 646–670. ISSN: 1751956X. DOI: 10.1049/itr2.12051.

[32] Alexander Katriniok et al. *Optimal Vehicle Dynamics Control for Combined Longitudinal and Lateral Autonomous Vehicle Guidance*. 2013. ISBN: 9783033039629. DOI: 10.23919/ECC.2013.6669331.

[33] “Towards longitudinal and lateral coupling control of autonomous vehicles using offset free MPC”. In: *Control Engineering Practice* 121 (Apr. 2022). ISSN: 09670661. DOI: 10.1016/J.CONENGPRAC.2022.105074.

[34] Bing Zhang et al. “Electrical Vehicle Path Tracking Based Model Predictive Control with a Laguerre Function and Exponential Weight”. In: *IEEE Access* 7 (2019), pp. 17082–17097. ISSN: 21693536. DOI: 10.1109/ACCESS.2019.2892746.